Analog Optical Links for Wide-Bandwidth Radar Receivers

A Major Qualifying Project Report
Submitted to the Faculty
of the
WORCESTER POLYTECHNIC INSTITUTE
In partial fulfillment of the requirements for the
Degree of Bachelor of Science
In Electrical & Computer Engineering
by:

_____

Sean Morris

_____

Brian Potts

Submitted:
October 15, 2009

Sponsor: MIT Lincoln Laboratory
Supervisor: Jeffrey Hargreaves

Approved:

_____

Professor Alexander Emanuel, Major Advisor

Abstract

This is a comprehensive report on the feasibility of using an analog optical link for transmission of a received radar signal from the antenna to the back-end of the receiver, located on the ground. Such a change from the coaxial cable, which is currently being used, to an analog optical link would allow for remoting of the back-end of the radar receiver. This is due to the much lower losses encountered in the use of analog optical links. This report examines instantaneous dynamic range and radar receiver sensitivity to determine if a commercially available link could seamlessly be inserted, or if an analog optical link needs to be designed at a component level in order to meet the radar receiver specifications.

Acknowledgements

We would like to thank Jeffrey Hargreaves, our supervisor at MIT Lincoln Laboratory, and Professor Alexander Emanuel, our WPI advisor, for their continued support throughout the project. Without their help this project would not have been possible.

Table of Contents

List of Figures

List of Tables

Executive Summary

MIT Lincoln Laboratory is a non-profit federally funded research and development center that was founded in 1951. It was originally founded primarily as a research center focusing on air defense [1]. Extensive work has been accomplished at MIT Lincoln Laboratory, in the area of radar and missile defense. The primary focus of this project involved working with a radar system developed by Lincoln Laboratory.

Radar systems are used in a wide variety of applications, ranging from weather sensing to defense. In defense applications, being able to accurately and precisely locate and/or identify a target is crucial. The ability to preserve the radar signal integrity is extremely important in achieving this. In order to do so, maintaining a sufficient dynamic range in the receiver side of the radar system is very important. Another primary concern is maintaining appropriate radar receiver sensitivity such that targets can be accurately identified over a range of distances. The radar system of interest for this project had a specified instantaneous dynamic range of 50 dB and a sensitivity corresponding to a signal-to-noise ratio of 30 dB for a 1 m^2 target at a distance of 1000 km.

Within the radar system of interest, coaxial cable is used for transmission of the received radar signal. The primary focus of this project was to investigate the feasibility of using an analog optical link to replace the coaxial cable transmission line for a number of reasons. Firstly, being able to receive the full bandwidth radar signal on the ground at the control center would be highly desirable, as opposed to the current setup in which the received radar signal is translated down to a lower frequency at the antenna, leading to a loss of information. Secondly, being able to have the receiver hardware on the ground would allow for easier access, therefore making

maintenance and operation easier. Lastly, being able to remote the radar receiver hardware at long distances away from the antenna can be highly desirable as well.

Analog optical links consist of a modulation device, which can be a direct or external modulator, an optical fiber, and a demodulation device, which is a photodiode. An RF signal is input to the modulator, which modulates an optical carrier signal, which is then converted back into RF at the demodulator. Optical fiber tends to have extremely low attenuation at long distances when compared to coaxial cable. Optical fiber also has a virtually flat frequency response throughout the RF and microwave spectrum, whereas coaxial cable attenuation rises with frequency. This characteristic of coaxial cable, along with having significantly higher attenuation than optical fiber, leads to a need for incorporating amplifiers and equalizers in the transmission line, which adds to design complexity as well as cost. The currently used coaxial cable costs $25 per foot with approximately $2,500 worth of amplifiers and equalizers within the transmission line. Low attenuation optical fiber can cost approximately $0.50 per foot, and a commercially available prepackaged analog optical link receiver and transmitter can typically cost up to $10,000. For this reason, from an economic perspective, the designer has to consider the specific distance of interest when deciding whether to use an analog optical link or coaxial cable. That is, although optical fiber is much cheaper and has much lower attenuation than coaxial cable, the cost of an analog optical link is primarily determined by the transmitter and the receiver.

There were three main deliverables for this project. The first deliverable consisted of simulation tools which could accurately model the performance of the entire radar receiver chain. These tools were developed in MATLAB®, and allow the designer to incorporate coaxial cable, an analog optical link at a component level, or an analog optical link at purely a link level into

the simulation of interest. The tool allows the user to specify the signal that is received at the antenna as well as state parameters values for each of the components in the radar receiver chain. Additional functions were written which adjust the signal primarily based on gain, saturation, and noise figure. After each component is specified MATLAB® will output the signal-to-noise ratio as well as a plot of the current time domain signal and amplitude spectrum. The second deliverable was a viable analog optical link design which could be incorporated into the current radar receiver chain. It was determined that there are no commercially available analog optical links which could be used within the existing radar receiver chain and still allow the entire receiver chain to meet the sensitivity specification. Therefore, it is recommended that future designers approach the analog optical link design from a component level. Three design cases were provided using an externally modulated link with different characteristics in order to demonstrate how different design variables affect overall performance. The last deliverable for the project was the testing of an evaluation analog optical link in order to realize any real world limitations not accounted for within the simulation tools, as well as to experimentally verify the fact that with significant increases in fiber distance, changes in optical fiber attenuation are negligible.

In conclusion, the simulation tools that were developed were successfully verified using real world specifications for comparison. All three component level analog optical link designs allow the radar receiver chain to meet both the dynamic range and sensitivity specifications, although given the first order nature of the simulation tools, these designs would probably have to be adjusted if implemented in the future. After testing the evaluation analog optical link with different length optical fibers, it was experimentally verified that any changes in attenuation were in fact negligible. In order to economically justify the usage of an analog optical link over

coaxial cable, the system of interest would have to require long distance signal transmission, whereas at shorter distance, coaxial cable is more economically feasible. From a performance perspective, the decision is more complicated since analog optical link performance is largely based upon whether or not it is a prepackaged link or not. As mentioned previously, designing an analog optical link from scratch is the recommended design solution since the desired link characteristics would be more easily achievable in this case.

Chapter 1: Introduction

MIT Lincoln Laboratory is a non-profit federally funded research and development center that was founded in 1951. It was originally founded primarily as a research center focusing on air defense. Correspondingly, it is particularly well known for the work it has done in radar development since it was first founded [1].

Radar systems are used in a wide variety of applications, ranging from weather sensing to defense. In defense applications especially, being able to accurately and precisely locate and/or identify a target is crucial. The ability to preserve the radar signal integrity is extremely important in achieving this. In order to do so, maintaining a sufficient dynamic range in the receiver side of the radar system is very important. Along with this, being able to remote the radar receiver hardware at a long distance from the antenna is highly desirable.

For this project, the primary radar system of interest is an X-Band radar system developed by MIT Lincoln Laboratory. This radar system operates at a center frequency of 10 GHz with a bandwidth of 1 GHz, making it one of the higher frequency radar systems developed by MIT Lincoln Laboratory. The problem arises in the transmission line currently used in the receiver side of the radar system, which is coaxial cable. Coaxial cable has been used in a number of different applications for decades, as it has a series of characteristics that make it desirable for radio frequency (RF) signal transmission. However, for the purpose of long distance signal transmission, as is the case when remoting receiver hardware, coaxial cable has less than desirable performance.

A possible solution to this problem is to use an analog optical link to replace the coaxial cable. Analog optical links function on the basis of transmitting light through optical fiber that has negligible loss over quite long distances, such as kilometers. The main goal of this project

was to examine the feasibility of using an analog optical link to replace the coaxial cable transmission line within the receiver side of a radar system. In order to successfully accomplish this, first, an in depth economic analysis was conducted in order to compare the advantages and disadvantages of coaxial cable and analog optical links. Once this was done, in order to aid future designers at MIT Lincoln Laboratory, a series of simulation tools were developed. These tools will allow the designer to observe the performance of the receiver side of a radar system given certain transmission line characteristics, either at an optical link component level or at purely a link level. Lastly, testing of an analog optical link was done in order to observe real world physical limitations, as well as the effect that fiber length may have on attenuation [2].

Chapter 2: Background

This chapter provides a general understanding of how radar works. Since this project deals with the receiver part of the radar, in particular the coaxial cable that is used to transmit the received signal from the equipment on the antenna to the equipment on the ground, the flow of the signal through the radar receiver is explained. The advantages and disadvantages of using coaxial cable are examined in depth. Also, since the ultimate goal of the project was to determine the feasibility of using an analog optical link instead of the currently used coaxial cable, a background of analog optical link theory at a component level is included.

2.1 Radar: Application and Theory

Radio detection and ranging (radar) was initially designed for defense against bomber aircraft in the 1930s. In fact, most developments in radar since it was first invented were funded by the government for the purpose of creating a stronger defense. Over the years the uses for radar have been broadened to include many civilian purposes as well, such as, for air-traffic controllers to keep the skies safe and for police to monitor the speed of traffic. While radar has advanced technologically throughout its history, there is still much more that can be done to improve it [3].

The theory behind how a radar system works is actually very simple. The first step is generating and transmitting a pulse of electromagnetic energy. This pulse will then propagate through the air at approximately the speed of light until it finds a target or until the signal dissipates and becomes too weak to return a detectable signal. A portion of the energy that reaches the target will then be reflected back towards the antenna from which it was transmitted.

Equation (1) is used to calculate the power that is seen at the receiver, and is known as the radar equation.

$$P_r = \frac{P_t G_t}{4\pi R^2} \times \frac{\sigma}{4\pi R^2} \times A_e \qquad (1)$$

where,

P_t= transmitted power (W),
G_t= transmitter gain,
R= range from antenna to target (m),
σ= cross sectional area of target (m^2),
A_e=effective aperture of antenna (m^2).

The first fraction in (1) deals with the transmission of the signal. The second fraction deals with the target and the signal that is reflected back to the antenna. Doing a simple reorganization of this equation and substituting the minimum detectable signal, S_{min}, into the equation for the received power allows one to solve for maximum range, R_{max}. This is defined by:

$$R_{max} = \left(\frac{P_t G_t A_e \sigma}{(4\pi)^2 S_{min}} \right)^{1/4} \qquad (2)$$

From (2) it is clear that an increase in the transmitted power has little effect on the maximum range of a radar system. If the desire is to double the maximum range, by changing only power, it would require the transmitted signal be 16 times as strong as before. Once a detectable signal returns to the antenna it is passed on to the receiver, as detailed in Figure 1, where the signal will be processed and analyzed. This processing is very complex and can be used to determine the location, trajectory, and many more characteristics of the target. Targets can then be displayed on a monitor for viewing [3].

This project deals with the receiver portion of the radar, specifically the link that is used to transport the signal from the receiver equipment on the antenna to the back end of the receiver which is located on the ground. Since, as was mentioned earlier, the signals that are received at

the antenna are very weak, it is extremely important to preserve the signal integrity as best possible.

2.2 The Radar Receiver

Any radar system can be broken down into two basic parts: the transmitter and the receiver. The receiver hardware serves the purpose of preserving and amplifying the received signal such that it can be successfully interpreted by the appropriate processing hardware used to detect targets. The configuration of such hardware can vary depending upon certain factors. One significant factor in determining which configuration to use is the bandwidth of the radar signal being used by the system. A block diagram of the receiver side of the radar system of interest can be seen in Figure 1.
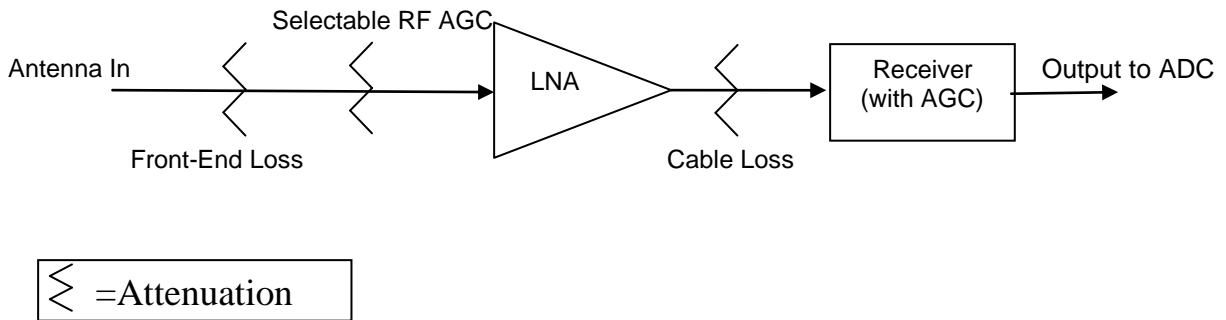
Figure 1: Receiver Side of Radar System

In Figure 1, AGC stands for automatic gain control, LNA stands for low noise amplifier, and ADC stands for analog to digital converter. AGC serves the purpose of reducing the amplitude of very high amplitude signals and increasing the amplitude of very low amplitude signals in order to achieve optimal signal reception [4]. The LNA boosts the received signal while inserting minimal noise into it. The ADC takes the analog, RF signal and converts it into a digital signal that can be processed by a computer system.

Regardless of the specific hardware configuration, the transmission line used to connect said hardware in each case remains the same. This is typically a low loss, 50Ω coaxial cable. Although coaxial cable has its advantages, it has inherent disadvantages as well. For the application at hand, it performs less than desirably when attempting to place the back-end receiver hardware on the ground. For this reason, there is a need to investigate other potential means of signal transmission. This is where analog optical links come into play.

2.2.1 Coaxial Cable

The coaxial cable has been popular in many high frequency applications for a number of decades. It made its first major appearance in the 1920's in telephone networks, and has seen a number of uses for communications and broadcasting networks since then [5]. Coaxial cable allows for the transmission of radio frequency (RF) and microwave signals with low attenuation, broad bandwidth, and almost ideal isolation from electromagnetic interference (EMI) [6]. The geometry of a typical coaxial cable is detailed in Figure 2.
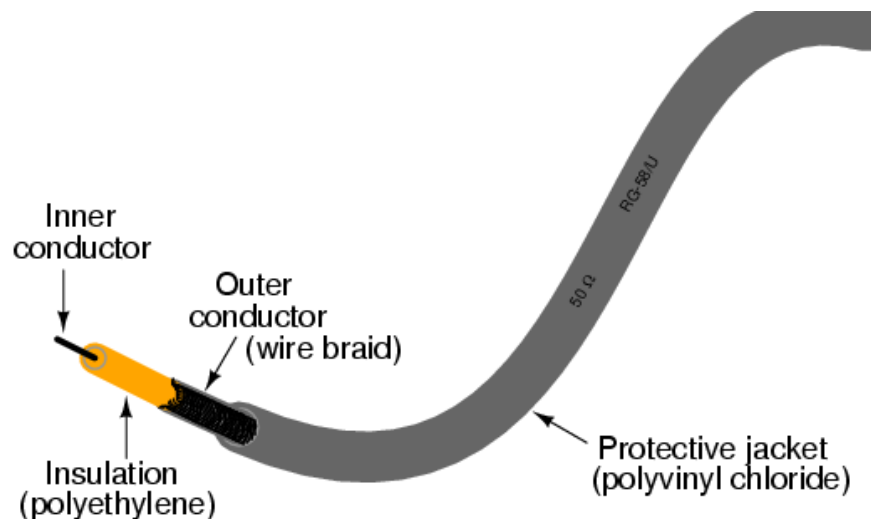
Figure 2: Typical Coaxial Cable [7]

The outer conductor of the coaxial cable is typically the return path or ground, while the inner conductor carries the transmitted signal to a load. The outer conductor shields the coaxial cable

[5]. Another important feature of the coaxial cable is that it does not generate electric or magnetic fields on the exterior of the outer conductor under ideal conditions [8]. What this means is that multiple coaxial cables can be bundled closely together in such a way that there is almost no cross talk, or destructive interference, between them. Another added benefit resulting from this feature of coaxial cable is that amplifiers can be placed farther apart on a given coaxial transmission line [5].

Although coaxial cable has many advantages regarding signal preservation, it also has a few disadvantages. One such disadvantage is the high price required for installation. Also, certain coaxial cables can, when struck by lightning, cause severe damage to electronics on either side of a given coaxial transmission line [5] At high frequencies in the GHz range, coaxial cable can have very high attenuation at a distance. Typical coaxial cable attenuation vs. frequency can be seen in Figure 3.
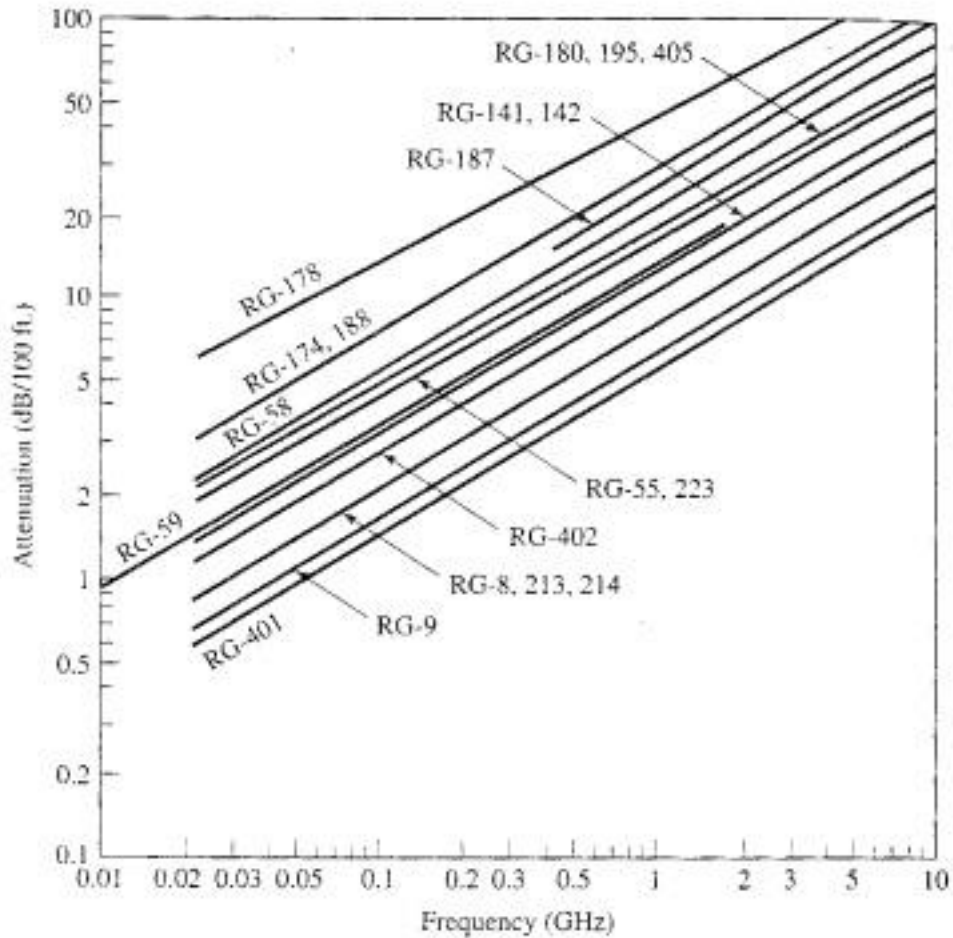
Figure 3: Attenuation vs. Frequency [9]

Figure 3 shows that at 10GHz, which is the center frequency of the radar signal for this project, the lowest attenuation achievable from RG-401 coaxial cable (the cable with the lowest attenuation in the figure) is approximately 20 dB/100ft. This amount of attenuation places a very strict limit upon how far away the back end of the radar receiver can be placed in relation to the antenna.

2.2.2 Analog Optical Links

The development of fiber optic links for communications applications started to take hold during the 1980's [10]. The primary reason that there was so much interest in this area is due to

the fact that fiber is highly efficient when it comes to optical transmission. While the most

common application for fiber optics has been digital communications, there has been increasing

interest in the area of analog signal transmission using fiber optics. The way in which such

analog signal transmission is accomplished is via an analog optical link [2]. A basic block

diagram of an analog optical link can be seen in Figure 4.
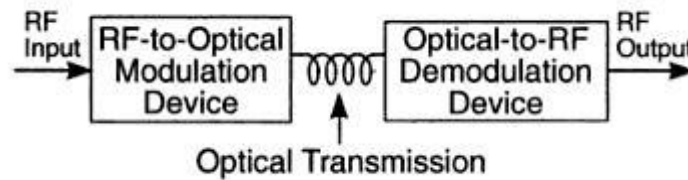
Figure 4: Analog Optical Link [2]

Typically, analog optical links are used in conjunction with RF and microwave signals as is

implied in Figure 4. An RF or microwave signal is input to the first stage of the analog optical

link, which is the modulation device. After this stage, optical transmission occurs along a fiber

optic transmission line. The signal carried by the fiber is then input to a demodulation device,

which converts the appropriate optical signal back to its RF or microwave equivalent.

Analog optical links are used in three different applications: transmission, distribution,

and receiving. For this project, the application of interest was receiving since we are dealing

with a radar receiver. An example of where such a link might be used is in the area of

cellular/PCS systems [2]. A diagram of this type of link is presented in Figure 5.
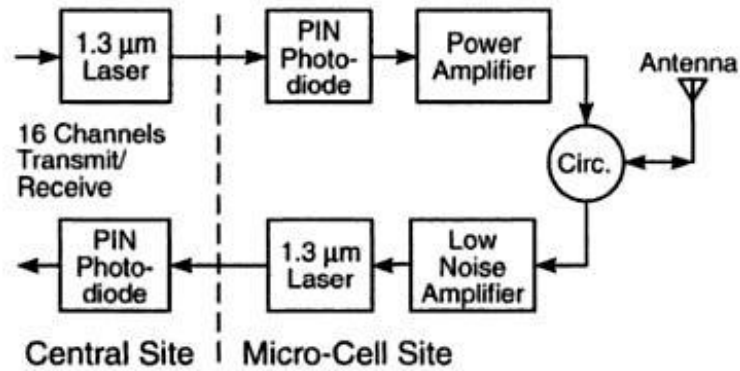
Figure 5: Cellular/PCS Link [2]

Due to the fact that the RF signal received in any given system is typically at a very low power level at the antenna, one of the primary concerns when designing an analog optical link in receiver applications is that of noise. While this is typically not a major design issue when dealing with lower frequency RF, noise can become a significant obstacle at higher frequencies due to increased link losses. This is usually dealt with by using a low noise RF pre-amplifier with a high gain before the analog optical link such that the analog optical link noise is kept very low and the determining factor in the chain of components is primarily determined by the pre-amplifier noise figure [2].

The other primary concern, when designing an analog optical link is that of distortion. Designing a link in order to avoid distortion is largely based upon the bandwidth of interest. Ultimately, balancing link noise and distortion, whether it is wide band or narrow band, is the primary design concern when dealing with distortion in analog optical links [2].

2.2.2.1 Analog Optical Modulators

The first stage in any analog optical link is the modulation stage. There are two types of modulation techniques that can be used: direct and external. Each of these modulation schemes has a number of advantages and disadvantages. The most important specification to consider

10

when selecting a modulation device is that of its modulation efficiency, or how efficiently the RF

input signal is converted to an optical signal [2].

Direct modulation, as its name implies, involves varying the intensity of an optical signal

directly from an RF modulation signal. The semiconductor diode laser is typically the means

used to achieve such a modulation scheme. Semiconductor diode lasers consist of the Fabry-

Perot diode laser, the distributed feedback diode laser (DFB), and the vertical cavity surface

emitting laser (VCSEL) [2].

The Fabry-Perot diode laser, shown in Figure 6, operates on the basis of utilizing the

properties of semiconductor diodes and optical waveguides.
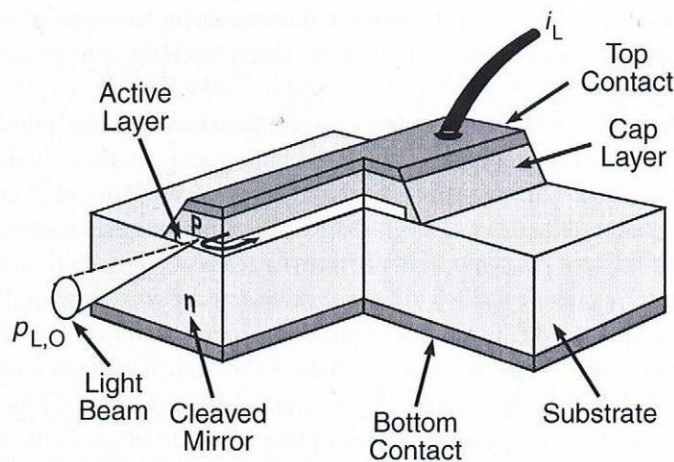
Figure 6: Fabry-Perot Laser Diode [2]

Firstly, a forward biased semiconductor diode can release radiation spontaneously given that the

p-n junction is the appropriate material. This process is random though, and for this reason, the

need for stimulated emission arises. Stimulated emission causes all photon emissions to be the

same. Once stimulated emission is accomplished, the optical waveguide comes into play. The

optical waveguide basically serves the purpose of resonating at the same wavelength as the

stimulated emissions. In the end, these processes successfully create what is commonly known

as a laser. What makes this particular type of laser a Fabry-Perot laser is the type of optical

waveguide employed [2].

There are a number of important parameters to be concerned with when selecting the

appropriate laser for modulation. One such parameter is the threshold current, I_T. I_T determines

at which point the optical gain of the laser is at least equal to the optical losses. A graph of

optical output power vs. laser current can be seen in Figure 7.
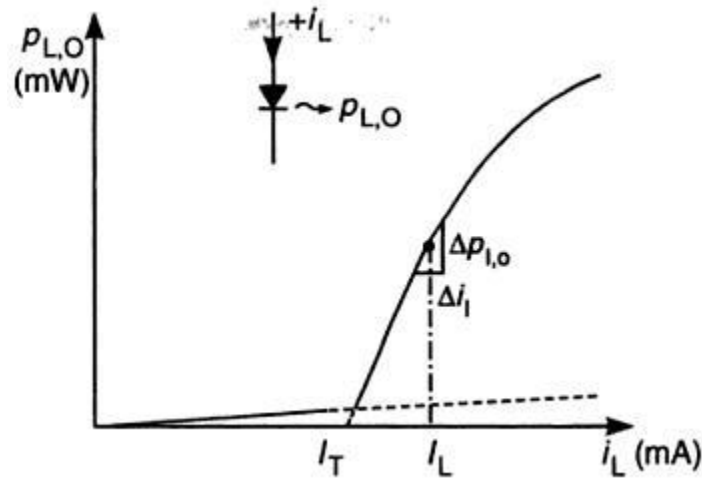
Figure 7: Optical Output Power vs. Laser Current [2]

As is shown in Figure 7, once the threshold current is achieved by the laser, there is an avalanche

effect on the optical output power of the laser. Usually the optical output power of an in-plane

laser, such as the Fabry-Perot, ranges from 10 to 100µW at the threshold current. Threshold

currents of 5 to 50mA are the most common. It is particularly important to be aware of this

value due to the fact that if the current applied is too high, the continuous wave (CW) laser

operation can be disrupted due to too much heat having been generated. Another important

consideration is that the threshold current usually rises with temperature [2].

Another important parameter of diode lasers is slope efficiency, s_l. The slope efficiency

is defined as the instantaneous rate of change, or the derivative, of the laser optical output power

with respect to the threshold current [2].

$$s_\ell \big|_{i_L=I_L} = \frac{dp_\ell}{di_\ell}$$

(3)

where,

s_ℓ = slope efficiency (W/A),
i_L = laser current (A),
I_L = DC bias current for laser (A),
p_ℓ = incremental laser output power (W),
i_ℓ = incremental laser current (A).

It can also be defined with regards to a parameter known as the external differential quantum

efficiency in order to demonstrate how its value is wavelength dependent [2].

$$s_\ell \big|_{I_L} = \frac{n_\ell hc}{q\lambda_o}$$

(4)

where,

n_ℓ = external differential quantum efficiency, "which is the ratio of change in number of emitted
photons to injected electrons",
h = Planck's constant (6.626×10^{-34} J/s),
c = speed of light in a vacuum (3×10^8 m/s),
q = electric charge (-1.602×10^{-19} C),
λ_o = free-space wavelength (m).

Regardless of how it is defined though, higher slope efficiency is desirable due to the fact that it

is used to determine just how efficient the modulator is. Fiber coupled slope efficiency is

derived from a combination of the laser slope efficiency and laser chip-to-fiber coupling

efficiency. It is of particular interest to a link designer since it is a performance metric providing

useful information at a link level. In reality, fiber coupled slope efficiency tends to be

13

significantly lower than any theoretically predicted maximum values when using laser diodes due to certain physical mismatches between the fiber and the diode laser [2].

Another important parameter of laser modulators is the incremental modulation efficiency. The mathematical definition of incremental modulation efficiency is defined as follows [2]:

$$\frac{p^2_{\ell,o}}{p_{s,a}} = \frac{s_\ell^2}{R_L + R_{MATCH}} \tag{5}$$

where,

$p_{\ell,o}$ = optical output power (W),
$p_{s,a}$ = available power to the load (W),
R_L = diode laser input resistance (Ω),
R_{MATCH} = resistor used to match modulation source with diode laser input resistance (Ω).

The schematic that corresponds to (5) can be seen in Figure 8 [2].
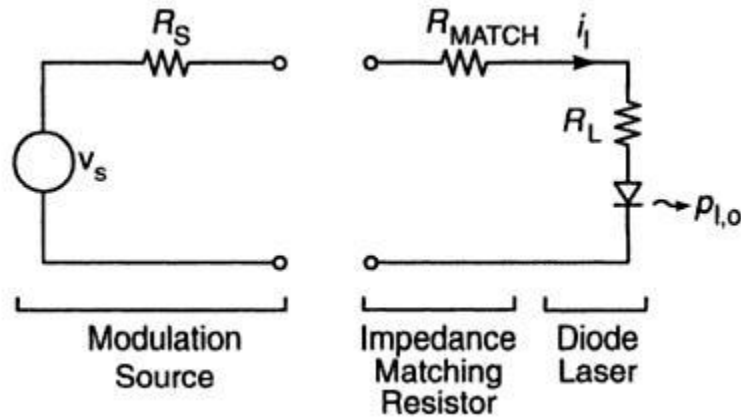
Figure 8: Small Signal Direct Modulation Model [2]

Another option for in-plane lasers is the DFB, which is shown in Figure 9.
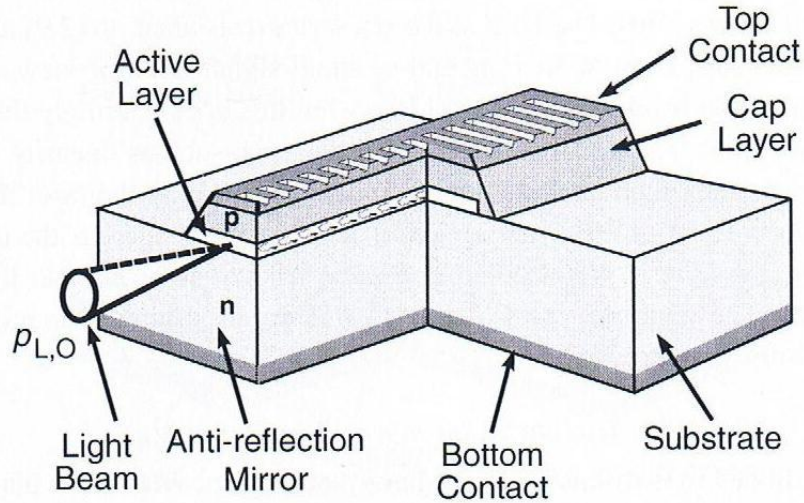
Figure 9: DFB Laser [2]

The need for DFB lasers stems from the spectral problems that can arise when using Fabry-Perot lasers. More specifically, the Fabry-Perot laser operates across a range of wavelengths. This limits its ability to be used in certain applications due to potential dispersion problems that can arise. Dispersion, specifically chromatic dispersion, is the propagation of different wavelengths at different velocities within a particular transmission medium. How DFB lasers overcome this is by utilizing an internal optical grating which, at a very basic level, finely tunes the optical output such that there is a single dominant wavelength. Other than this device level difference, the DFB laser is very similar to the Fabry-Perot laser, and for this reason can be treated the same way at a small-signal modeling level [2].

The third option available for direct modulation lasers is the vertical cavity surface emitting laser (VCSEL), shown in Figure 10.

15
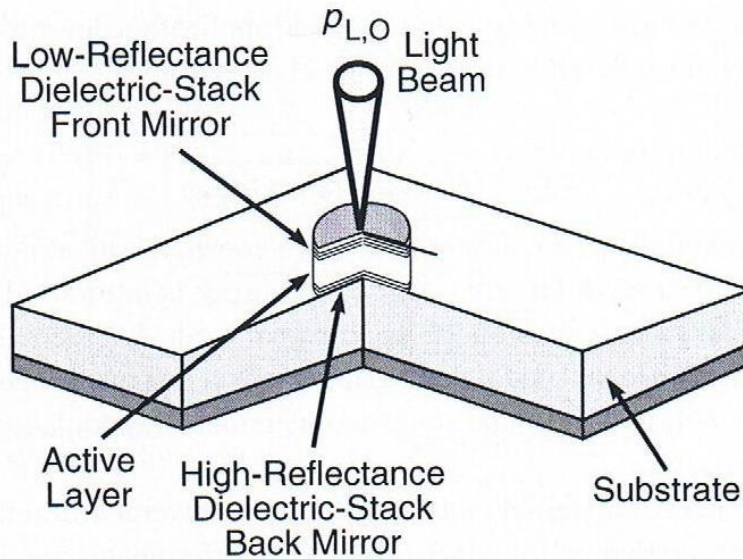
Figure 10: VCSEL [2]

The need for VCSEL's stems from the fact that firstly, in-plane laser testing is difficult, and secondly, that in-plane lasers are very limited for usage in two- dimensional laser arrays. The way the VCSEL addresses this is by having a vertical, perpendicular to wafer, laser. VCSEL's tend to have better fiber-coupling efficiency as a result of this. As was the case with the DFB laser, the VCSEL can be treated the same as the Fabry-Perot laser from a small-signal modeling perspective [2].

External modulation is the alternative to direct modulation. External modulation, on a basic level, involves using a CW laser in conjunction with a separate modulating device. One advantage to this approach is that the designer has a much broader range of lasers to choose from for the application of interest. The primary concern of the designer when selecting an external modulator should be how effectively a change in electric properties translates into a change in optical properties (electro-optic sensitivity), how much optical loss can be tolerated, what the maximum optical power is of the device, and what is necessary in terms of optical/thermal stability. There are a number of different materials that have been used in the development of

external modulators, but inorganic lithium niobate tends to be the most commonly used. This is primarily due to the ability to achieve a good balance between all of the previously mentioned parameters when using the material. The three main external modulators known to date are the Mach-Zehnder modulator, the directional coupler modulator, and the electro-absorption modulator [2].

The Mach-Zehnder modulator (MZM) is shown in Figure 11.
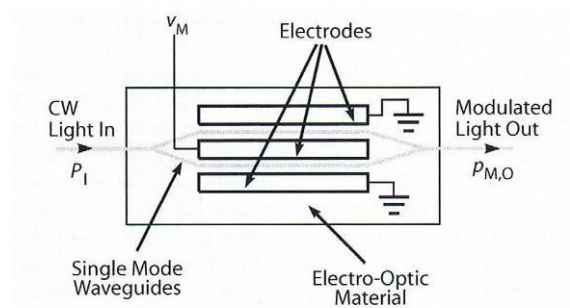
Figure 11: Mach-Zehnder Modulator [2]

It consists of electrodes connected to a slab of lithium niobate used to induce changes in the electric field, therefore changing the optical phase of light passing through the slab. This change in optical phase thereafter gets translated into a change in optical intensity, which corresponds to intensity modulation. This is all possible due to the fact that light propagates at different velocities through different mediums, and in this case, the electric field indirectly controls the propagation speed [11]. To make the modulator more sensitive to electric field changes, the usage of an optical waveguide can be employed [2].

Within the Mach-Zehnder modulator, the external CW laser is fed into the optical waveguide, which is split into two equally long sections, eventually recombining back into one section. The significance of this is that when there is no voltage applied, the maximum optical transmission is achieved. When a specific voltage known as V_π is applied, there is minimum

optical transmission. The transfer function for the Mach-Zehnder modulator is defined as

follows [2]:

$$p_{M,O} = \frac{T_{FF} P_I}{2} [1 + \cos(\frac{\pi v_M}{V_\pi})] \qquad \textbf{(6)}$$

where,

$p_{M,O}$ = modulated output power (W),
T_{FF} = excess modulator loss represented as a linear ratio (usually about 0.5 = 3 dB of loss),
P_I = input power (W),
v_M = modulation voltage signal applied to electrode (V).

Since the transfer function of the Mach-Zehnder modulator is an elevated sinusoid with a

minimum at zero, V_π can be effectively thought of as the linear region of operation for the

modulator, as is detailed in Figure 12. That is, the ideal DC bias point for the modulator is

located at half of V_π (or a whole number multiple of it) [12] [2]. More importantly, this DC bias

point allows the designer to achieve theoretically maximum incremental modulation efficiency.

As an appropriate analogy, this is essentially the same analysis that is applied to a transistor

when attempting to determine an appropriate DC bias point in linear amplifier applications.
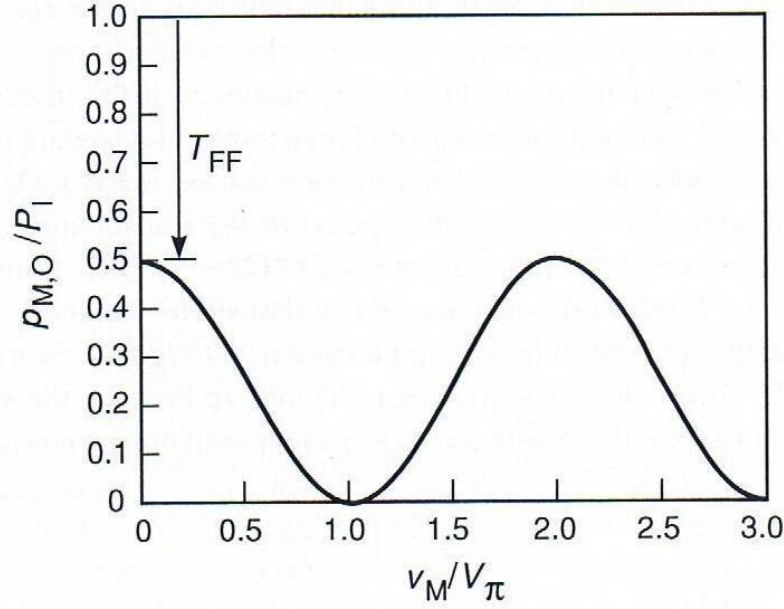
Figure 12: Mach-Zehnder Modulator Transfer Function [2]

The general form of fiber-coupled slope efficiency for a Mach-Zehnder modulator can be

derived using (6) and is defined as follows [2]:

$$s_{mz} = \frac{T_{FF} P_I \left[\cos(\pi V_M / V_\pi)\cos(\pi v_m / V_\pi) - \sin(\pi V_M / V_\pi)\sin(\pi v_m / V_\pi)\right] R_S}{2 v_m} \tag{7}$$

where,

s_{mz} = fiber-coupled slope efficiency (W/A),
V_M = DC bias voltage (V),
v_m = RF modulation voltage (V),
R_S = modulation source resistance (Ω).

By comparing direct modulators to Mach-Zehnder modulators, statistically and theoretically, one

learns that Mach-Zehnder modulators tend to offer better slope efficiencies while simultaneously

utilizing high power, external CW lasers [2].

There are two forms of wavelength dependence to consider when dealing with the fiber-

coupled slope efficiency of Mach-Zehnder modulators. The first of these is that the fiber-

coupled slope efficiency is related to the inverse of wavelength when considering a single modulator. Also, given different modulators designed to handle different wavelengths, fiber-coupled slope efficiency is roughly related to the inverse of wavelength squared [2].

The directional coupler is another type of external modulator that is very similar in its design to the Mach-Zehnder modulator. Through the modification of certain physical properties such as waveguide spacing and electrode alignment within the lithium niobate, what is known as a directional coupling modulator is achievable. The transfer function for a directional coupler is defined as follows [2]:

$$p_{D,O} = T_{FF} P_I \frac{\sin^2[(\pi/2)\sqrt{1+3(v_M/V_S)^2}]}{1+3(v_M/V_S)^2} \tag{8}$$

where,

$p_{D,O}$ = power output for the directional coupler (W),
V_S = voltage needed to induce no coupling (no optical output power) (V).

V_S can be treated similarly to V_π in the case of the Mach-Zehnder modulator for analysis purposes. The analysis for the directional coupler is not as straight forward as in the case of Mach-Zehnder due to the fact that the transfer function is not periodic in this case. Nonetheless, $0.43 V_S$ turns out to be the ideal DC bias voltage to achieve maximum incremental modulation efficiency for a directional coupler. Assuming this DC bias voltage, (9) is the slope efficiency for a directional coupler [2].

$$s_{dc}\big|_{V_M \cong 0.43V_S} = \frac{5.24 T_{FF} P_I R_S}{V_S} \tag{9}$$

where,

s_{dc} = slope efficiency for a directional coupler (W/A).

After comparing the transfer function for a Mach-Zehnder modulator and a directional coupler modulator, given the same lengths for the electrodes in each case, it is evident that the directional coupler modulator has higher incremental modulation efficiency by about 1.6. After comparing the slope efficiencies for the two, it is also evident that the directional coupler modulator achieves better slope efficiency than the Mach-Zehnder modulator. However, the directional coupler modulator is more difficult to manufacture, and is usually only the preferred modulator in switching applications. It is important to note that for both the directional coupler modulator and the Mach-Zehnder modulator, the incremental modulation efficiencies and slope efficiencies are not inherent characteristics of the devices, but rather derived based upon a selected DC bias value [2].

Another type of external modulator that can be used is the electro-absorption modulator. This modulator differs from the previous two in that it utilizes what is known as the electro-absorption (EA) effect. The inherent behavior of the electro-absorption modulator relies upon the behavior of a PIN junction when utilizing certain wavelengths. The incremental modulation efficiency and slope efficiencies in this case can be given in a general form as a function DC bias voltage rather than having to be derived assuming a particular DC bias voltage. The incremental modulation efficiency for an electro-absorption modulator is defined as follows [2]:

$$\frac{p^2_{a,o}}{p_{s,a}} = \left(\frac{T_{FF} P_I T_N}{V_\alpha}\right)^2 R_S \tag{10}$$

where,

$p_{a,o}$ = modulated optical power output (W),
T_N = light absorption due to DC bias voltage,
V_α = effectively the same as V_π (V).

The slope efficiency for an electro-absorption modulator is defined as follows [2]:

21

$$s_{ea}\Big|_{V_M} = \frac{T_{FF}\,P_I\,T_N(V_M)\,R_S}{V_\alpha(V_M)} \tag{11}$$

where,

s_{ea} = slope efficiency for the electro-absorption modulator (W/A).

Electro-absorption modulators have certain inherent physical limitations to be considered when selecting an external modulator. One such limitation is the maximum optical power is significantly lower than what Mach-Zehnder modulators are currently capable of. Also, electro-absorption modulators impose certain limitations on the usable CW laser wavelength [2].

2.2.2.2 Optical Fibers

Once the RF signal has been converted to an optical signal, a transmission line is needed to carry the signal to the optical receiver, where the signal will be converted back to RF. Analog optic links typically use a fiber made of silica glass, a very low-loss material [13]. Fabrication of a suitable fiber was not easy during the early years of development. It took until the 1970s for a fiber to be made with an attenuation as little as 20 dB/km, thus making it useful for telecommunication transmission [14]. This was a major breakthrough, but was by no means an end point. Currently, optical fibers are available with attenuation as low as 0.15 dB/km [13].

An optical fiber consists of a core, a cladding, and a buffer. The optical signal is passed down the core using internal reflection. The refractive index of the core is slightly higher than the refractive index of the cladding which causes the light from the core to reflect off the cladding and remain in the core. The buffer is just there to protect the fiber from physical damage. There are two main types of optical fibers which are used; single-mode and multi-mode. Figure 13 shows the typical geometry of a single-mode and a multi-mode fiber. Due to

the differing diameter of the two cores, the manner in which the signal will pass through the fiber

is very different [2].
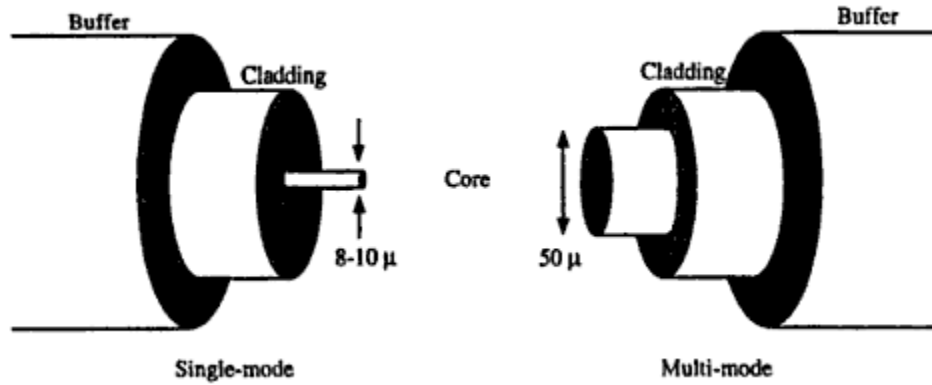
Figure 13: Typical Optical Fibers [13]

An example of how the signal travels through a multi-mode fiber is show in Figure 14.

One of the paths is straight down the middle, but in the other paths the signal is continually

reflected back and forth within the core as it travels down the fiber. The reflected signal has a

longer path to follow than the direct path. This creates some distortion at the output of the fiber

as the same signal will arrive at the end at slightly differing times [14].
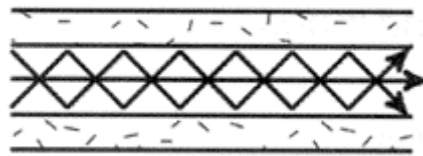
Figure 14: Multi-mode Signal Path [14]

In some applications this amount of distortion may be acceptable, but not for all. One

method of avoiding this distortion is to use a single-mode fiber. The path the signal will follow

down a single-mode fiber is shown in Figure 15. Because the core of the single-mode fiber is

much smaller, there is only one path for the light to follow, yielding a cleaner signal [14].
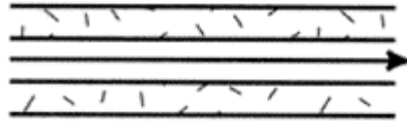
Figure 15: Single-mode Signal Path [14]

There are also some special optic fibers that are fabricated such as polarization maintaining fiber. In order for an optic fiber to maintain polarization, stress within the fiber must not change. This is accomplished by using stress rods; however, bends in the fiber significantly degrade the ability to maintain the polarization. Figure 16 shows an end view of the three types of fiber that have been discussed. The illuminated portion in the center of each fiber is the core. The single-mode core is much smaller than that of the multi-mode fiber. The rightmost image in Figure 16 illustrates the rods on either side of the core that are used to avoid changes in stress within a polarization maintaining fiber [2].
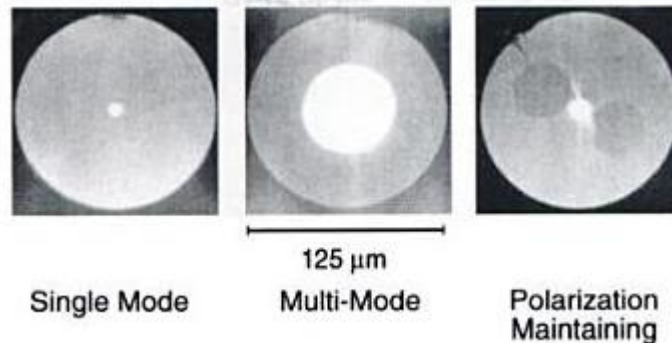
Figure 16: End View of Three Different Types of Fiber [2]

It is also important to consider the wavelength of the laser that is being used to modulate the signal that is launched into the fiber. As was mentioned earlier, lasers are available in several different wavelengths. Attenuation of the fiber changes with the wavelength that the laser uses. Figure 17 is a plot of the wavelength of the laser versus the fiber attenuation. Three wavelengths that have been used extensively in optics are 0.85 μm, 1.30 μm, and 1.55 μm. The 0.85 μm wavelength was primarily chosen because it was widely available in laser diodes when the first

fiber optic links were made. From the figure it is clear why 1.30 μm and 1.55 μm have been

chosen, since the desire of the fiber is to preserve the signal as best as possible [2].
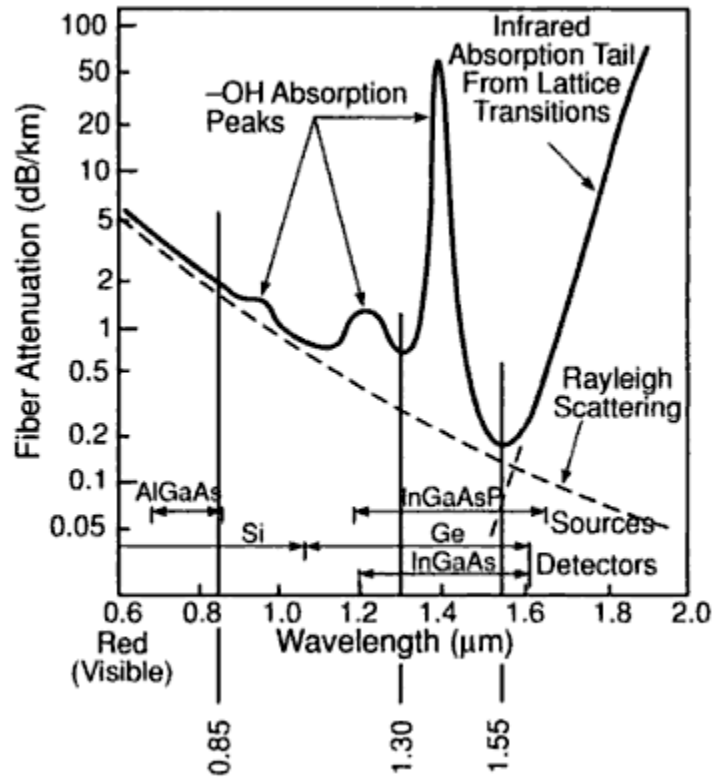
Figure 17: Attenuation vs. Wavelength [2]

While attenuation is very important when deciding frequency, it is not the only factor.

The ultimate goal of the fiber is to transmit the signal as uncorrupted as possible, which means

the signal should not be degraded significantly by dispersion either. Conventional optical fibers

have zero dispersion at a wavelength of 1.3 μm, but if 1.55 μm was used on this fiber, dispersion

could become a problem. One solution to this problem was the development of dispersion

flattened fiber. With this type of fiber the dispersion remains relatively flat between 1.3 μm and

1.55 μm wavelengths, but it is still not perfect. If the desire is to use a wavelength of 1.55 μm

(due to the lowest attenuation), a dispersion shifted fiber is made which has zero dispersion when

using a 1.55 μm wavelength laser. This fiber will take advantage of the lowest attenuation

available as well as avoid major dispersion. A plot of dispersion versus wavelength is shown in Figure 18 for conventional, dispersion flattened, and dispersion shifted fiber [13].
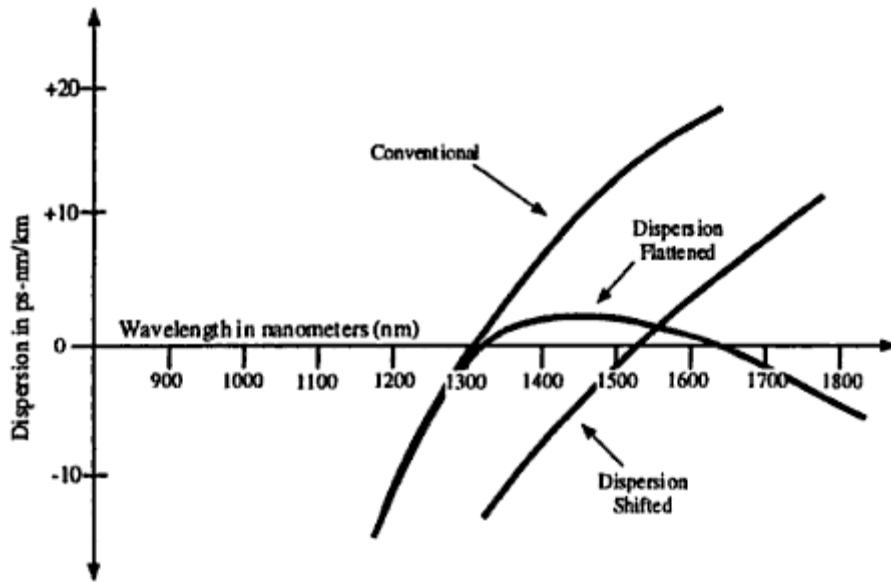
Figure 18: Dispersion vs. Wavelength for Three Types of Fiber [13]

When designing a fiber optic link, the optical fiber that is chosen has to be a major consideration. As with many designs, there needs to be a balance between the cost of the fiber and the performance that needs to be achieved.

2.2.2.3 Photodetectors

The intensity modulated optical signal that is transmitted by the optical fiber is of no use unless it can be converted back to an RF signal. This conversion must also be done efficiently so as not to significantly attenuate or distort the signal. A photodetector made from a semiconductor material is able to accomplish this task. For an optical signal with a wavelength of 0.85 μm the semiconductor used is typically silicon, whereas, for a wavelength of 1.30 μm or 1.55 μm, it is germanium or indium-gallium-arsenide. These materials were chosen for this purpose for three main reasons: they can absorb an optical wave, they can transport the absorbed energy to an external circuit, and they can be easily constructed as a structure. The most

26

common photodetector used for this application is the p-intrinsic-n (PIN) photodiode. It consists

of three main layers (shown in Figure 19). The p-layer has an excess of positive holes carriers,

the n-layer has an excess of negative electrons carriers, and the I-layer is undoped. The

absorption of the optic signal occurs in the I-layer [2]. There is also an anti-reflection coating to

avoid reflections of the optical signal back through the fiber. This is shown as the green layer in

Figure 19 [15].
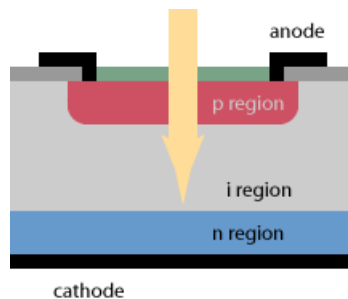
Figure 19: PIN Photodiode [15]

For this application, a PIN Photodiode is operated with a few volts of reverse bias. This

can be seen in Figure 20.
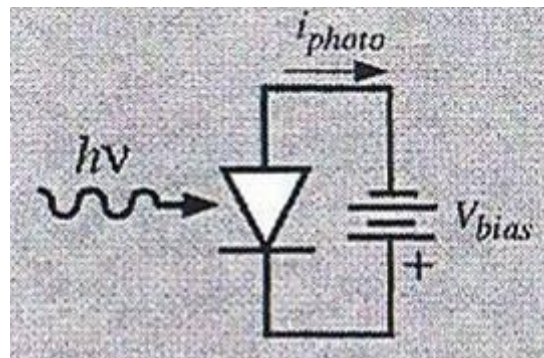
Figure 20: Reverse Biased Photodiode [13]

The actual value is of this voltage can vary slightly with little effect on the output current of the

photodiode. Figure 21 shows several curves, each corresponding to a different optical power that

the photodiode is receiving.
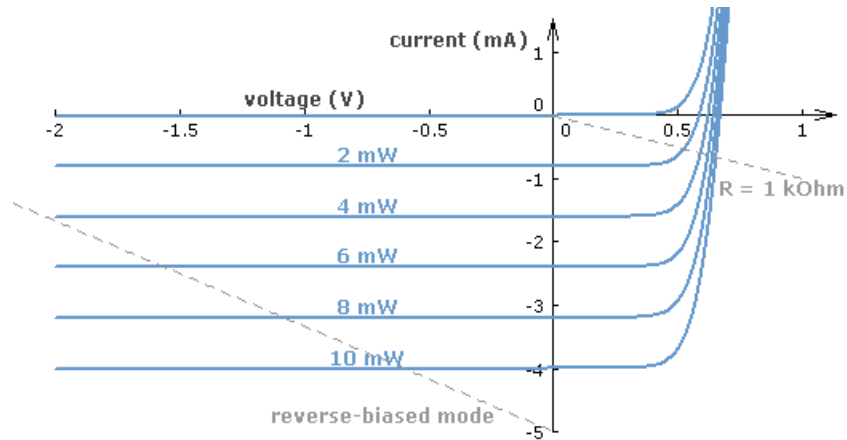
Figure 21: Characteristic Curve of Photodiode [16]

If the photodiode is operated with zero bias there will be no photo-generated current when there is no optical power present, but an increase in the optical power does not cause a linear increase in the output current. This will cause distortion of the signal. If a positive bias is used, the bias current will be much greater than the photo-generated current and thus will be hard to detect. If operated in the negative bias region of the photodiode, when the optical power is zero there will be no photo-generated current (which is desired). Also, as the optical power increases, the photo-generated current will increase very linearly [16]. A plot of photo-generated current versus optical power for a reverse bias photodiode is shown in Figure 22.
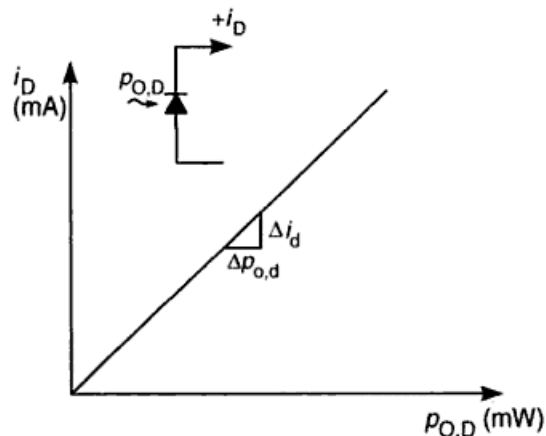
Figure 22: Current vs. Optical Power of PIN Photodiode [2]

28

Clearly, photo-generated current changes linearly with optical power. The slope of this line is known as the responsivity of the photodiode and is the ratio of photo-generated current to optical power. The responsivity of a photodiode can be calculated using the following expression [2]:

$$r_D = \frac{\eta_D q \lambda_0}{hc} \tag{12}$$

where,

r_D = total photodiode responsivity (A/W),
η_D = external quantum efficiency of photodiode.

The photo-generated current can then be calculated from the following expression:

$$i_d = r_d p_{od} \tag{13}$$

where,

i_d = photodiode current (A),
r_d = small signal photodiode responsivity (A/W),
p_{od} = optical power detected by photodiode (W).

The output power (RF power) can also be calculated using the photo-generated current and the load resistance [2].

$$p_{load} = i_d^2 R_{LOAD} \tag{14}$$

where,

p_{load} = power delivered to load resistance connected to photodiode (W),
R_{LOAD} = load resistance connected to photodiode (Ω).

Simply substituting (13) into (14), we then show the output power based on the responsivity of the photodetector and the optical power being delivered to the photodetector. The resultant is shown as equation 15 [2].

$$p_{load} = r_d^2 R_{LOAD} p_{od}^2 \tag{15}$$

One interesting note to make at this point is that the converted RF power is related to the square of the optical power, as defined by (15). Due to this relationship, a 1dB loss of optical power will become a 2dB loss of RF power [17].

When choosing a photodetector to be used in an analog optic link it is important to consider the wavelength of the laser that is used to generate the signal as well as the conversion efficiency that is required of the photodetector. For some applications a weaker signal may be sufficient, but for many applications it is important to receive as much of the signal as possible because an inefficient photodetector may lose important information.

Chapter 3: System Requirements and Analysis

The primary goal of this project was to examine the feasibility of using an analog optical link in the transmission of the received signal in a radar receiver chain. In order to conduct this feasibility study, the radar receiver chain in its current form had to be analyzed appropriately. Once such an analysis was conducted, a comparison between analog optical links and coaxial cable had to be done from both an economic and technical perspective to determine whether or not it was worth considering the usage of an analog optical link given certain possible performance benefits.

3.1 Radar Receiver Specifications

The primary specification that had to be met in this project was to maintain a radar receiver instantaneous dynamic range of at least 50 dB. Instantaneous dynamic range is defined as the difference between P1dB, which is the point where the output signal starts to saturate, and the minimum detectable signal (MDS), or in this case, the noise floor of the system.

$$DR = P1dB - MDS \qquad\qquad (16)$$

where,

DR = instantaneous dynamic range (dB),
$P1dB$ = system signal compression point (dB),
MDS = minimum detectable signal (dB).

In order to meet this specification, an analysis of what instantaneous dynamic range was currently being achieved by the radar receiver with the coaxial transmission line in place had to be done [17].

The ADC in the current radar receiver chain had 14 bits of resolution, which corresponds to an instantaneous dynamic range of 84 dB since 1 bit of resolution is approximately equal to 6

dB of dynamic range. The specification for the ADC stated that the three least significant bits (LSB) had to be reserved for the noise floor. The AGC prior to the ADC would never allow the received signal to reach a level corresponding to the most significant bit (MSB) of the ADC either. This meant that the currently used ADC only had an effective instantaneous dynamic range of 60 dB yielding 10 bits of resolution.

What the radar receiver was achieving prior to the ADC was an instantaneous dynamic range of 79 dB. However, since inputting a signal with such a dynamic range into the ADC would cause signal saturation, the AGC inside the receiver effectively prevents the received signal from reaching a power level corresponding to the most significant bit of the ADC.

The second specification that had to be met in this project had to deal with radar sensitivity. Given a certain signal-to-noise ratio (SNR) for a target at a given distance, it can be seen whether the appropriate sensitivity is achieved for the radar receiver.

$$SNR = \frac{P_{pk} PL \lambda^2 G^2 RCS}{(4\pi)^3 R^4 KTL} \tag{17}$$

where,

SNR = signal-to-noise ratio,
P_{pk} = radar peak power (W),
PL = pulse length (s),
λ = wavelength of radar signal (m),
G = radar gain,
RCS = target cross section (m^2),
R = range from radar to target (m),
K = Boltzmann's constant (1.38×10^{-23} J/K),
T = noise temperature (K),
L = transmit path and receive path losses.

The variable that was of concern in this project was the noise temperature T, since ultimately this was the primary variable impacted by modifying the transmission line used in the receiver

side of the radar system. Noise temperature can be defined in terms of cascaded noise factor, a concept which will be discussed further in depth in Section 3.2.

$$T = (F - 1) * 290 \qquad \textbf{(18)}$$

where,

F = noise factor.

In order to control the noise temperature, the noise factor of each device in the receiver of the radar system has to be considered as part of a larger cascaded system. By changing the coaxial cable transmission line to an analog optical link, this can have an impact on the overall cascaded noise factor, therefore changing the noise temperature of the entire system. Given the current system in place, the overall noise temperature of the radar receiver system is 307 K. The SNR that corresponds to this noise temperature can be calculated using the values shown in Table 1.

Table 1: Radar Values for SNR Calculation

PARAMETER	VALUE	UNITS	dB
PEAK POWER	**100,000**	Watts	50.00
PULSE LENGTH	**0.001000**	Seconds	-30.00
WAVELENGTH	0.030	Meters	-15.23
GAIN	663,457		58.22
RCS	1	M^2	0.00
RANGE	**1,000,000**	Meters	60.00
TEMPERATURE	307	K	24.87
LOSSES	2.51		4.0
(4*pi)^3	1,984		32.98
K (Boltzman)	1.38E-23	Joules/K	-228.60
SNR			32.74

The result of using these values as inputs to (17) is an SNR of approximately 33 dB.

The noise temperature of the receiver chain is largely dependent on the link that is used. Since cascaded noise temperature of the chain as a whole is dependent on the noise figure and gain of each of the components, which for this analysis is a set value for all of the components except the link itself, a plot of the cascaded noise temperature values is shown in Figure 23 for various gain and noise figure combinations of the link. The drop-off that is seen after the gain

reaches -10 dB is due to the fact that the receiver chain is built around a coaxial cable which has

a loss of 10 dB. In order to avoid saturating the receiver, attenuation is added before the link if

the gain is greater than -10 dB such that the total gain of the attenuator and the link is equal to -

10 dB. Adding this attenuation before the link increases the cascaded noise figure of the link, a

concept which is explained later in Section 3.2. That is, the data shown in Figure 23 is purely

based on using a link until -10 dB of gain is reached. Once this point is reached, the data

represents what link noise figure and gain would be required for the corresponding noise

temperature value assuming an attenuator is inserted prior to it in order to maintain a net gain of -

10 dB. The same applies to Figure 25.
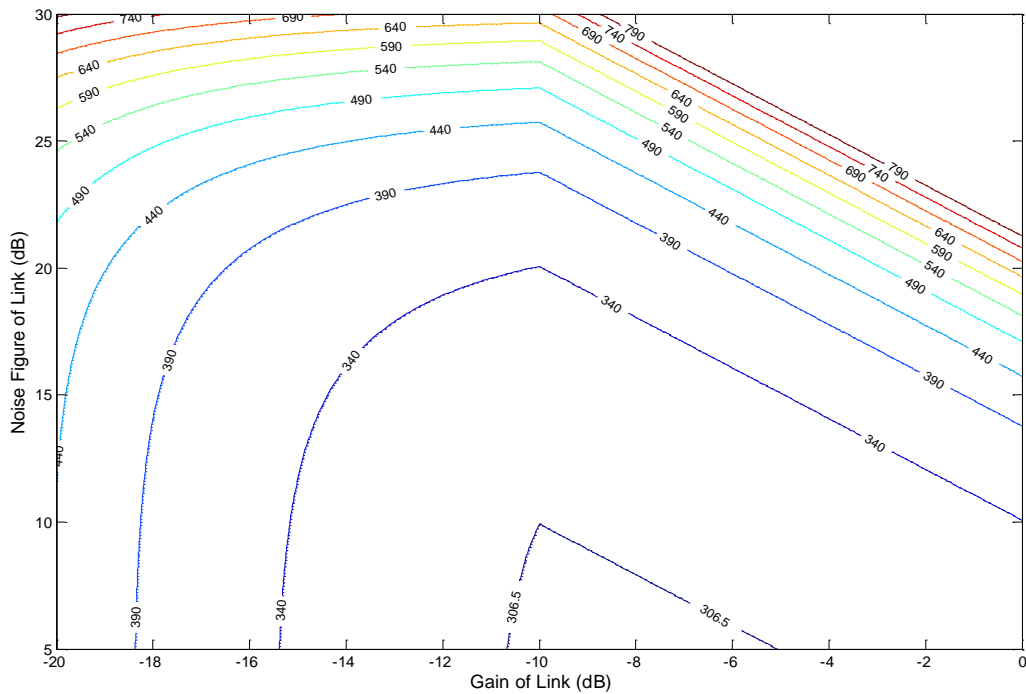
Figure 23: Overall Noise Temperature of Receiver (K) for Various Link Noise Figure and Gain Combinations

It is also important to know what noise temperature is required to achieve the desired

SNR for the specified target. A plot of SNR versus noise temperature is shown in Figure 24.
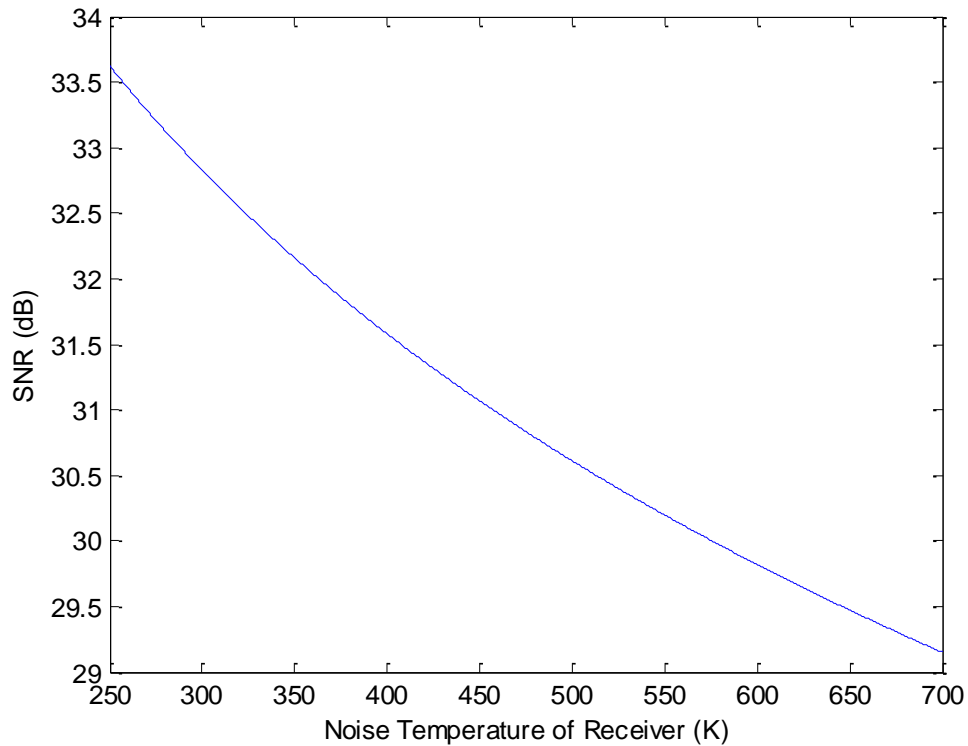
Figure 24: SNR for 1 m^2 Target at a Distance of 1000 km vs. Noise Temperature

Finally, it is important to plot the SNR for the specified target that is achieved for various configurations of the link. The plot shown in Figure 25 is of the SNR for the specified 1 m^2 target at a distance of 1000 km based on the noise figure and gain of the link. Once again, the drop-off that is seen after the gain reaches -10 dB is due to the attenuation that must be added before the link to ensure the overall gain of the link does not exceed -10 dB. If such attenuation were not added, the receiver would become saturated for large signals.
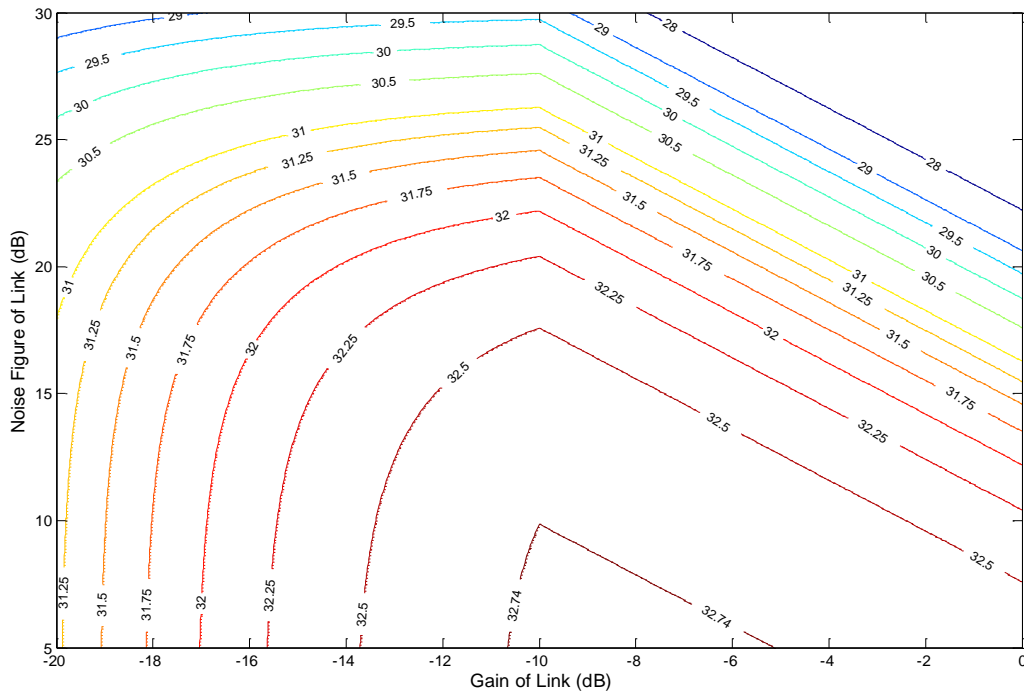
Figure 25: SNR (dB) for 1 m² Target at a Distance of 1000 km for Various Link Noise Figure and Gain Combinations

3.2 Comparison of Analog Optical Links and Coaxial Cable

As was mentioned previously, coaxial cable at a distance can have very high signal attenuation. This prevents the radar back-end receiver hardware from being remoted a significant distance away from the antenna. One possible solution to this problem is to substitute the coaxial transmission line between the LNA and the ADC of the radar receiver with an analog optical link. The main advantage provided via the usage of an analog optical link is the ability to achieve a much greater remoting distance away from the antenna without significantly attenuating the signal. This is primarily due to the fact that fiber optic cable has very low signal attenuation at a distance. A direct comparison of attenuation vs. frequency for typical electric cabling and fiber optic cabling can be seen in Figure 26 [2].

36
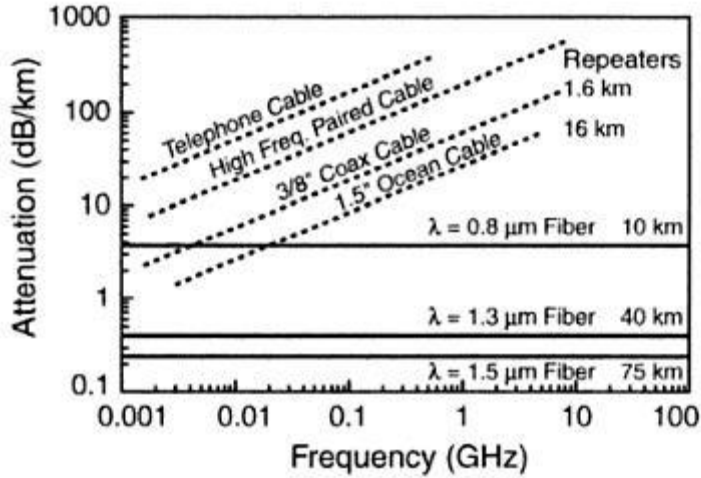
Figure 26: Attenuation vs. Frequency [2]

It is important to note in this case that the data plotted in Figure 26 applies to systems that utilize

repeaters, and therefore does not contradict the data presented in Figure 3. Having considered

the low loss that can be achieved with fiber optic cable, one might be led to think that the

solution to the problem is therefore obvious. However, the performance of an analog optical link

is very heavily dependent upon the optical transmitter and the optical receiver. This idea is

reinforced by the graph shown in Figure 27.
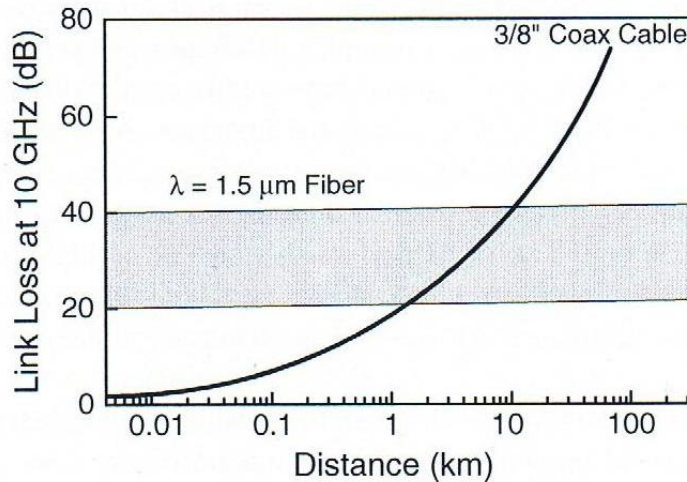
Figure 27: Loss vs. Length at 10 GHz [2]

Even though coaxial cable attenuation increases much faster than fiber as a function of distance (at 10GHz), the intrinsic analog optical link loss sets a lower bound on the total link loss. This loss is primarily due to the fact that the modulation and photodetection circuits in this specific link are not very efficient in converting between RF and optical power. Only when these inefficiencies are successfully overcome, especially at distances less than approximately one kilometer, can the designer finally justify the usage of an analog optical link. Otherwise, given such inefficiencies, the applications where analog optical links can be used are strictly limited to those that require distances greater than approximately ten kilometers of transmission distance. It is important to note that the data in Figure 27 dates back to 2004, so in general, analog optical links to date may perform better on average, but the same fundamental problem of conversion inefficiency still is a major determining factor in justifying the usage of an analog optical link over a coaxial transmission line, especially over short distances [2].

From an economic perspective, one has to consider that the bulk of the cost of an analog optical link will mostly be dependent upon the transmitter and receiver since low loss fiber optic cable is extremely inexpensive compared to low loss coaxial cable. Figure 28 represents a cost comparison of the currently used coaxial cable vs. a typical 100MHz to 11GHz analog optical link.
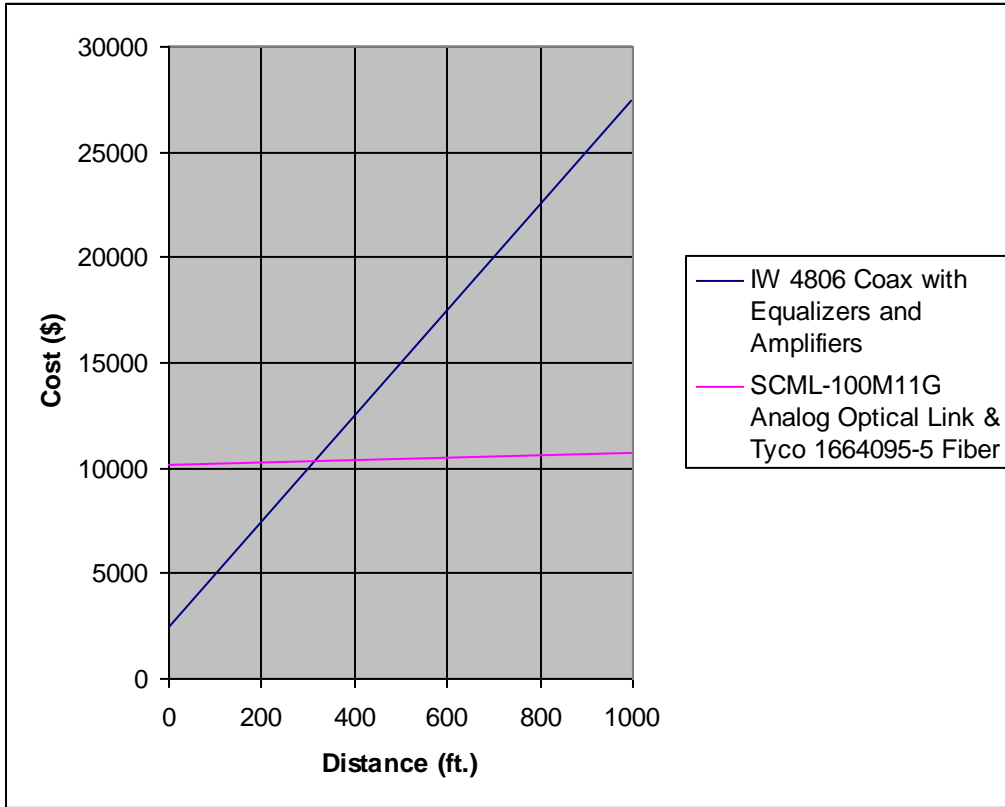
Figure 28: Cost Comparison of Coax vs. Analog Optical Link

The data in Figure 28 is based on IW 4806 coaxial cable [20] which costs approximately

$25/foot, repeater equipment in the coaxial transmission line that costs approximately $2,500 in

total, the MITEQ® SCML-100M11G analog optical transmitter which costs $8,250, the

MITEQ® SCML-100M11G analog optical receiver which costs $1,900, and Tyco 1664095-5

single mode fiber which costs $0.54/foot. At distances less than approximately 300 feet, coaxial

cable is the cheaper alternative. Once the transmission line extends beyond 300 feet though, the

cost of coaxial cable rises at a significantly higher rate than that of the analog optical link.

Therefore, the designer has to judge whether or not the performance benefits, if any, of using an

analog optical link at a distance of less than 300 feet outweigh the fact that coaxial cable is the

cheaper alternative.

One of the major disadvantages of coaxial cable to consider when making such a decision is that the loss per unit of distance tends to rise significantly with frequency due to the skin effect, which is the tendency for electrical current to reside purely on the conductor surface as frequency rises, therefore reducing the effective conductor cross sectional area, and thus in turn increasing the effective resistance of the conductor. The consequences of such an effect can be seen for the IW 4806 cable in Figure 29 [18] [19].
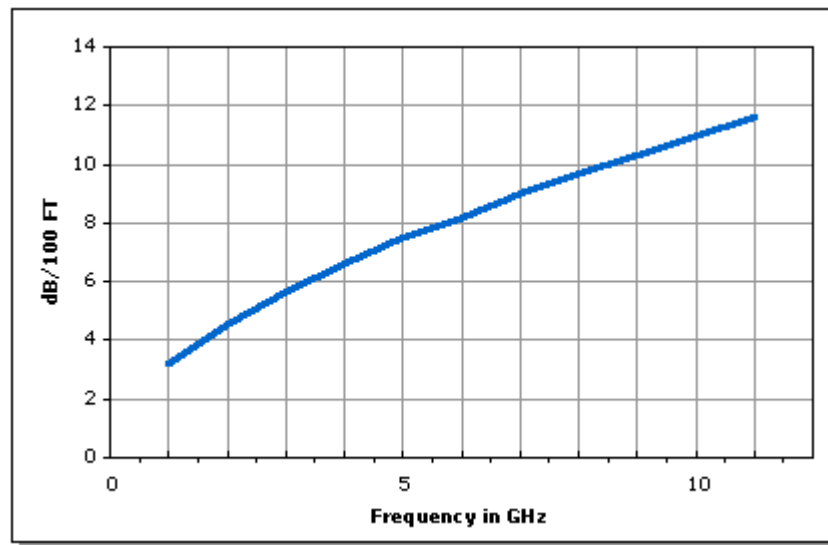
Figure 29: IW® 4806 Loss/100 ft. vs. Frequency [20]

Taking this data and replicating it over a 1GHz bandwidth centered at 10GHz for multiple distances yields the data shown in Figure 30.
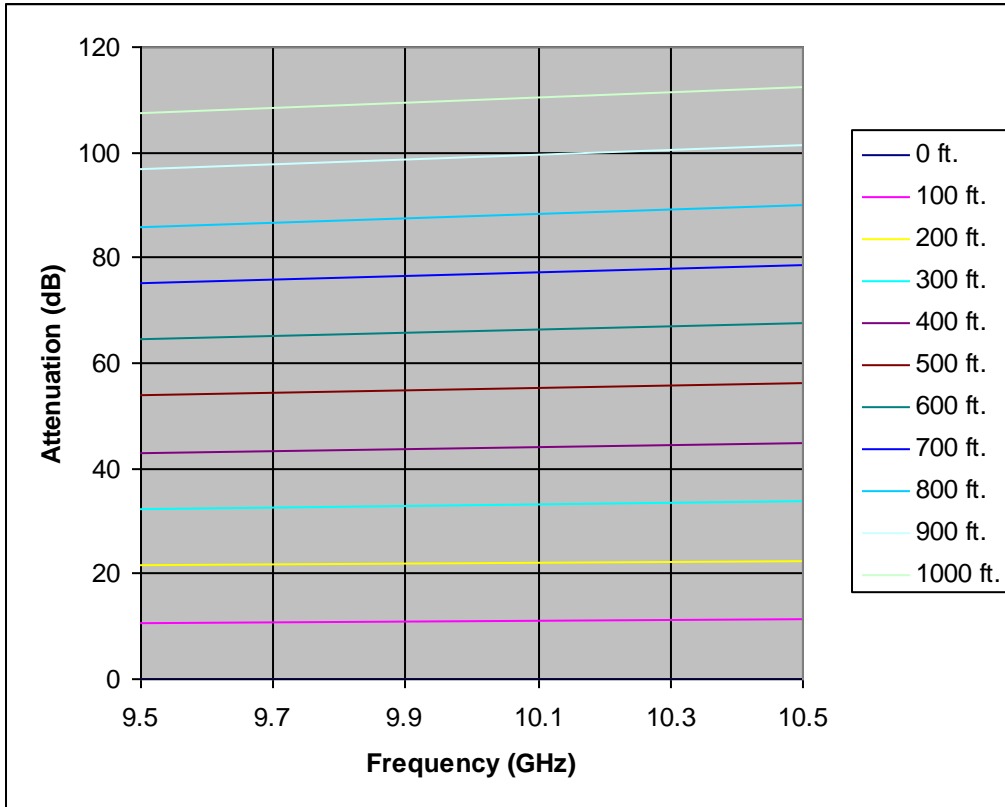
Figure 30: Attenuation vs. Distance for IW® 4806

In order to emphasize the rising attenuation slope of coaxial cable at increasing distances, Figure 31 shows relative attenuation at each distance for the IW 4806 coaxial cable. It should be noted that each set of data represented in Figure 30 and Figure 31 is in both cases an approximation of the data shown in Figure 29.
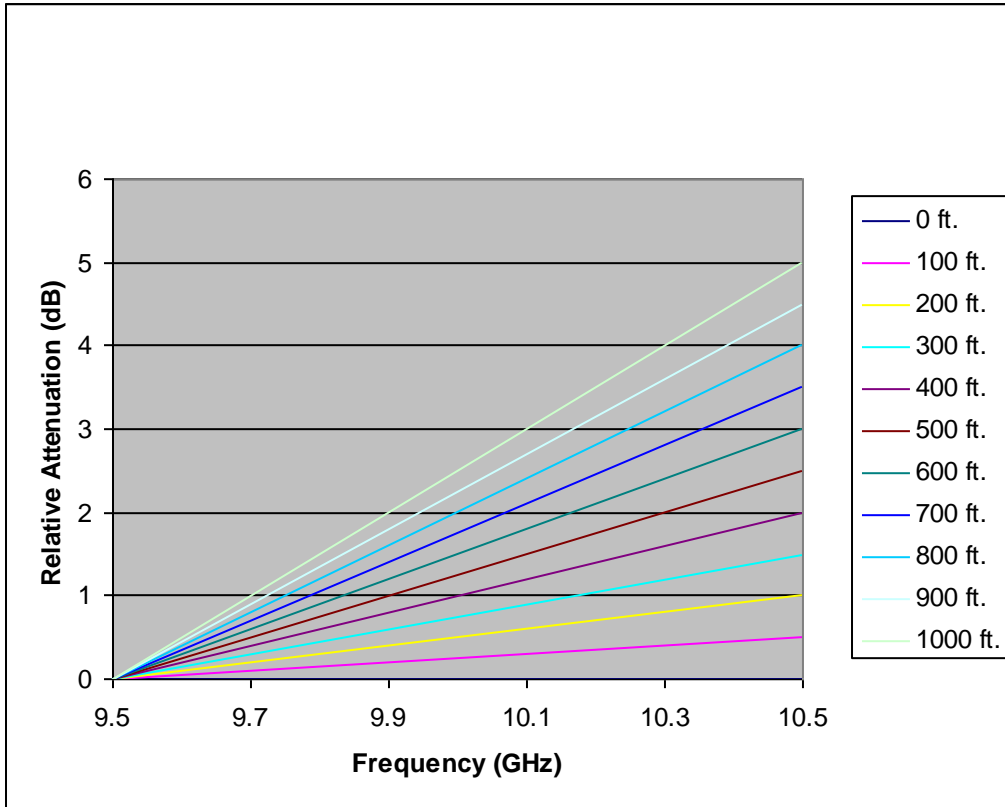
Figure 31: Relative Attenuation vs. Frequency for IW® 4806

This means, given all other variables are ideal, the received radar signal amplitude is not unity over a given signal bandwidth. This effect becomes even more pronounced as the distance increases. Therefore, amplitude equalizers, which are devices that serve the purpose of reducing or increasing the power at certain frequencies, have to be inserted into the transmission line. This ends up contributing to a significant amount of the overall cost of the coaxial transmission, especially at a short distance.

Optical fiber does not experience the skin effect since it transmits light, not electrical current. This is not to say that there are no wavelength dependent losses in optical fiber. One might be led to ask how bandwidth dependent attenuation/distance could be an issue if all that is being transmitted is one wavelength of light [2]. The reality is that all lasers generate more than one wavelength of light [21]. The relationship between attenuation/distance and wavelength for

silica optical fiber is shown in Figure 17. It can be seen from this data that the degree to which the attenuation/distance varies with wavelength in single mode fiber is practically negligible compared to that of coaxial cable given a transmitter such as the MITEQ® SCML-100M11G which can vary in output wavelength from 1530 to 1560 nm. Even aside from this fact though, Tyco 1664095-5 fiber, which represents a typical single mode fiber, is quoted as having an attenuation of 0.5 dB per km, whereas the IW 4806 coaxial cable attenuation is at least 328 dB per km for the bandwidth of interest. Simply put, any attenuation/distance variation for optical fiber is going to be negligible when compared to coaxial cable attenuation/distance over the same distance for the same bandwidth [2].

Once again though, the designer also has to consider that the optical transmitter and optical receiver losses could be greater than the coaxial losses at shorter distances. This is not always the case though given the current state of the art for analog optical links. In fact, based on what was advertised by MITEQ®, analog optical links tend to have net positive gain. The reason that such a net positive gain is achievable is due to external amplifiers being added in addition to the modulator, the fiber, and the photodetector. What this suggests is that the cost of an analog optical link can be significantly reduced by removing such external components from the design, but at an expense to the overall noise figure and intrinsic gain. To better realize this, the general form of noise figure is defined in (19), and intrinsic gain is defined for a directly modulated link in (20) and an externally modulated link in (21) [2].

$$NF = 10\log\left(1 + \frac{n_{add}}{g_i n_{in}}\right) \tag{19}$$

where,

NF = noise figure (dB),
n_{add} = noise contribution of the device (W),
n_{in} = input noise (W).

$$g_{iDM} = \frac{s_\ell^2}{R_{IN}} r_d^2 (R_{LOAD}) T_{MD}^2 \tag{20}$$

where,

g_{iDM} = intrinsic gain of directly modulated link (RF gain),
T_{MD} = linear ratio representing power losses in optical fiber,
R_{IN} = input resistance of entire transmitter including any diode laser matching resistance (Ω).

$$g_{iEM} = \frac{s_{mz}^2}{R_S} r_d^2 (R_{LOAD}) T_{MD}^2 \tag{21}$$

where,

g_{iEM} = intrinsic gain of externally modulated link (RF gain),

It is important to note that noise figure is inversely proportional to intrinsic gain because in a cascaded system, higher gain at the input results in a better overall noise figure for the system. This can be seen by first defining noise factor, which is the linear equivalent of noise figure and is defined as follows [2]:

$$F = 1 + \frac{n_{add}}{g_i n_{in}} \tag{22}$$

Once noise factor for a single device is defined, the result can be applied to a cascaded system as defined by the following expression.

$$NF = 10\log\left(F1 + \frac{F2-1}{G1} + \frac{F3-1}{G1G2} + \frac{F4-1}{G1G2G3} + ...\right) \qquad \textbf{(23)}$$

where,

$F1$ = noise factor of first component from input,
$F2$ = noise factor of second component from input,
$F3$ = noise factor of third component from input,
$F4$ = noise factor of fourth component from input,
$G1$ = gain of first component from input,
$G2$ = gain of second component from input,
$G3$ = gain of third component from input.

By inserting LNA's at the input of the analog optical link, the overall noise figure and attenuation can in fact be reduced significantly. Once again though, such performance improvements come at a fairly steep cost as quality LNA's are not without cost [2].

Given a commercially available link such as the MITEQ® SCML-100M11G, for the purpose of long distance signal transmission, it is difficult to justify the usage of coaxial cable over an analog optical link. If the designer wishes to reduce costs at the expense of gain and noise figure, the best option would be to design an analog optical link from separately purchased components rather than to purchase a pre-packaged link. At shorter distances though, this would simply be achieving the same end as using lower quality coaxial cable which would be cheaper and have higher attenuation. At long distances, however, an analog optical link designed in this way would still be the better option from both a performance and cost perspective if the designer is primarily concerned with dynamic range. This is due to the extremely low attenuation achievable with optical fiber over long distances. Table 2 summarizes the tradeoffs between using an analog optical link vs. coaxial cable [2].

Table 2: Tradeoffs between Analog Optical Links and Coaxial Cable

	Coaxial Cable	Analog Optical Link
Advantages	Less expensive for shorter distances, typically has lower attenuation than analog optical links at shorter distances (assuming no external circuitry in the analog optical link)	Less expensive for longer distances than coaxial cable, can have lower attenuation than coaxial cable at all distances (assuming external circuitry in the analog optical link), has a virtually constant attenuation/distance slope over all distances given a 1310 nm or 1550 nm laser with a reasonably narrow output spectrum
Disadvantages	More expensive and may have higher loss than analog optical links, especially at longer distances, has an attenuation/distance slope that can rise steeply at increasing distances for a given bandwidth	More expensive at shorter distances, typically has higher loss than coaxial cable at shorter distances (assuming no external circuitry in the analog optical link)

Chapter 4: Simulated and Experimental Results

There were three primary deliverables for this project. The first was the development of modeling tools that were produced in order to simulate the receiver side of a radar system. These simulation tools can be applied purely at the link level, or at the link component level. The second was the testing of the MITEQ® LBL-10M4P5G analog optical link. The link was tested using a network analyzer first to determine that it met specification. Once this was completed, the link was tested using different lengths of optical fiber to observe the length effect on the analog optical link attenuation. The third deliverable was to design an analog optical link at the component level that would satisfy the design specifications of the radar receiver chain.

4.1 Modeling

In order to determine if an analog optical link was capable of accomplishing the desired task, a model had to be created to give a tool for testing values. The main focus of the model was on gain, saturation, noise figure, and dynamic range of the receiver chain that was shown in Figure 1 (page 5). This model was created using MATLAB®. (An initial attempt was made to use Simulink® for the model but it was later decided that more control could be had over the models using MATLAB®.)

The main function of the model, is called "Radar Receiver," When called, it begins by asking the user how the main signal should be setup. The user is requested to enter the frequency of the main signal (10 GHz for the purpose of this project) and the power level of the signal. The user is then asked for parameters of the front-end losses, the LNA, the link, and the receiver, respectively. After each of these, the user is asked if they want to see a plot of the current time domain signal and amplitude spectrum.

The front-end losses are defined by the loss of the received signal before it reaches the LNA. The parameters asked for are the gain and noise figure of these losses. Since this describes insertion loss, the gain entered should be a negative number. The LNA parameters the user is asked to enter are the gain, P1dB, and the noise figure. Once the signal passes through the LNA it reaches the link (which this project is trying to improve).

The user is given four different choices as to how the link will be specified. These choices are to use a coaxial cable, a direct modulation analog optical link at the component level, an external modulation analog optical link at the component level, and an analog optical link at the link level (such as an off the shelf link). Depending on the choice made, a different set of parameters will be requested of the user. The coaxial cable option simply asks for the gain and the noise figure of the link. If either the direct or the external modulation analog optical link is selected, several more parameters are asked for. In the direct modulation case the user is asked to enter the RIN of the transmitter, laser slope efficiency, laser bias current, laser threshold current, fiber attenuation, fiber length, and photodiode responsivity. For the external modulation case the user is asked for total excess modulator loss, V_π, DC bias voltage of the modulator, optical output power from CW laser, fiber attenuation, fiber length, and photodiode responsivity. The final option, link level analog optical link, was created to model a prebuilt link for which the gain, P1dB, and noise figure are all known. This was used to model commercially available links within the receiver chain.

The final component the signal must go through is the receiver. The parameters of interest for the receiver were the gain, P1dB, and noise figure. Since the receiver consists of several components, including mixers which translate the frequency of the signal, the user is also

asked to enter the frequency of the signal that the receiver outputs as well as the new bandwidth

of the system. Values for the current system are shown in Table 3.

Table 3: Set Values for System

Component	Parameter	Value
Front End Losses:	Gain (dB)	-1
	Noise Figure (dB)	1
	System BW (GHz)	1
LNA:	Gain (dB)	30
	Output P1dB (dBm)	10
	Noise Figure (dB)	2
	System BW (GHz)	1
Coaxial Link:	Gain (dB)	-10
	Noise Figure (dB)	10
	System BW (GHz)	1
RCVR:	Gain (dB)	10
	Output P1dB (dBm)	10
	Noise Figure (dB)	7
	Output Freq (MHz)	70
	System BW (MHz)	20

Since the system has been designed around a 10 dB loss from the link, it is important to

maintain this same loss even when replacing the coaxial link with an analog optical link. In

order to achieve this, since the analog optical link will most likely have a gain greater than -10

dB, attenuation must be added either directly before or directly after the link. It is also important

to ensure that a power of 0 dBm can be delivered to the receiver from the output of the link,

which limits the amount of attenuation that can be added after the link. When the link level

analog optical link is selected the user will be presented with the option to add attenuation before

and/or after the link. If either one of the component level links is selected the program will

automatically add the appropriate attenuation to the system based on the gain and P1dB values

returned from the component level models. It first uses the P1dB value to determine the

maximum attenuation that can be added after the link, since there are advantages to having the

attenuation later in the chain (explained in Modeling Noise Figure section), and then adds the

remaining necessary attenuation before the link.

The main function of the model calls on several different functions to accomplish the

processing of the signal based on the entered parameters. The following sections will discuss the

various code modules that were used to accomplish the desired functionality.

4.1.1 Modeling Gain

The signal that is being passed through the chain is a voltage. Since gain is specified in

dB the gain function begins by converting the specified gain to a linear gain in terms of voltage.

This was accomplished using the following expression:

$$G_V = 10^{\frac{G_{dB}}{20}} \tag{24}$$

where,

G_{dB} = User specified gain (dB),
G_V = Linear gain in terms of voltage.

The signal entering the component was simply multiplied by G_V to obtain the new signal with

the appropriate gain. It was important to consider the fact that even though a component has a

certain gain, this gain is not achievable when the signal power levels become too high. This was

considered in the saturation code module.

4.1.2 Modeling Saturation

One limitation of a component that needs to be considered is the saturation. Within the

main function of the model the user is asked for P1dB of several of the components. This is the

point where the gain will begin to drop off, but since this was first order modeling, it was viewed

as a strict cutoff. P1dB is given as an average output power in dBm. This was converted to a

peak voltage using:

$$V_{pk} = \sqrt{50 \left(10^{\frac{(P1dB-30)}{10}} \right)} \sqrt{2} \qquad\qquad (25)$$

where,

V_{pk} = Peak voltage (V),
$P1dB$ = User specified P1dB (dBm).

The code module will then take the signal and change any values above V_{pk} to V_{pk}. Also, any

values below $-V_{pk}$ are changed to $-V_{pk}$.   The signal generated after this will resemble

something between a sine wave and a square wave depending on how much it has been clipped

by. The peak voltage that was calculated using (25) should be the peak of the fundamental

frequency, not necessarily the peak of the signal. For a sine wave the peak of the fundamental

frequency is the same as the peak of the signal, but not for a square wave. The peak of the

fundamental frequency of a square wave is actually $4/\pi$ greater than that of the square wave itself

[22]. This means that if the signal is significantly clipped (such that it more closely resembles a

square wave) according to the calculated peak voltage the power of the fundamental will actually

be stronger by a factor of $4/\pi$. This needed to be accounted for because, after clipping occurs,

the signal would be something in between a square wave and a sine wave, but neither exactly, it

needed to be clipped somewhere in between the calculated V_{pk} and $\frac{\pi}{4}V_{pk}$. The clipping function

begins by clipping the signal at V_{pk} and then checks to see if the amplitude of the fundamental

frequency is correct. If the amplitude is too large it will then lower the value of V_{pk} iteratively

until it reaches a suitable amplitude of the fundamental frequency.

4.1.3 Modeling Noise Figure

The last of the three main attributes that needed to be modeled was the noise figure. This is essentially the added noise above the thermal noise floor. The noise figure code module begins by calculating the thermal noise floor using:

$$p_t = 10\log(kTB) + 30 \tag{26}$$

where,

p_t = Mean power of thermal noise (dBm)
k = Boltzmann's constant (1.38×10^{-23} J/K),
T = Ambient temperature (K),
B = System bandwidth (Hz).

The bandwidths that were used in the case of this project were 1GHz and 20MHz dependent on where in the system the noise floor was being calculated for. The noise level is then calculated using the thermal noise floor as a starting point. The sum of the previous gains (in dB) is then added to the noise as well as the cascaded noise figure of the system. The cascaded noise figure is the additive noise by the components and is calculated using (23) on page 45. As can be seen from (23), there is a great advantage to having gain, from a LNA, early in the chain of system receiver components. The higher the previous gains, the lower the additive noise of a later component. This is why, if attenuation must be added, it should be added as late in the chain as possible while still achieving the desired results.

Once the thermal noise floor (in dBm), the gain (in dB), and the cascaded noise figure (in dB) of the system have all been calculated they can be added together to find the noise level (in dBm). The noise figure code module will then add the proper noise to the signal at each stage of the system as the user proceeds through.

4.1.4 Modeling Directly Modulated Analog Optical Link

In order to simulate a directly modulated analog optical link, a mathematical model generated by Charles H. Cox, III, was used [2]. This model assumes that the directly modulated link is relative intensity noise (RIN) dominated since this tends to be the case for most directly modulated links. RIN noise is the result of laser output power fluctuations, and is defined as follows [2]:

$$\left\langle i_{rin}^2 \right\rangle = \frac{\left\langle I_D \right\rangle^2}{2} 10^{RIN/10} \Delta f \tag{27}$$

where,

$\left\langle i_{rin} \right\rangle$ = relative intensity noise current (mean value) (A),
$\left\langle I_D \right\rangle$ = photodiode current (mean value) (A),
RIN = relative intensity noise power (dB/Hz),
Δf = system bandwidth (Hz).

The circuit corresponding to this model can be seen in Figure 32.
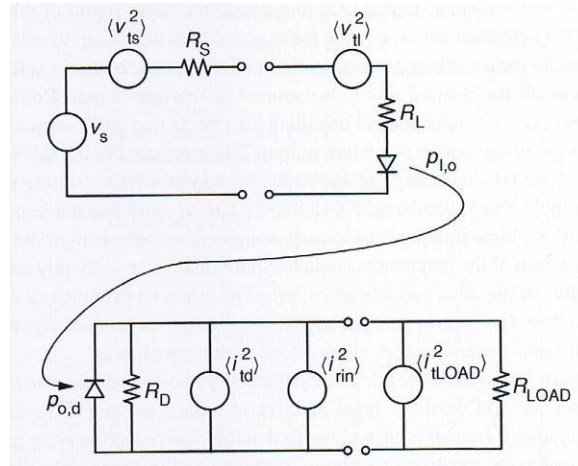

Figure 32: Direct Modulation Model Circuit [2]

All other noise sources in this model are thermal noise sources resulting from individual components (hence the t in the subscripts). For the purposes of this specific model, the thermal noise resulting from the photodiode, $\left\langle i_{td}^2 \right\rangle$, and the thermal noise resulting from the load,

$\langle i_{tLOAD}^2 \rangle$, were excluded due to the fact that it is not uncommon in directly modulated links, for these sources to be dominated by RIN noise. Given these conditions, the noise figure for a directly modulated, RIN noise dominated link is defined as follows [2]:

$$NF = 10\log\left(2 + \frac{\langle i_{rin}^2 \rangle R_{LOAD}}{g_{iDM}\, kT} \right) \tag{28}$$

Since the average photodiode current, $\langle I_D \rangle$, can be derived from the laser bias and threshold currents assuming that it is approximately proportional to laser bias current above threshold, the following assumption was made for the model [2]:

$$\langle I_D \rangle = s_\ell r_d (I_L - I_T) T_{FF} T_{MD} \tag{29}$$

The gain of a directly modulated link was modeled using (20).

P1db of the directly modulated link is by far the most significant limitation of this simulation tool, as it simply relies on an arbitrary user input rather than being derived from intrinsic device properties. For this reason, there was no point to validating this parameter [2].

The direct modulation link simulation tool was then verified using the commercially available MITEQ® LBL-10M4P5G analog optical link for a test simulation. This was more difficult than initially anticipated due to the fact that most commercially produced analog optical links are designed with external components, primarily amplifiers, in an effort to improve performance. Therefore, the advertised performance specifications are usually listed with such external circuitry in mind. Another problem was that component level specifications are not usually disclosed on datasheets for pre-packaged links. After corresponding with an engineer at MITEQ®, the values shown in Table 4 were obtained for the link. MITEQ® stated that the link had been tested using 0.2 dB/km single mode optical fiber, so incorporating fiber losses into the simulation was unnecessary. It should be noted that in the currently coded model, it is assumed

that all resistances are 50 Ω matched and that the ambient temperature is 290 K, although these assumptions can be easily modified by simply uncommenting specific lines of code in the model.

Table 4: LBL-10M4P5G Component Level Specifications

Component	Parameter	Value
LBL-10M4P5G Diode Laser	Slope efficiency (W/A)	0.15
	Threshold current (mA)	12
	Bias current (mA)	70
	RIN (dB/Hz)	-150
LBL-10M4P5G Photodiode	Photodiode responsivity (A/W)	0.85

Using these values as inputs for the simulation, the results were then compared to the link performance specifications shown in 5, assuming no external circuitry and negligible fiber loss for the link.

Table 5: LBL-10M4P5G Expected Values vs. Simulated Values

Component	Parameter	Expected Value	Simulated Value
LBL-10M4P5G Analog Optical Link with no external circuitry and negligible fiber loss	Gain (dB)	-22 to -23	-17.9
	Noise Figure (dB)	45 to 50	43.2

The most likely explanation for the noise figure discrepancy is that the noise figure data provided by MITEQ® was obtained deductively. That is, MITEQ® stated that the noise figure analyzer they normally use cannot measure noise figure over 35 dB, therefore requiring there to be an external amplifier inserted before the link when performing measurements. The noise figure values were therefore obtained partly from analytical prediction rather than pure measurement. MITEQ® stated that these values were an approximation and should range from 40-50 dB. For this reason, the discrepancy of 2 dB is acceptable [2].

As for the gain discrepancy, the most likely explanation is that the simulation did not account for excess losses in the link, which would most likely be coupling losses. It is worth noting that for the coded model, a term representing all other losses in the link, such as coupling and modulator loss denoted as T_{FF} in (29), were included to account for this discrepancy.

However, in Cox's mathematical model of slope efficiency for the direct modulator, defined by (3), there is no such term. Cox does discuss possible coupling losses that exist when using semiconductor lasers though, therefore at least partially justifying its addition in this coded model [2].

Regardless of such discrepancies though, the simulation can at the very least be used for the purpose of first order modeling. The actual simulation can be found in Appendix A [2].

4.1.5 Modeling Externally Modulated Analog Optical Link

In order to simulate an externally modulated analog optical link, once again, a mathematical model generated by Charles H. Cox, III, was used [2]. For this specific model, it is assumed that a Mach-Zehnder modulator is used since it is typically the most commonly used external modulator in industry (at least as of 2004). This model assumes that the dominant noise source for the Mach-Zehnder modulated link is shot noise. Shot noise results from the random arrival of photons at the photodetector. Shot noise is defined as follows [2]:

$$\left\langle i_{sn}^2 \right\rangle = 2q\left\langle I_D \right\rangle \Delta f \tag{30}$$

where,

i_{sn} = shot noise current (A).

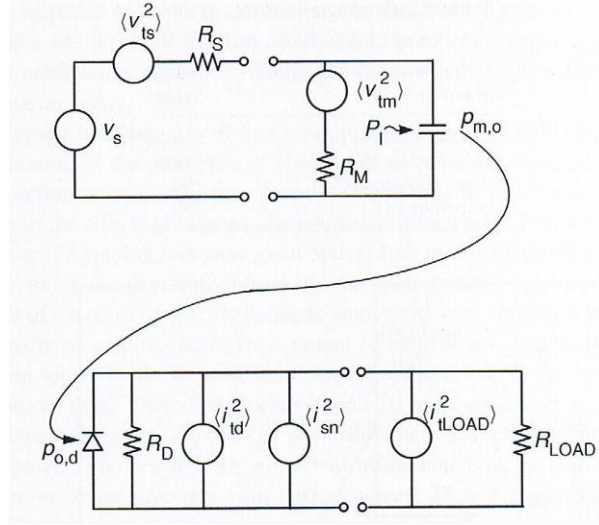The circuit corresponding to this model can be seen in Figure 33.

Figure 33: External Modulation Model Circuit [2]

Once again, all other noise sources in this model are thermal. Since it is assumed that shot noise dominates, as is often the case for externally modulated links, the thermal noise sources can therefore be neglected. Given these assumptions, the noise figure for a Mach-Zehnder modulated link is defined as follows [2]:

$$NF = 10\log\left(2 + \frac{2qI_D R_{LOAD}}{g_{iEM} kT}\right) \tag{31}$$

Since I_D can be derived, in this case in terms of P_I, the following assumption was made [2]:

$$I_D = T_{FF} T_{MD} r_d P_I \tag{32}$$

The gain of the Mach-Zehnder modulated link was modeled using (21). The P1dB of the Mach-Zehnder modulated link was modeled using [2]:

$$P1dB = \frac{V_\pi^2}{2\pi^2 R_S} \tag{33}$$

It was much more difficult to find a commercially available Mach-Zehnder modulated link, but after speaking to an engineer at MITEQ®, a link, although not commercially available at the time, could be defined by the characteristics shown in Table 6. Once again, it should be noted

57

that in the currently coded model, it is assumed that all resistances are 50 Ω matched, that the

ambient temperature is 290 K, and that there is no excess modulator loss since this specific piece

of information was not readily available, although these assumptions can be easily modified by

simply uncommenting certain lines of code in the model.

Table 6: Mach-Zehnder Modulated Analog Optical Link Component Level Specifications

Component	Parameter	Value
External Modulator	V_π (V)	5.5
	DC bias voltage (V)	2.75
	Excess modulator loss (dB)	4
	CW laser output power into modulator (W)	0.01
Photodiode	Photodiode responsivity (A/W)	0.5

Using these values as inputs for the simulation, the results were then compared to the link

performance specifications shown in Table 7, assuming no external circuitry and negligible fiber

loss for the link [2].

Table 7: Mach-Zehnder Modulated Analog Optical Link Expected Values vs. Simulated Values

Component	Parameter	Expected Value	Simulated Value
Mach-Zehnder Modulated Analog Optical Link with no external circuitry and negligible fiber loss	Gain (dB)	-34	-31
	Noise Figure (dB)	49	40
	Output P1dB (dBm)	-17	-16.1

Regarding the noise figure discrepancy, the same explanation that applied in the direct

modulation case applies to the Mach-Zehnder modulated case as well. The gain discrepancy can

also most likely be explained by the same reasoning used in the direct modulation case as well.

It is worth noting that the maximum excess loss for the modulator can actually be 5 dB.

Therefore, using this value as an input to the simulation could possibly improve the simulated

values. Nonetheless, the Mach-Zehnder modulated analog optical link model is validated and

can be used for first order modeling. The actual simulation can be found in Appendix B [2].

4.1.6 Modeling Frequency Translation

The final component that the signal is passed through is the receiver. An important piece of this component is that the signal is translated to a lower frequency suitable to be passed on to the ADC. This was modeled by adjusting the time vector of the signal to appropriately reflect the new frequency.

4.1.7 Modeling Results

A sample execution of each of the link cases (coaxial cable, component level direct modulation analog optical link, component level external modulation analog optical link, and link level analog optical link), using the signal input power that would not result in saturation of any of the components (-19 dBm), is shown in Appendix C – Appendix F. The values that were used in each of these cases reflect the aforementioned values of the system. The figures have been inserted at the point at which they would appear to the user. In the case of the link level analog optical link the values used are based on the MITEQ® SCML-100M11G link. The actual values that were used are shown in Table 8.

Table 8: Link Level Analog Optical Link Parameters

Component	Parameter	Value
Attenuation Before Link:	Gain (dB)	-24
	Noise Figure (dB)	24
Analog Optical Link:	Gain (dB)	18
	Output P1dB (dBm)	4
	Noise Figure (dB)	20
Attenuation After Link:	Gain (dB)	-4
	Noise Figure (dB)	4
All:	System BW (GHz)	1

In order to demonstrate the saturation part of the model, an additional model execution for the coaxial cable model is shown in Appendix G with an larger input signal (-10 dBm). The figures of the time domain signal show that the signal has been clipped at the saturation point of

59

the components. It is difficult to see the noise on the time domain signal in the previous model

executions since the signal is so much larger than the noise, a coaxial model execution was

completed with a smaller input power (-60 dBm) to decrease the signal-to-noise ratio. This

execution is shown in Appendix H.

As can be seen in the sample execution of the model for the link level analog optical link,

the instantaneous dynamic range after the receiver is greater than the 50 dB that was required by

the specifications. This means that based on the model, and if dynamic range was the only

driver, this link should be suitable for replacing the coaxial cable. However, as was mentioned

earlier, sensitivity was also a consideration, which turns out to be a more stressing specification.

4.2 Analog Optical Link Design

A commercially available prepackaged link that can be simply switched with the

currently used coaxial cable appeared to be unattainable. The only commercially available

prepackaged link that came close was the SCML-100M11G MITEQ® link, primarily due to the

fact that it fit the necessary bandwidth requirements. The main problem with this and other

prepackaged links is that the gain tends to be significantly higher than -10 dB. This is due to the

fact that such links contain external amplification circuitry, which in part serves the purpose of

reducing the overall noise figure of the link at the expense of having a higher overall gain.

Another reason for such high link gains though could simply be due to the fact that selling a link

with high loss up front might appear to completely negate the purpose of utilizing low loss fiber

in most applications. As can be seen though, a thorough cost-benefit analysis should be

performed based on the distance of interest before completely dismissing the possibility of using

a higher loss analog optical link for such a reason. Although having a higher link loss up front

might appear to negate the advantages of using optical fiber, this tends to only be the case in the short run.

In order to use the SCML-100M11G MITEQ® link, attenuation would have to be inserted prior to the link. As the simulation of the SCML-100M11G MITEQ® link in the entire receiver chain showed, the dynamic range specification can in fact be met assuming these conditions. However, the sensitivity specification would not be achievable. The actual achievable SNR corresponding to the sensitivity of the radar receiver chain when using the SCML-100M11G MITEQ® link in conjunction with 28 dB of attenuation would be approximately 18 dB. The problem exists in that a 24 dB attenuator would have to be placed prior to this link (4 dB of attenuation can be placed after the link since the output P1dB is 4 dBm), thereby almost completely negating the gain contribution of the LNA to the overall noise figure. This means that the noise figure of the link becomes a major contributor to the overall noise figure of the radar receiver chain at this point. The only way to improve the SNR without inserting an attenuator would be to reduce the gain of the link, but this would result in a higher link noise figure. This might be acceptable though given the LNA's gain contribution to the entire receiver chain noise figure. Ultimately, since most commercially available links appear to have positive gains and at best, moderate noise figures, the best solution would be to custom design a link from scratch.

To design a link, the first decision that has to be made is what type of modulation scheme to use. After examining the specifications for the two different links presented by MITEQ®, the SCML-100M11G directly modulated link and the Mach-Zehnder modulated link, it appeared that it would be easier to obtain a lower noise figure after raising the gain to the desired level of approximately -10 dB by using a Mach-Zehnder modulated link in part due to the following

explanation. According to Cox, increasing the optical power in a directly modulated link simply increases the overall noise figure assuming that said link is RIN dominated. However, in the case of external modulation, increasing the CW laser output power effectively decreases the overall noise figure of the link assuming that the link is shot noise dominated. The implication of this is that in a shot noise dominated Mach-Zehnder modulated link, increasing the optical power leads to a simultaneous increase in gain and decrease in noise figure, whereas for a RIN noise dominated direct modulation link, noise figure alone increases with an increase in optical power. Therefore the designer has control over two link performance metrics via a single variable, the optical power of the CW laser, in the case of a shot noise dominated Mach-Zehnder modulated link, which allows the design to be less complex. According to Cox, the noise figure of shot noise dominated links in general can also be controlled via changing the photodiode responsivity and the modulation slope efficiency, unlike in the case of a RIN noise dominated link, whereas only the latter has an effect on noise figure. Aside from this, simply being able to use a CW laser separate from the modulator means greater overall flexibility in the design of a Mach-Zehnder modulated link. Another added benefit of utilizing external modulation is the ability to troubleshoot and maintain the system more easily given separate parts, unlike in the case of a directly modulated link where if something were to go wrong with the modulator, the entire part (the diode laser) would have to be replaced. This is not to say that direct modulation would not necessarily work, because ultimately, the decision to utilize external modulation was a design choice that had to be made given certain constraints. If a future designer prefers to utilize direct modulation instead, the appropriate modeling tools are available [2].

In order to have a starting point for the design, the specifications provided by MITEQ®
were used to represent realistic values. After careful consideration, the following set of possible
designs was established, as shown in Table 9.

Table 9: Mach-Zehnder Modulated Design Scenarios

		Case 1	Case 2	Case 3
Component Specifications:	Excess Modulator Loss (dB)	4	4	4
	$V\pi$ (V)	3.14	3.5	3.5
	DC bias (V)	1.57	1.75	1.75
	Optical Power from CW Laser (W)	0.1	0.045	0.05
	Photodiode Responsivity (A/W)	0.5	0.8	0.8
Link Specifications:	Noise Figure (dB)	25.28	27.60	27.15
	P1dB Out (dBm)	3.76	0.94	1.85
	RF Gain (dB)	-6.24	-10.00	-9.09
Overall:	Overall Noise Temp (K)	428.13	513.08	492.83
	Instantaneous Dynamic Range (dB)	78.0	77.8	77.9
	SNR (dB)	31.29	30.5	30.68

It is important to remember that the minimum instantaneous dynamic range specification is 50

dB and the minimum SNR is 30 dB. The reason for having considered multiple designs is to

show the tradeoffs that occur in the design when manipulating different component level

characteristics of the analog optical link.

The first design case consisted of selecting a V_π of 3.14 V, which may seem arbitrary at a

first glance, but was in fact derived using (33) with the constraint that the maximum input signal

to the analog optical link will be 10 dBm. The excess modulator loss of 4 dB is typical of

lithium niobate modulators, the DC bias is based upon biasing the modulator at $0.5V_\pi$ in order to

obtain maximum linearity, the photodiode responsivity of 0.5 A/W is from the MITEQ® Mach-

Zehnder modulated link specifications, and the optical power from the CW laser was also a

specification provided for the MITEQ® Mach-Zehnder modulated link. With these

characteristics set to the previously mentioned values, the simulation yielded an SNR of 31.29

dB, meeting the minimum sensitivity specification of 30 dB. It is also important to note that the

achieved gain in this case was -6.24 dB, while the output P1dB out was 3.76 dBm. Ideally, the

gain should be -10 dB for the link with an output P1dB of 0 dB. Therefore, in this case, although the SNR specification was met, an attenuator would in fact have to be inserted into the overall design, although it could come after the link since the appropriate output to the receiver could still be met, thus having a minimal effect on the overall receiver chain noise figure [2].

For the second design case, the primary concern was adjusting any unrealistic values used in the first design case to be more realistic. The only unrealistic value used in the first design was a V_π of 3.14 V, which although it falls within the range of currently available Mach-Zehnder modulator V_π values, seemed too specific. For this reason, a V_π of 3.5 V was used instead, and the DC bias voltage was adjusted accordingly. In order to meet the sensitivity specification again, two more component level specifications were changed. The photodiode responsivity was adjusted to be 0.8 A/W, and the CW laser optical output power was adjusted to be 45 mW, both realistic values. The reason for changing photodiode responsivity was that by increasing its value, the noise figure of a shot noise dominated Mach-Zehnder modulated link decreases while the gain simultaneously increases. By increasing CW laser optical output power, the noise figure also drops while simultaneously leading to a gain increase. With these characteristics set in the simulation, an SNR of 30.5 was achieved, therefore meeting specification once again. In this case, the appropriate gain and P1dB were extremely close to being met (within 1 dB), and is therefore worth noting as the most likely design to work in practice without additional attenuation [2].

For the third design case, the only change made from the second design case was to increase the CW laser optical output power to 50 mW, simply since it is a less specific number, therefore probably more easily achievable in terms of obtaining commercially available parts. Nonetheless, the sensitivity specification was still met in this case, by a slightly higher margin

than the second case. However, of note is both the gain and output P1dB changed by approximately 1 dB. Therefore, a small change in the CW laser optical output power can in fact have a dramatic effect on gain and P1dB accordingly, as was expected given the Mach-Zehnder modulated link model [2].

It is worth noting that if the sensitivity specification was met in each of the design cases, then the corresponding dynamic range specification could be met as well. This is due to the fact that for the sensitivity specification of a 30 dB SNR, an overall maximum noise figure of 4.75 dB is required for the receiver chain. In order for the instantaneous dynamic range specification to be met, a maximum noise figure of 32 dB is required, therefore making it necessary for the primary constraint to be in terms of noise figure, and the sensitivity. It is important to note lastly that if these designs were to actually be implemented, due to the first order nature of the simulation tools provided, actual achieved noise figure and gain values might very well differ for the links. Therefore, although these designs appear to meet specification based on simulation, adjustments will most likely have to be made to obtain close to perfect performance in an implemented design.

In order to see if such designs would be practically realizable given currently available commercial analog optical link components, a brief online survey of available parts was conducted. This was primarily done for the purpose of finding a Mach-Zehnder modulator since the photodiode values of 0.5 and 0.8 A/W, based upon MITEQ® links and Cox, should be realizable [2]. One Mach-Zehnder modulator manufactured by Thorlabs®, Inc., was specified as having a V_π between 2.75-3 V at a frequency of 10 GHz. This was not exactly equal to the value of 3.14 V used in the first case design, but nonetheless, reinforces the notion that such a value is

very close to being achievable given currently available parts throughout the analog optical link industry.

4.3 Testing

An important aspect of the project was to test a commercially available link and measure its capabilities. As was mentioned earlier, the LBL-10M4P5G analog optical link was obtained from MITEQ® as a demonstration link. A picture of this link is shown in Figure 34. Since this link was used for demonstration purposes, the transmitter and receiver are physically adjacent, but in an actual implementation of the link the two could be located great distances from each other. The transmitter is on the left and the receiver is on the right. The blue cables are coaxial and transport the RF signal. The white cable with the green connectors is the optical fiber that is used to transport the signal from the optic transmitter to the optic receiver.

Figure 34: MITEQ® LBL-10M4P5G Analog Optical Link

The testing of the demo link was accomplished using an Agilent Technologies E8363B network analyzer. A diagram of the setup that was used is shown in Figure 35.
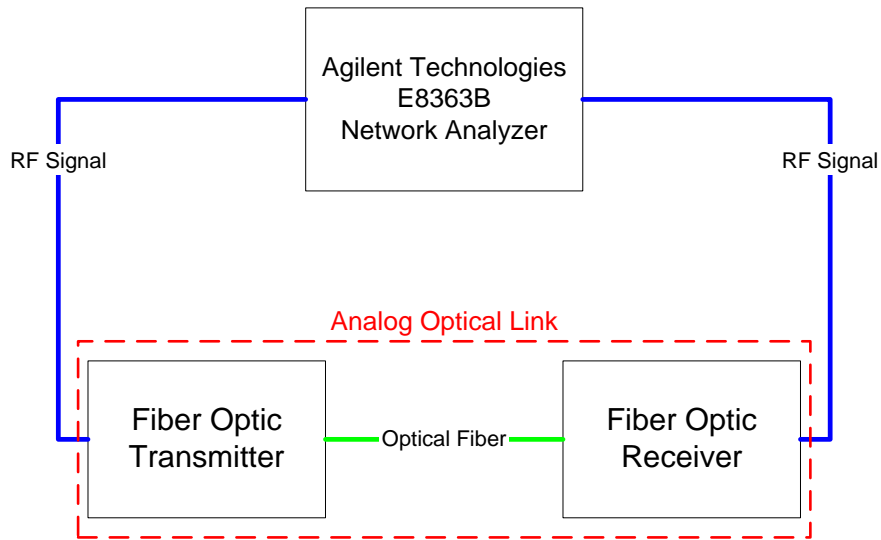
Figure 35: Diagram of Test Setup

First, the gain of the analog optical link was measured with an input power of -14 dBm, which is the input P1dB of the link, and a frequency sweep from 10 MHz to 4.5 GHz, which is the operating frequency of the link. A screenshot of the measurement (as displayed on the network analyzer) is shown in Figure 36.
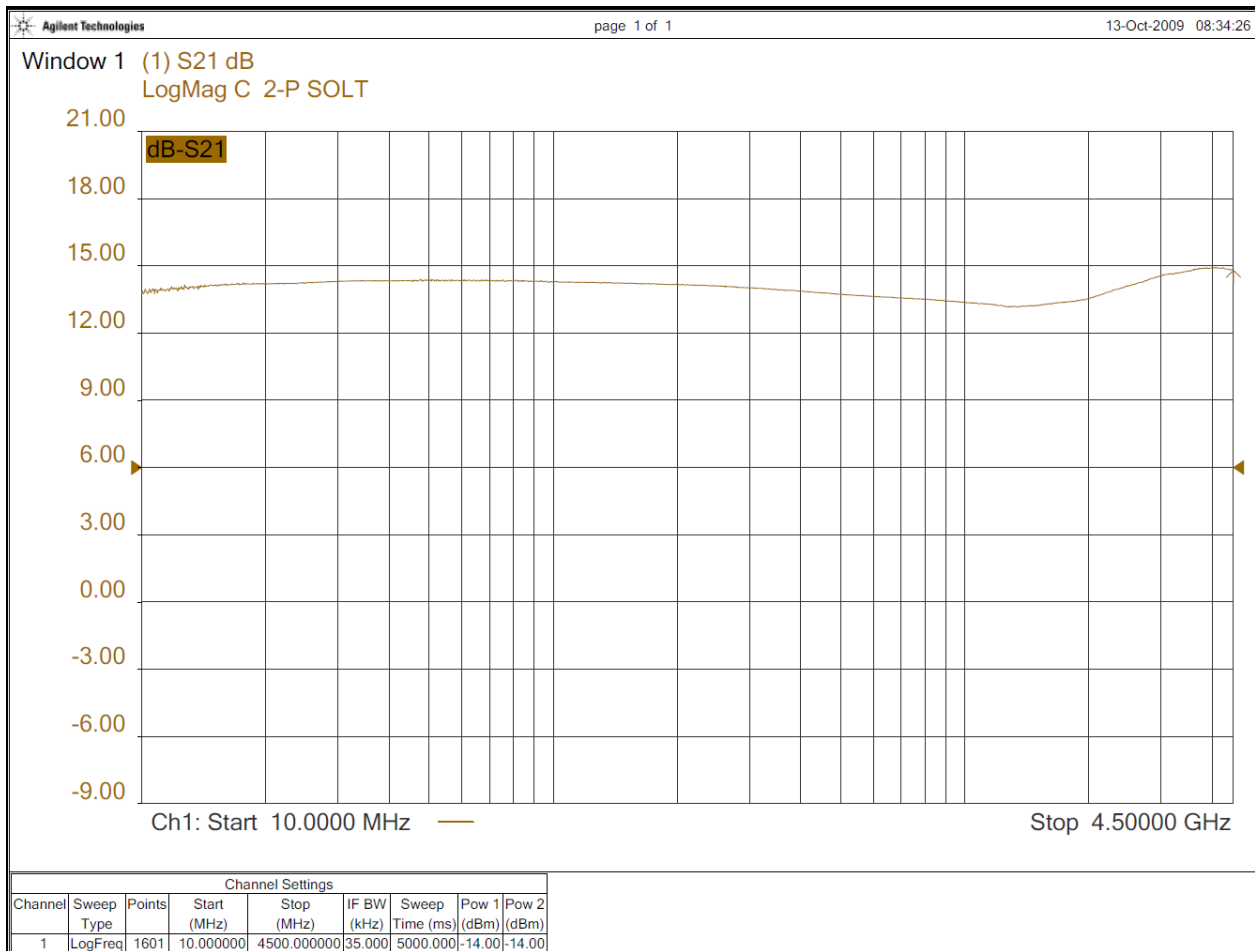
Figure 36: Gain of Demo Link for 2 Meter Long Fiber

From the image it can be seen that the gain of the link varies slightly across the usable bandwidth

but is approximately 14 dB. This test was done using a 2 meter long optical fiber. Comparisons

were made to the gain of a 50 meter long fiber to see how much difference the length of the fiber

would have on the gain of the link. The frequency response for this case is shown in Figure 37.
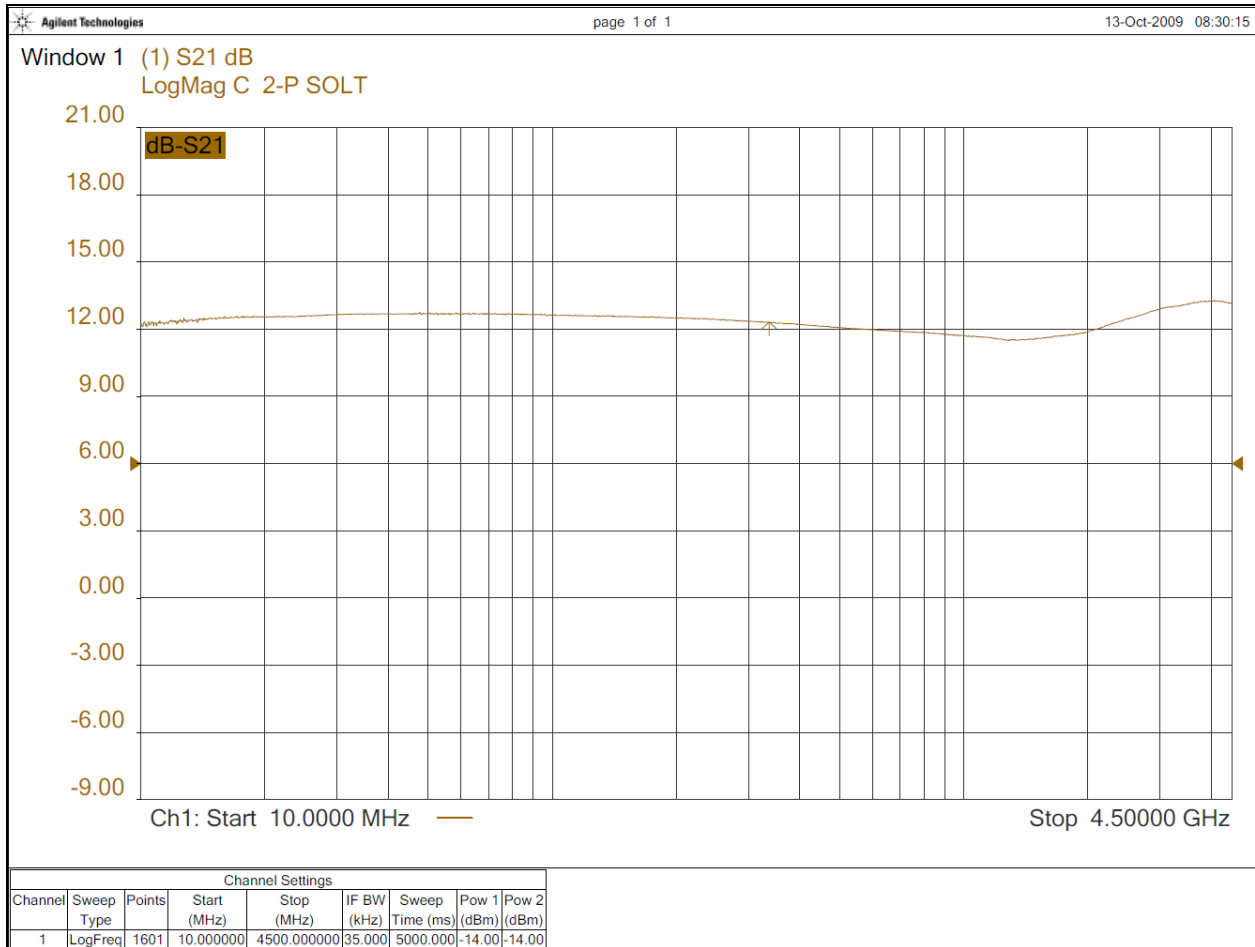
Figure 37: Gain of Demo Link for 50 Meter Long Fiber

If Figure 36 is compared with Figure 37, it becomes apparent that the link behaves very similarly

for the different lengths of fiber. While the absolute attenuation varies slightly, the slope of the

attenuation is nearly identical for the two different length fibers. This is shown in Figure 38.

The actual fiber that was used for the 50 meter long fiber needed adapters due to a different

connector type. These adapters could account for at least some of the added attenuation.
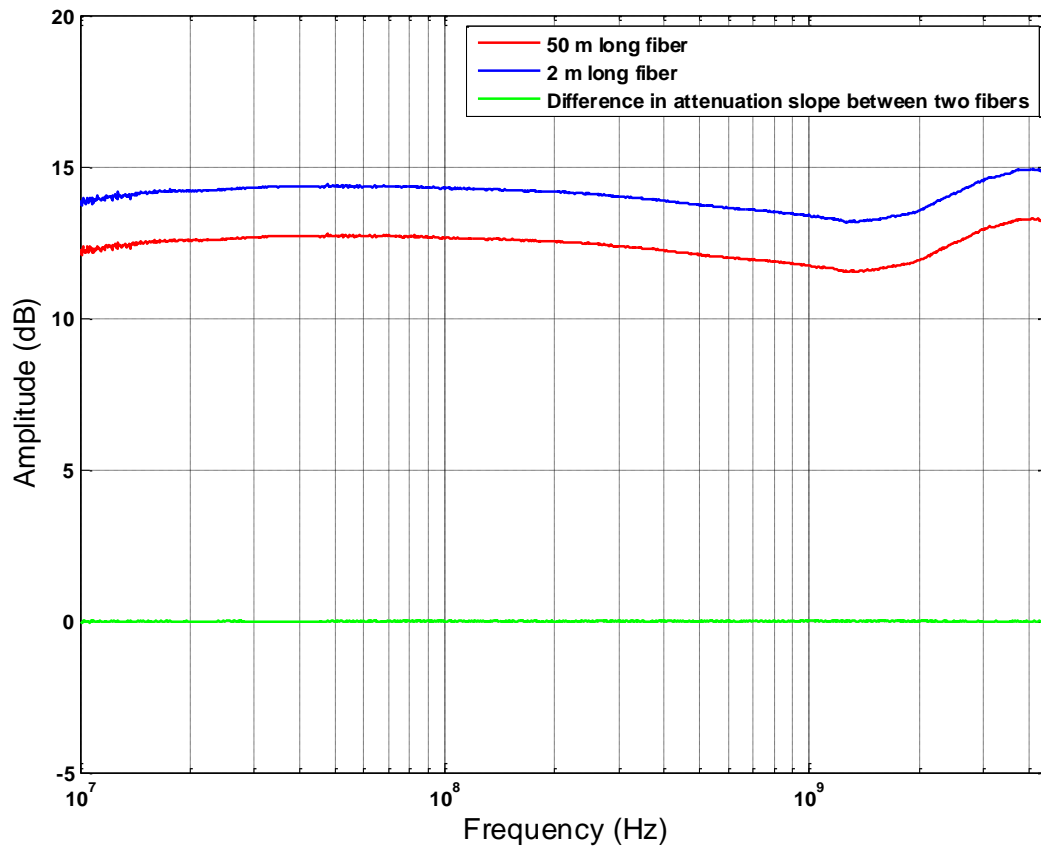
Figure 38: Absolute Attenuation vs. Frequency for 2 and 50 Meter Long Optical Fibers and Difference in Attenuation Slope of the Two Fibers vs. Frequency

The difference in the attenuation slope of the two length fibers is nearly zero over the entire spectrum. The importance of this lies in the comparison to a coaxial cable. As was discussed earlier in this report, as length increases for a coaxial cable, the slope of the attenuation across the bandwidth also increases. This is not the case with an analog optical link. Any slope that is seen at the output is due to the optical transmitter and receiver, not the fiber itself. This is why the slope of the attenuation does not change with a change in fiber length.

Other measurements of the demo link included the reverse isolation and the reflection coefficient of both the input and the output of the link. The reverse isolation is shown in Figure 39.
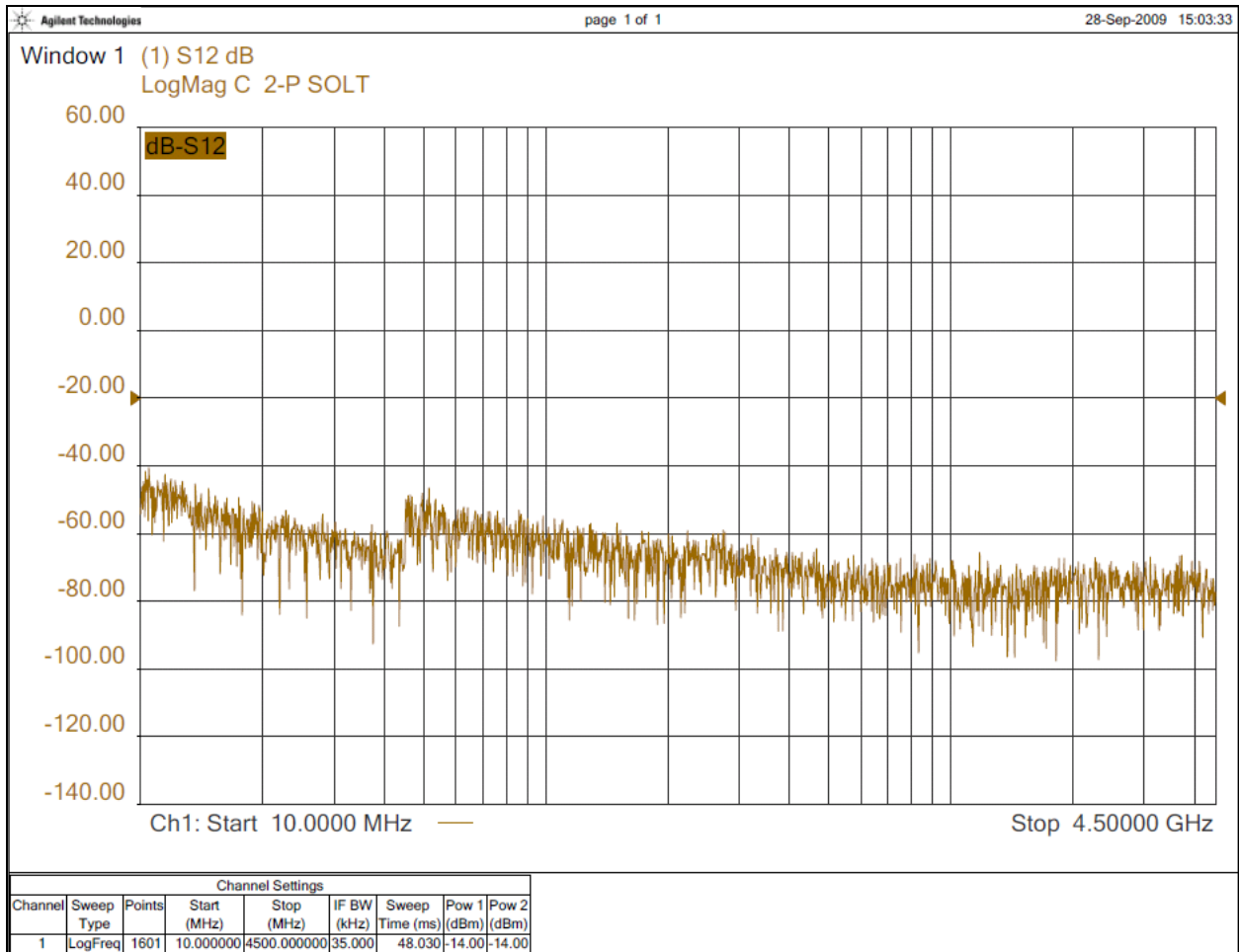
Figure 39: Reverse Isolation of Demo Link

This shows that signal transmission through the link is unidirectional from the transmitter to the receiver, which is desired.

It was also desired that the reflections at each port of the link be minimal in order to prevent distortion of the signal as much as possible. The reflections at the input port of the link are shown in Figure 40 and the reflections at the output port of the link are shown in Figure 41.

Window 1 (1) S11 dB
          LogMag C 2-P SOLT
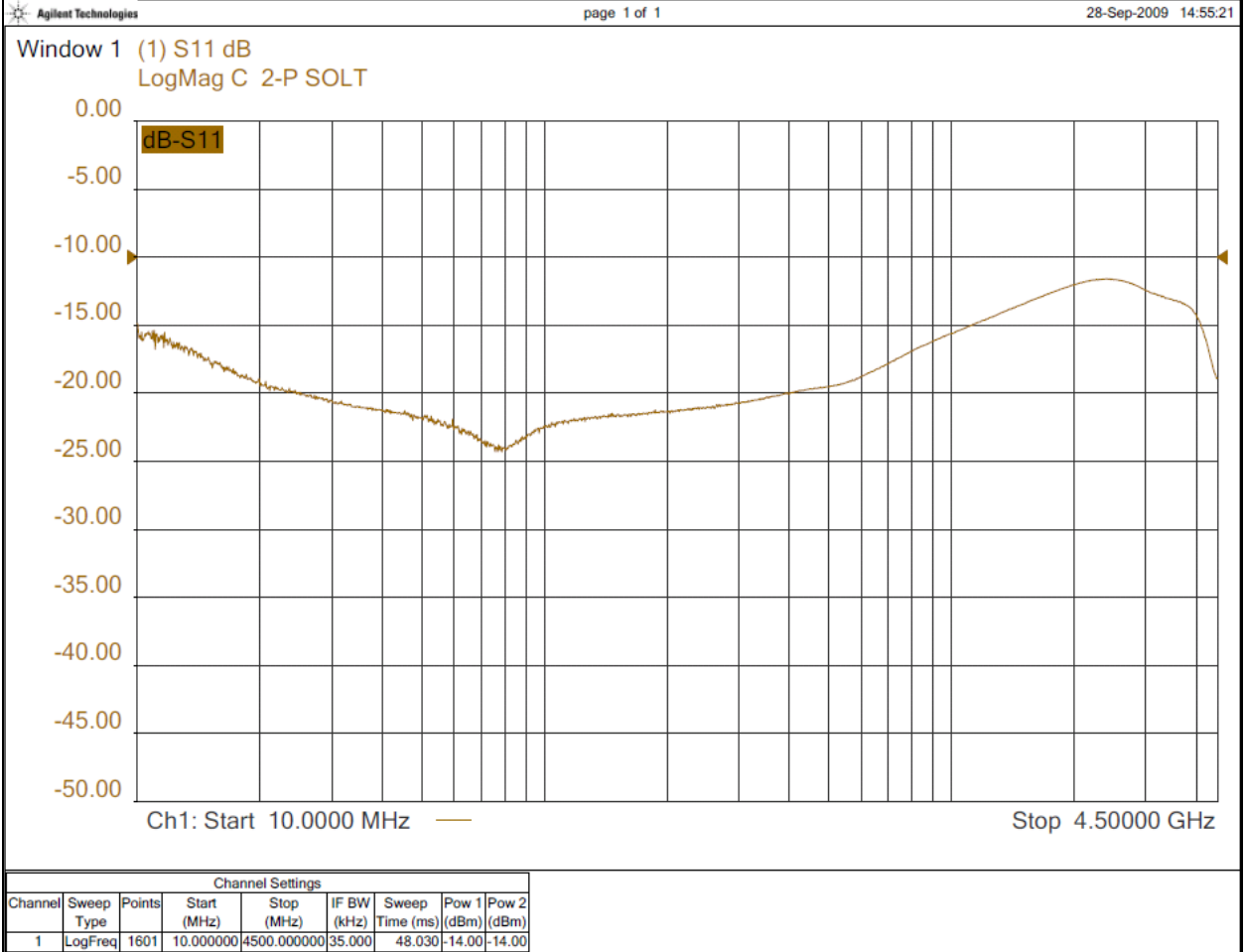
Figure 40: Reflections at Input Port of Demo Link
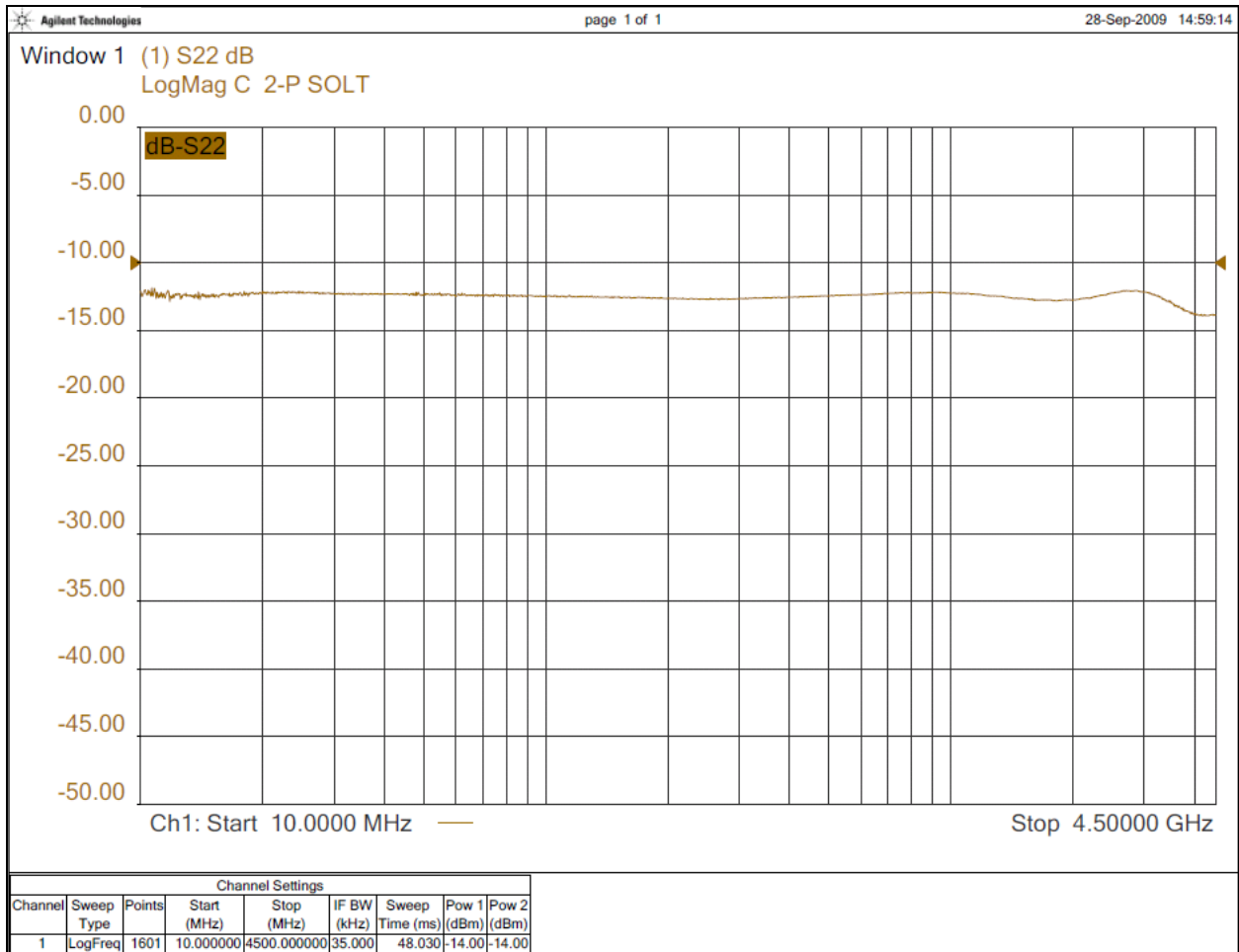
Figure 41: Reflections at Output Port of Demo Link

In both of these cases the reflections are much smaller than the actual signal.

From this test data it can be seen that the link performs well in the test setup. The biggest advantage of the analog optical link over a coaxial cable was confirmed through this testing, which is, the length of the fiber has negligible effect on the performance of the link. Most of the performance loss associated with the link is due to the transmitter and the receiver inefficiencies.

Chapter 5: Conclusion

For the purpose of long distance signal transmission, analog optical links are a better alternative to coaxial cable. This is primarily due to the fact that coaxial cable has higher attenuation than optical fiber overall. This is also due to the fact that coaxial cable attenuation varies significantly over a 1 GHz bandwidth, therefore requiring the designer to insert equalizers into the transmission line design in order to maintain signal integrity. Optical fiber does not experience wavelength dependent attenuation to the same degree that coaxial cable does, therefore making it ideal for remoting radar receiver hardware at a long distance from the antenna. That being said, the cost of an analog optical link tends to be large when compared to coaxial cable for short distance signal transmission. This is due to the fact that an analog optical link consists of components that convert RF to optical and vice versa, whereas coaxial cable is purely a transmission medium. Ultimately, it is up to the designer to weigh the costs and benefits of coaxial cable vs. analog optical links to determine which should be used for the particular application of interest.

Currently available commercial analog optical links would most likely need to be supplemented by attenuation in order to be used in the radar receiver chain. For this reason, designing a link from scratch is highly recommended. In order to design a link that can meet the appropriate specifications, simulation and modeling tools have been developed. These simulation tools have been verified using real world data and correspondingly can be used for the purpose of first order analog optical link modeling. These tools were also used to develop three Mach-Zehnder modulated link design cases in which both the dynamic range and sensitivity specifications would be met, either with or without extra attenuation required. Using these tools

in conjunction with the overall radar receiver chain analysis, future designers should be able to successfully develop links at the component level that will meet overall system specifications.

References

[1] Anonymous MIT Lincoln Laboratory: History. *2009(10/2),* pp. 1. Available: http://www.ll.mit.edu/about/History/history.html

[2] C. H. Cox, *Analog Optic Links: Theory and Practice.* Cambridge, UK: Cambridge University Press, 2004, pp. 288.

[3] M. I. Skolnik, *Radar Handbook.* ,Third ed. New York: McGraw-Hill, 2008, pp. 1300.

[4] Anonymous Radar basics- gain control methods. *2009(8/28),* Available: http://www.radartutorial.eu/09.receivers/rx08.en.html

[5] L. Goleniewski, *Communications Essentials: The Complete Global Source for Communications Fundamentals, Data Networking and the Internet, and Next-Generation Networks.* Addison-Wesley, 2002,

[6] Anonymous (2008, Coax. *2009(8/21),* Available: http://www.microwaves101.com/encyclopedia/coax.cfm

[7] Anonymous A 50-ohm cable? *2009(9/8),* pp. 1. Available: http://www.allaboutcircuits.com/vol_2/chpt_14/1.html

[8] K. Lonngren, S. Savov and R. Jost, *Fundamentals of Electromagnetics with MATLAB.* Raleigh, NC: Scitech Publishing, Inc., 2007,

[9] Anonymous (2007, General information about coaxial cable. *2009(9/17),* Available: http://www.linx-sat.com/coaxialcable.asp

[10] ORTEL, RF and microwave fiber-optic design guide.

[11] Anonymous Refraction of light. *2009(9/2),* Available: http://hyperphysics.phy-astr.gsu.edu/Hbase/geoopt/refr.html

[12] SHF Communication Technologies AG, Tutorial note #5 modulation schemes, pp. 3.

[13] S. B. Alexander, *Optical Communication Receiver Design.* Bellingham, Washington: SPIE Optical Engineering Press, 1997, pp. 314.

[14] Anonymous The basics of fiber optic cable. *2009(8/27),* Available: http://www.arcelect.com/fibercable.htm

[15] D. R. Paschotta. (2008, p-i-n photodiodes. *2009(9/1),* Available: http://www.rp-photonics.com/p_i_n_photodiodes.html

[16] D. R. Paschotta. (2009, Photodiodes. *2009(9/1),* Available: http://www.rp-photonics.com/photodiodes.html

[17] MITEQ®, Fiber optics specification definitions.

[18] T. Engdahl, "Cable impedance," vol. 2009, pp. 1,

[19] Anonymous "More on the "skin effect". *2009(9/28),* pp. 1. Available: http://www.allaboutcircuits.com/vol_2/chpt_3/6.html

[20] Anonymous IW products page 4 4806- 4808. *2009(9/25),* pp. 1. Available: http://www.iw-microwave.com/html/480.htm

[21] Anonymous Fiber dispersion. *2009(9/28),* pp. 1. Available: http://www.fiber-optics.info/articles/fiber_dispersion

[22] Anonymous Square wave signals. *2009(9/28),* Available: http://www.allaboutcircuits.com/vol_2/chpt_7/2.html

Appendix A : Direct Modulation Analog Optical Link Model Verification

```
>> [RFgain P1dBout NoiseFigure] = AnalogOpticLink_Direct

Analog Optical Link Component Parameters (Direct Modulation)
  Transmitter Parameters
    Relative Intensity Noise (RIN) of transmitter (dB/Hz): -150
    Laser slope efficiency (W/A): .15
    Laser bias current (A): .07
    Laser threshold current (A): .012
  Fiber Parameters
    Fiber Attenuation (dB/km): 0
    Length of Fiber (km): 0
  All other excess losses, including coupling losses (dB): 0
  Receiver Parameters
    Photodiode responsivity (A/W): .85

RFgain =

  -17.8898


P1dBout =

    0.1102


NoiseFigure =

  43.2256
```

Appendix B : External Modulation Analog Optical Link Model Verification

```
>> [RFgain P1dBout NoiseFigure] = AnalogOpticLink_External(10)

Analog Optical Link Component Parameters (External Modulation)
  Transmitter Parameters
    Total excess modulator loss (dB): 4
    Vpi (V): 5.5
    DC bias voltage of modulator (V): 2.75
    Optical output power from CW laser being input into modulator (W): .01
  Fiber Parameters
    Fiber Attenuation (dB/km): 0
    Length of Fiber (km): 0
  Receiver Parameters
    Photodiode responsivity (A/W): .5

RFgain =

  -30.9852


P1dBout =

  -16.1209


NoiseFigure =

   39.9996
```

Appendix C : Sample Model Execution – Coaxial Cable

```
>> RadarReceiver
Signal Setup:
  Frequency of Main Signal (GHz): 10
  Average Power of Main Signal (dBm): -19
  System Bandwidth (GHz): 1
Plot signal and amplitude spectrum of initial signal?(y/n): y
```
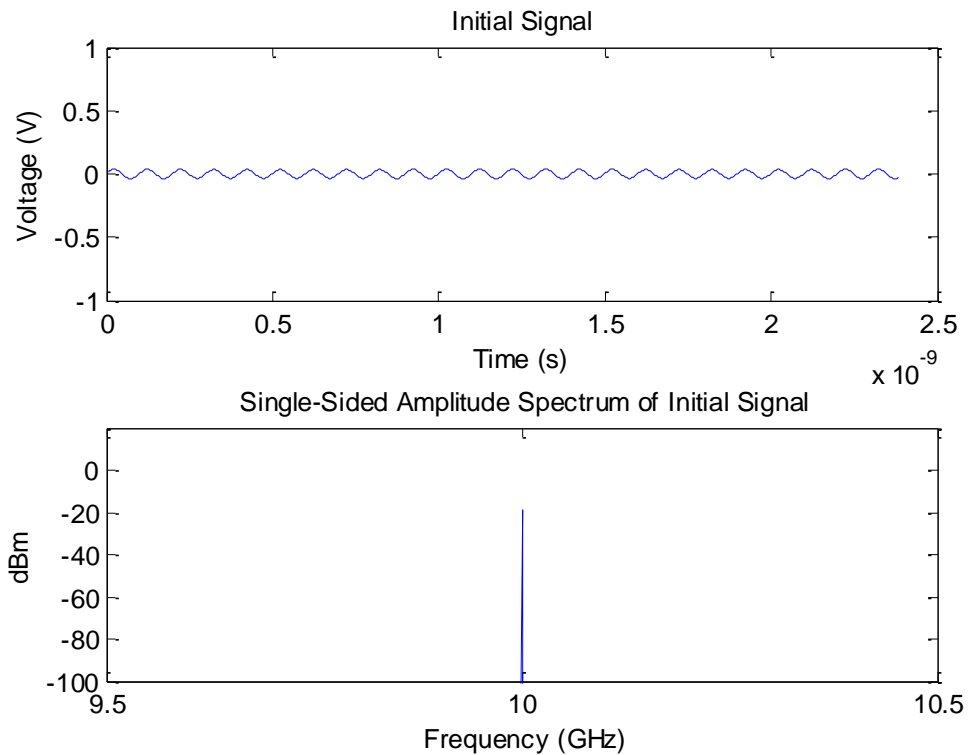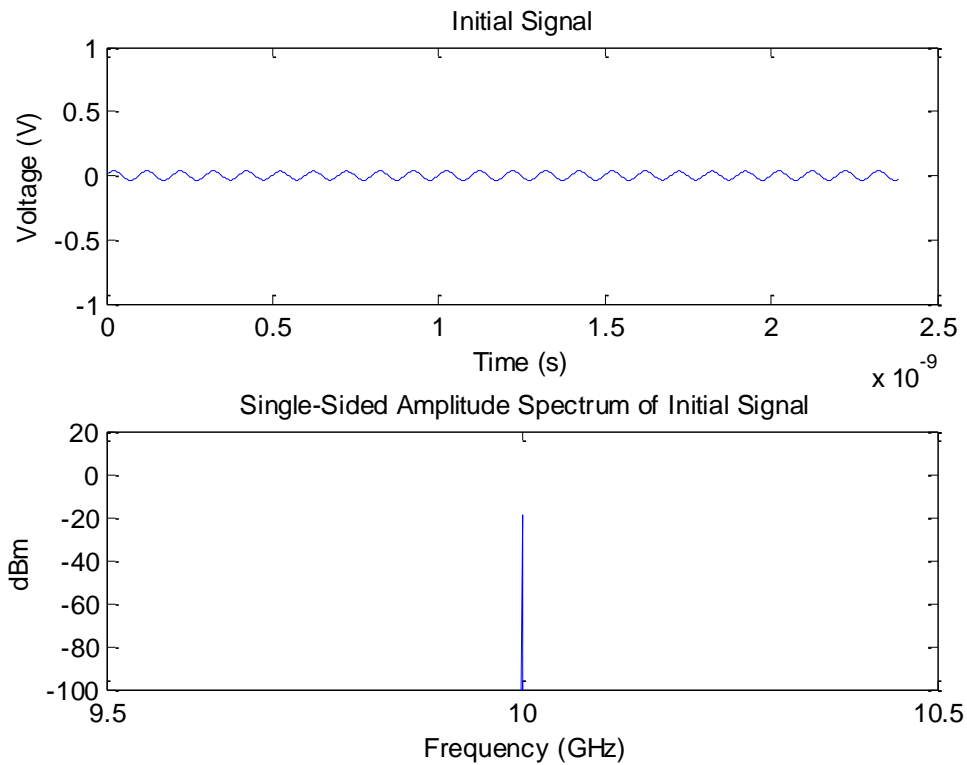

Figure 42: Coaxial Model - Initial Signal and Amplitude Spectrum

```
Front-End Parameters
  Gain of Front-End (dB): -1
  Noise Figure of Front-End (dB): 1
  System Bandwidth (GHz): 1
Plot signal and amplitude spectrum of current signal?(y/n): y
```
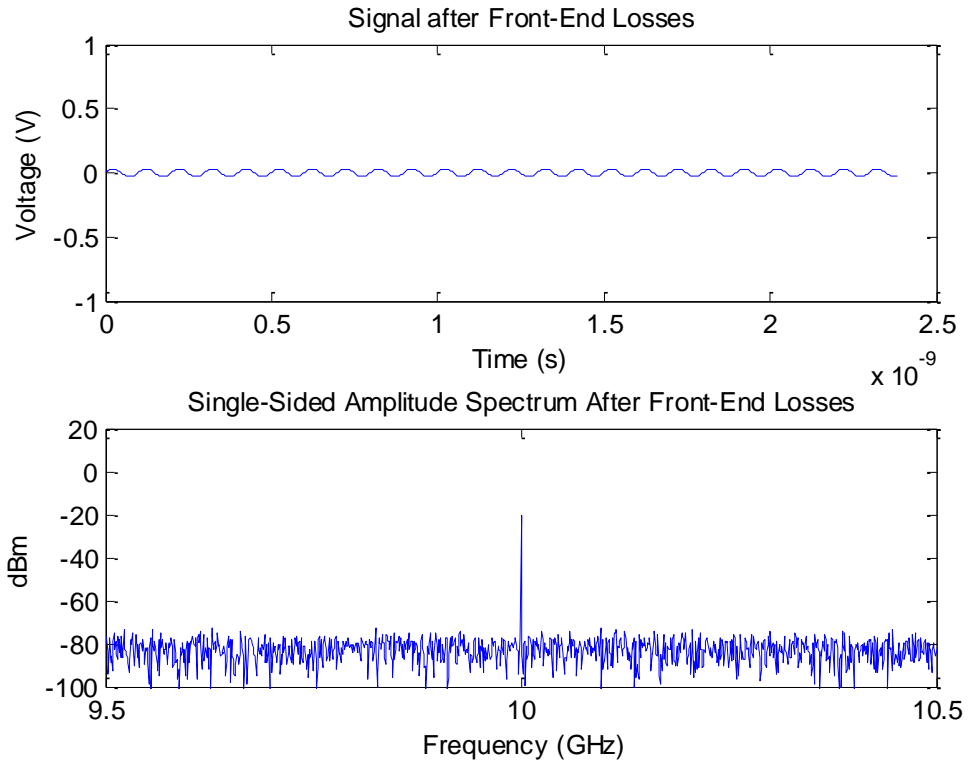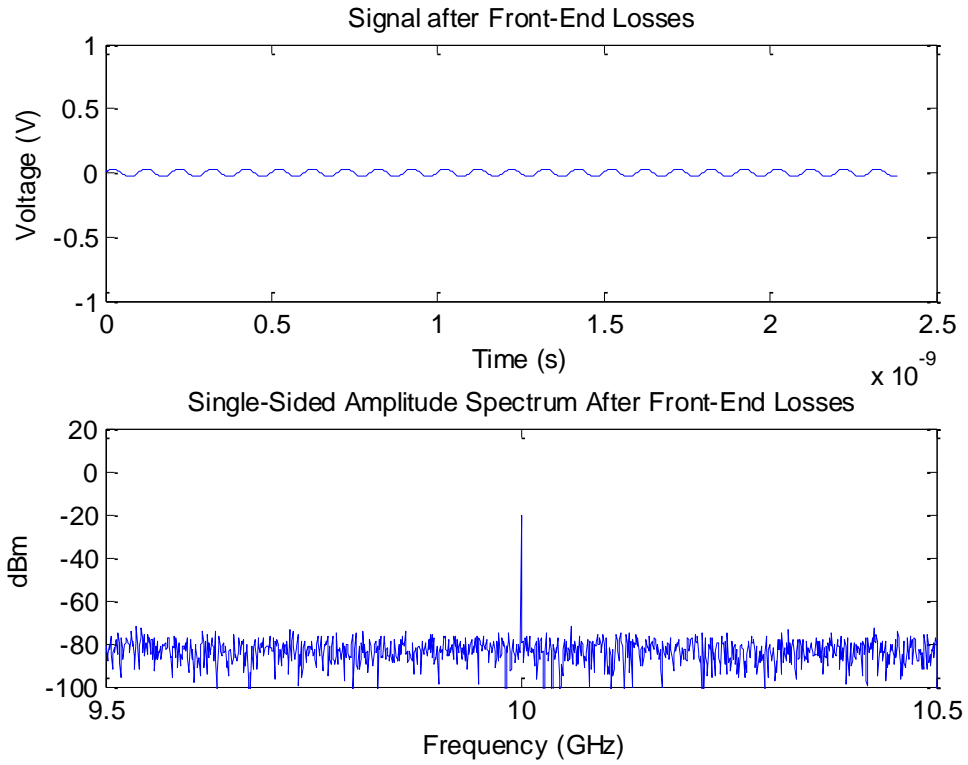
Figure 43: Coaxial Model - Signal and Amplitude Spectrum after Front-End Losses

```
SNR =

   63.9759



LNA Parameters
  Gain of LNA (dB): 30
  Output P1dB of LNA (dBm): 10
  Noise Figure of LNA (dB): 2
  System Bandwidth (GHz): 1
Plot signal and amplitude spectrum of current signal?(y/n): y
```
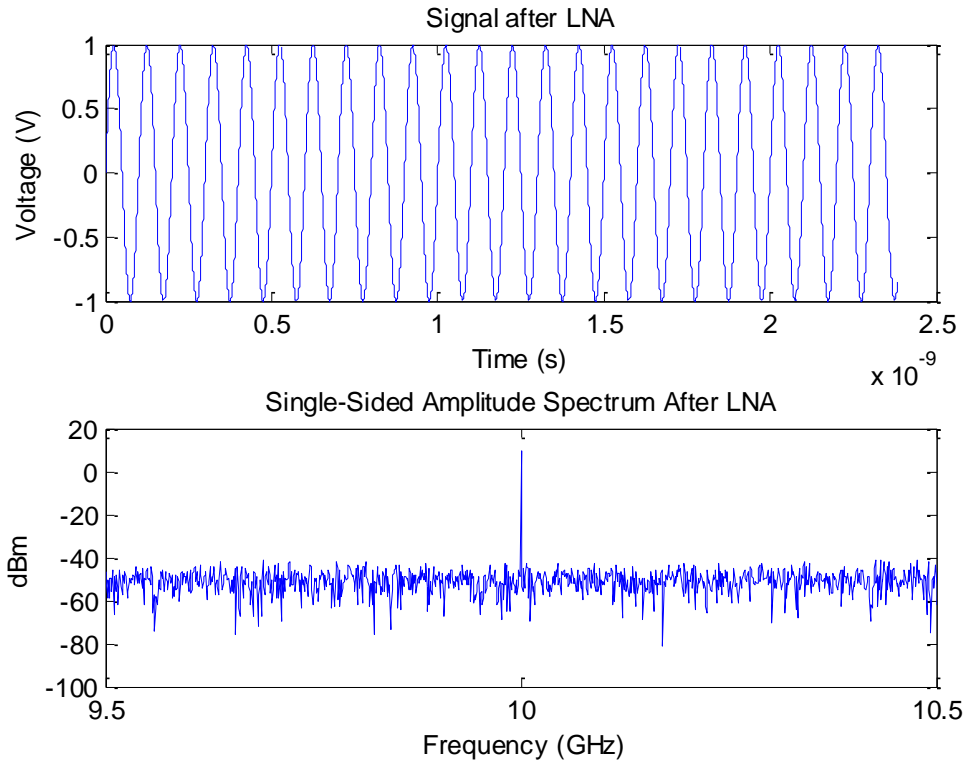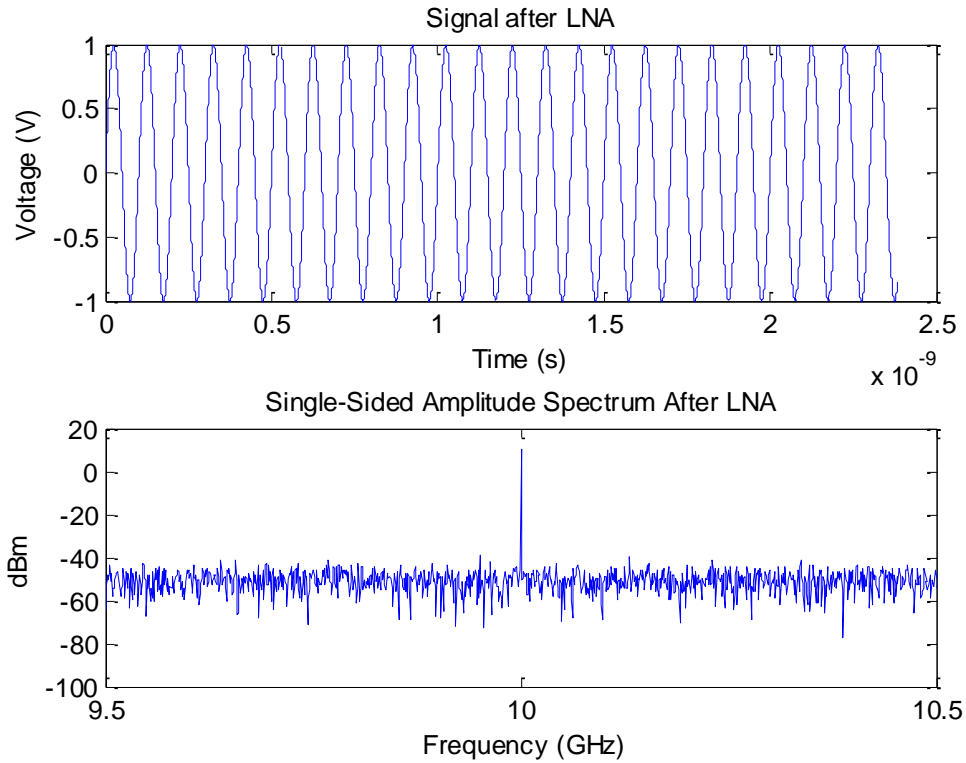
Figure 44: Coaxial Model - Signal and Amplitude Spectrum after LNA

```
SNR =

   61.9808


Specify Type of Link
  1) Coaxial
  2) Analog Optical (Component Level - External Modulation)
  3) Analog Optical (Component Level - Direct Modulation)
  4) Analog Optical (Link Level)
Enter #: 1

Coaxial Link Parameters
  Gain of Link (dB): -10
  Noise Figure of Link (dB): 10
  System Bandwidth (GHz): 1
Plot signal and amplitude spectrum of current signal?(y/n): y
```
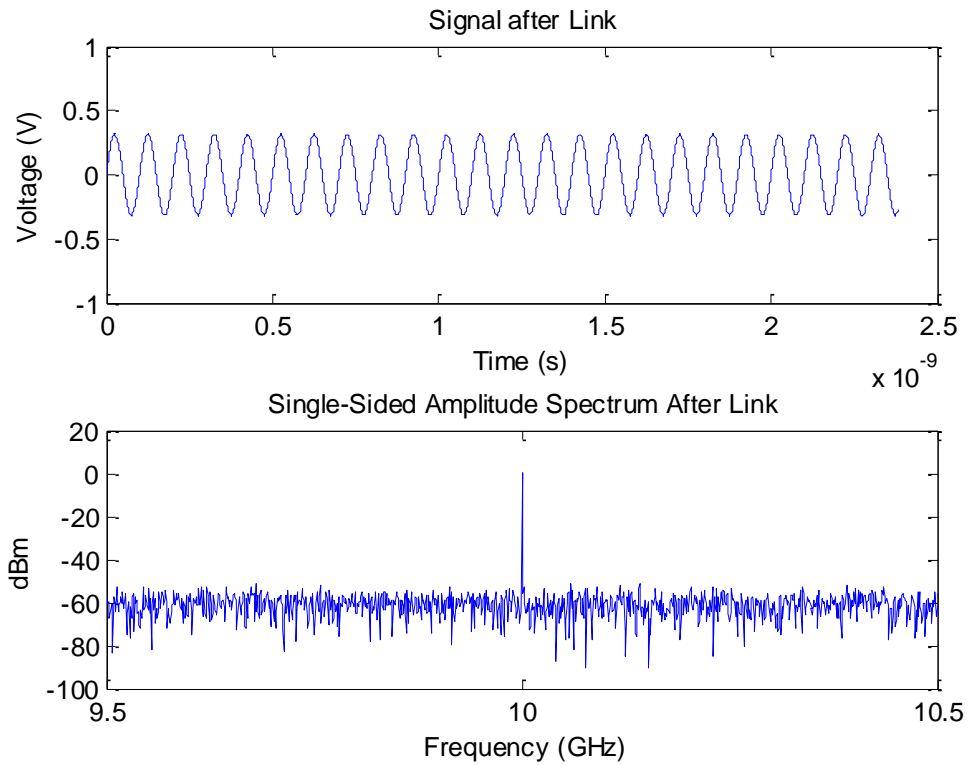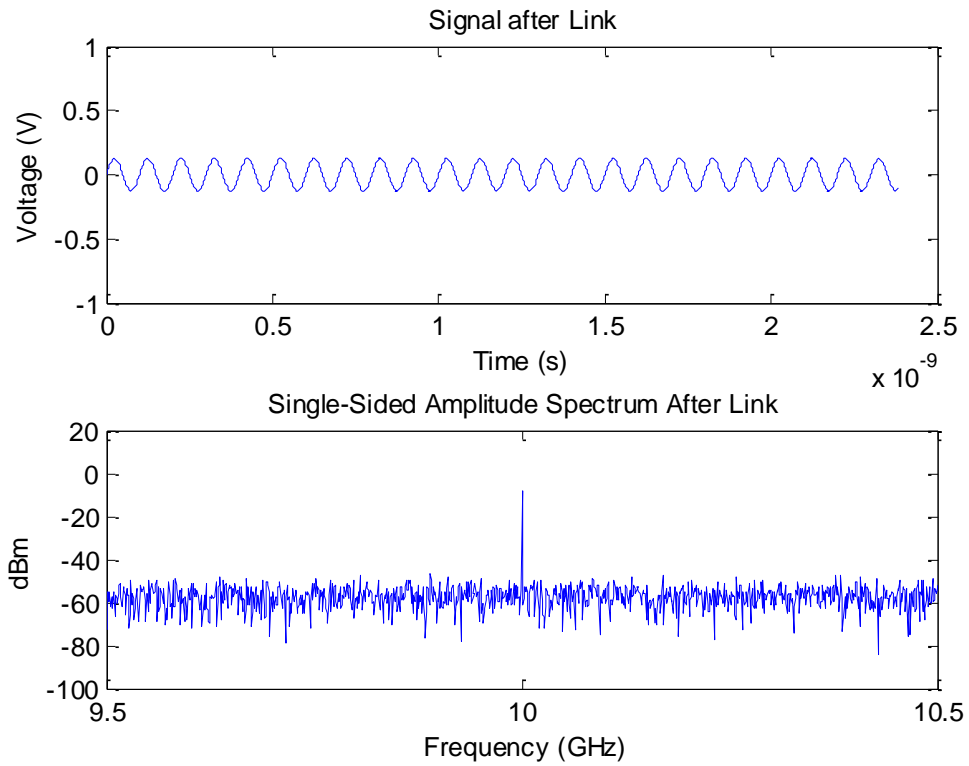
Figure 45: Coaxial Model - Signal and Amplitude Spectrum after Link

```
SNR =

   61.9536


RCVR Parameters
  Gain of RCVR (dB): 10
  Output P1dB of RCVR (dBm): 10
  Noise Figure of RCVR (dB): 7
  Output Frequency of RCVR (MHz): 70
  System Bandwidth (MHz): 20
Plot signal and amplitude spectrum of final signal?(y/n): y
```
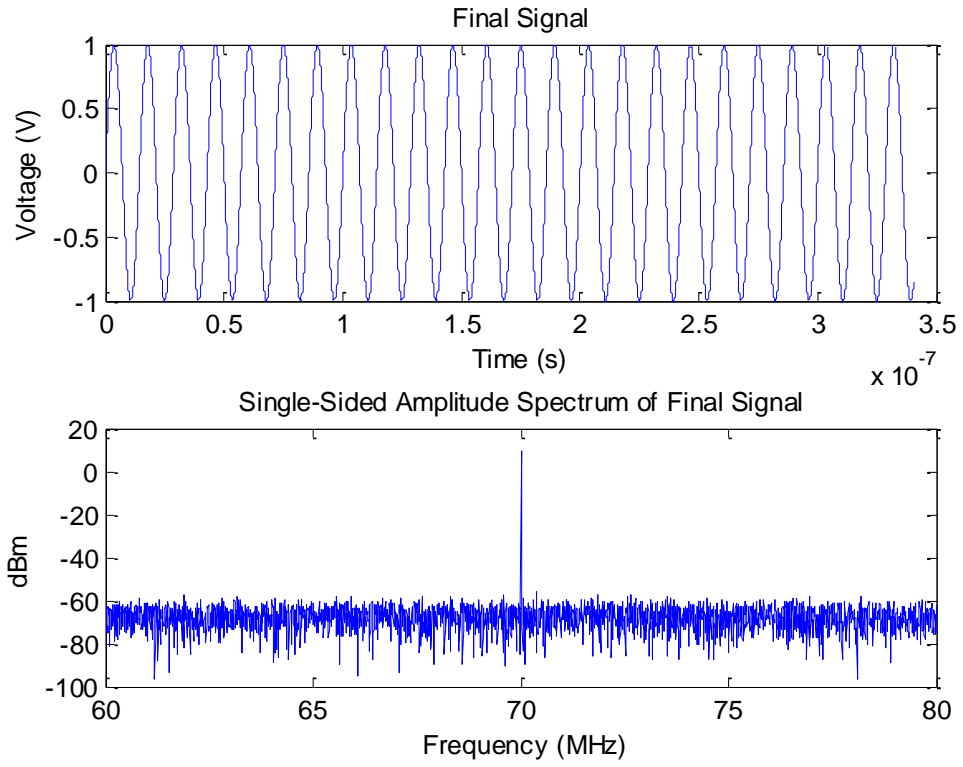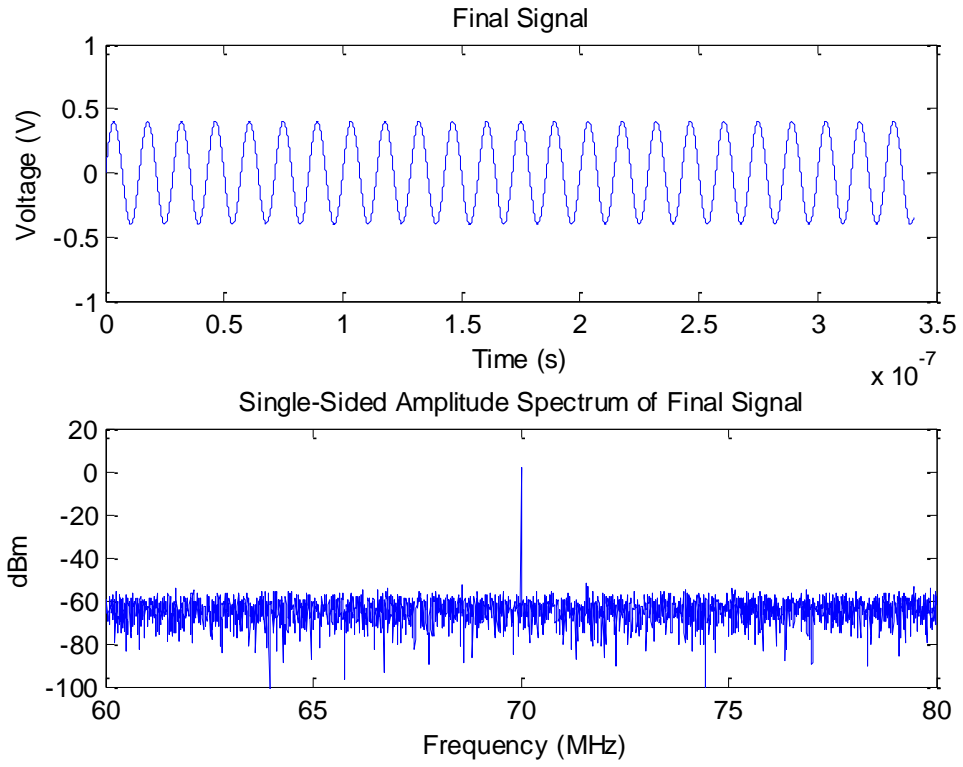
Figure 46: Coaxial Model - Final Signal and Amplitude Spectrum

```
SNR =

    78.8342
```

Appendix D : Sample Model Execution – Direct Modulation Analog Optical Link (Component Level)

```
>> RadarReceiver
Signal Setup:
  Frequency of Main Signal (GHz): 10
  Average Power of Main Signal (dBm): -19
  System Bandwidth (GHz): 1
Plot signal and amplitude spectrum of initial signal?(y/n): y
```
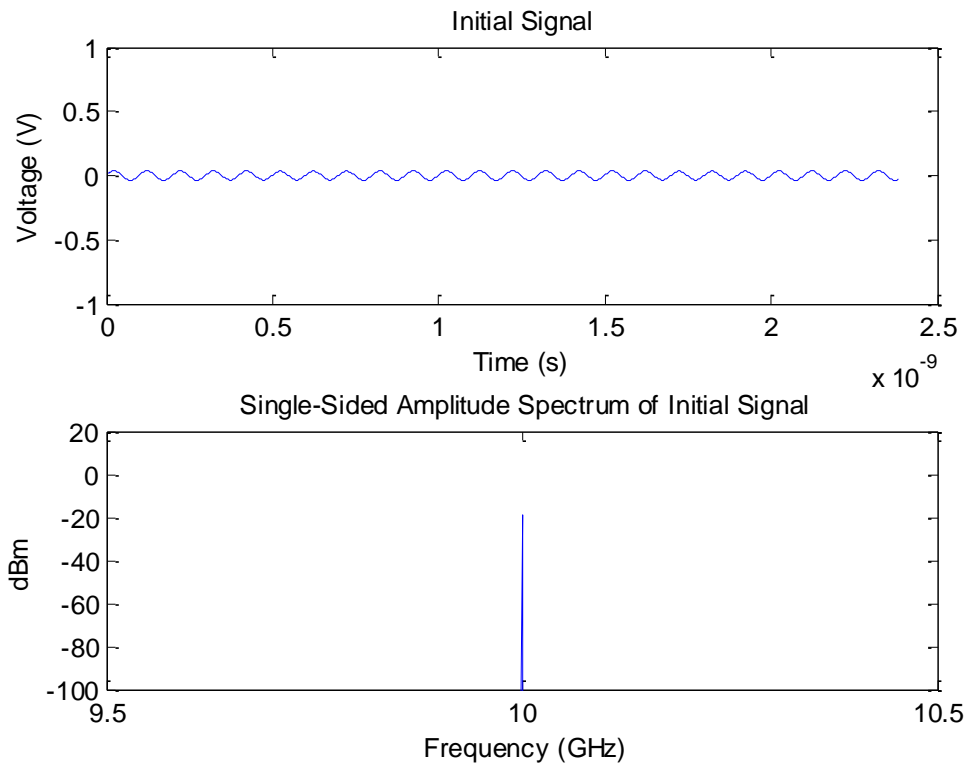

Figure 47: Direct Modulation Model - Initial Signal and Amplitude Spectrum

```
Front-End Parameters
  Gain of Front-End (dB): -1
  Noise Figure of Front-End (dB): 1
  System Bandwidth (GHz): 1
Plot signal and amplitude spectrum of current signal?(y/n): y
```
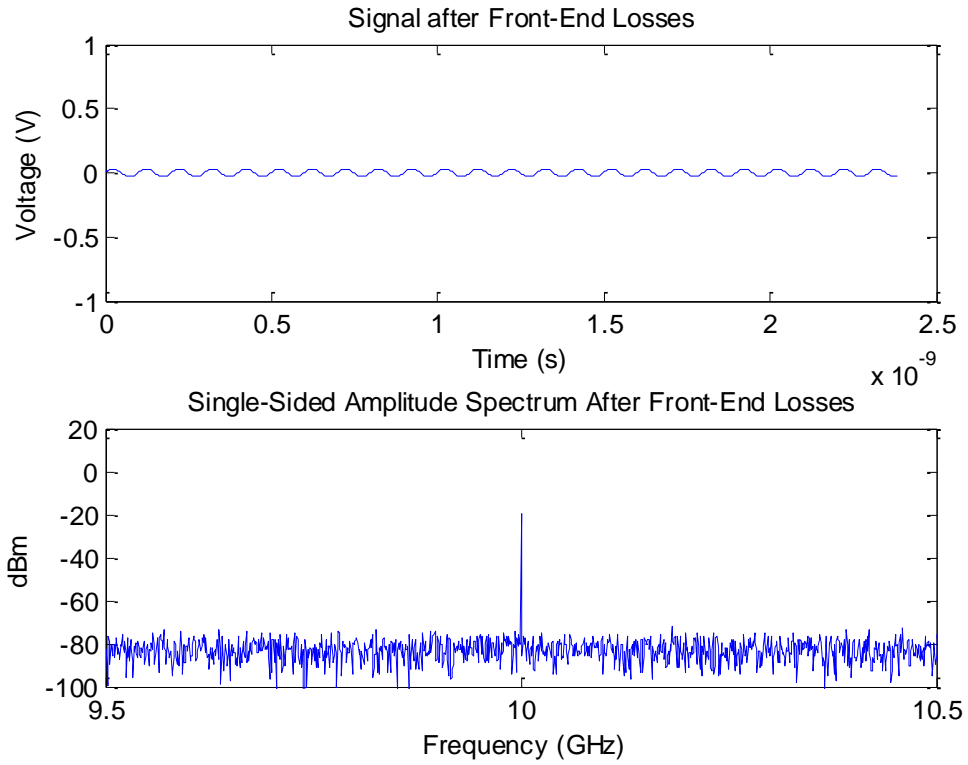
Figure 48: Direct Modulation Model - Signal and Amplitude Spectrum after Front-End Losses

```
SNR =

   63.9789



LNA Parameters
  Gain of LNA (dB): 30
  Output P1dB of LNA (dBm): 10
  Noise Figure of LNA (dB): 2
  System Bandwidth (GHz): 1
Plot signal and amplitude spectrum of current signal?(y/n): y
```
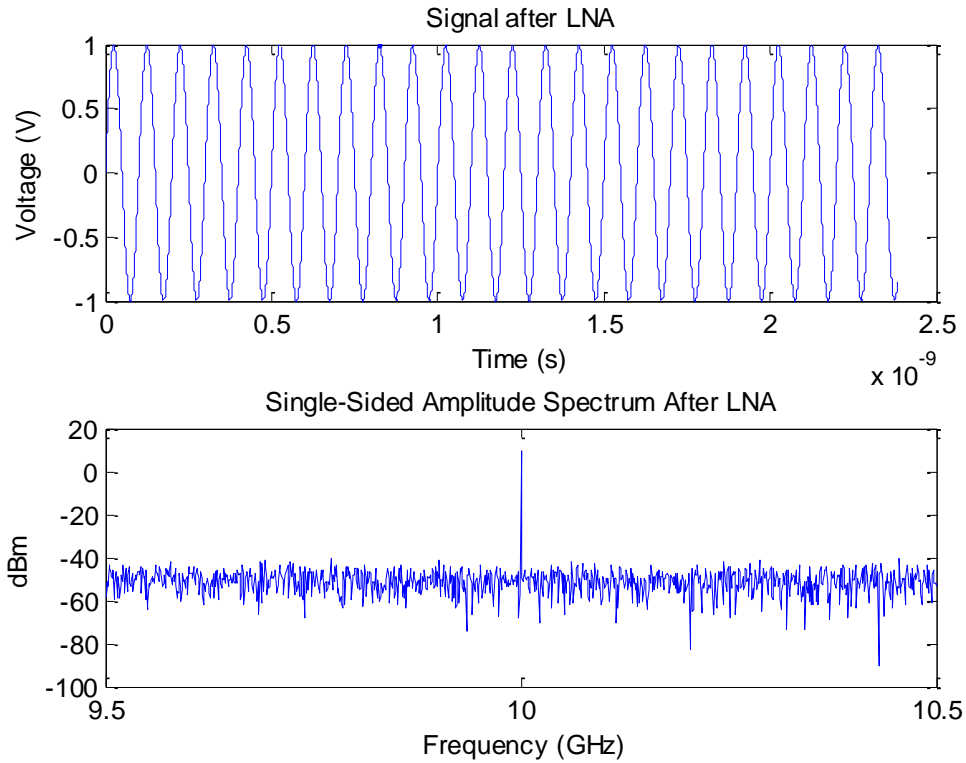
Figure 49: Direct Modulation Model - Signal and Amplitude Spectrum after LNA

```
SNR =

   61.9791



Specify Type of Link
  1) Coaxial
  2) Analog Optical (Component Level - External Modulation)
  3) Analog Optical (Component Level - Direct Modulation)
  4) Analog Optical (Link Level)
Enter #: 3

Analog Optical Link Component Parameters (Direct Modulation)
  Transmitter Parameters
    Relative Intensity Noise (RIN) of transmitter (dB/Hz): -150
    Laser slope efficiency (W/A): .15
    Laser bias current (A): .07
    Laser threshold current (A): .012
  Fiber Parameters
    Fiber Attenuation (dB/km): .5
    Length of Fiber (km): .03
  All other excess losses, including coupling losses (dB): 0
  Receiver Parameters
```

```
   Photodiode responsivity (A/W): .85
 System Bandwidth (GHz): 1
Plot signal and amplitude spectrum of current signal?(y/n): y
```


Figure 50: Direct Modulation Model - Signal and Amplitude Spectrum after Link

```
   SNR =

      50.4400


RCVR Parameters
   Gain of RCVR (dB): 10
   Output P1dB of RCVR (dBm): 10
   Noise Figure of RCVR (dB): 7
   Output Frequency of RCVR (MHz): 70
   System Bandwidth (MHz): 20
Plot signal and amplitude spectrum of final signal?(y/n): y
```

Figure 51: Direct Modulation Model - Final Signal and Amplitude Spectrum

```
SNR =

   67.3772
```

Appendix E : Sample Model Execution – External Modulation Analog Optical Link (Component Level)

```
>> RadarReceiver
Signal Setup:
  Frequency of Main Signal (GHz): 10
  Average Power of Main Signal (dBm): -19
  System Bandwidth (GHz): 1
Plot signal and amplitude spectrum of initial signal?(y/n): y
```


Figure 52: External Modulation Model - Initial Signal and Amplitude Spectrum

```
Front-End Parameters
  Gain of Front-End (dB): -1
  Noise Figure of Front-End (dB): 1
  System Bandwidth (GHz): 1
Plot signal and amplitude spectrum of current signal?(y/n): y
```

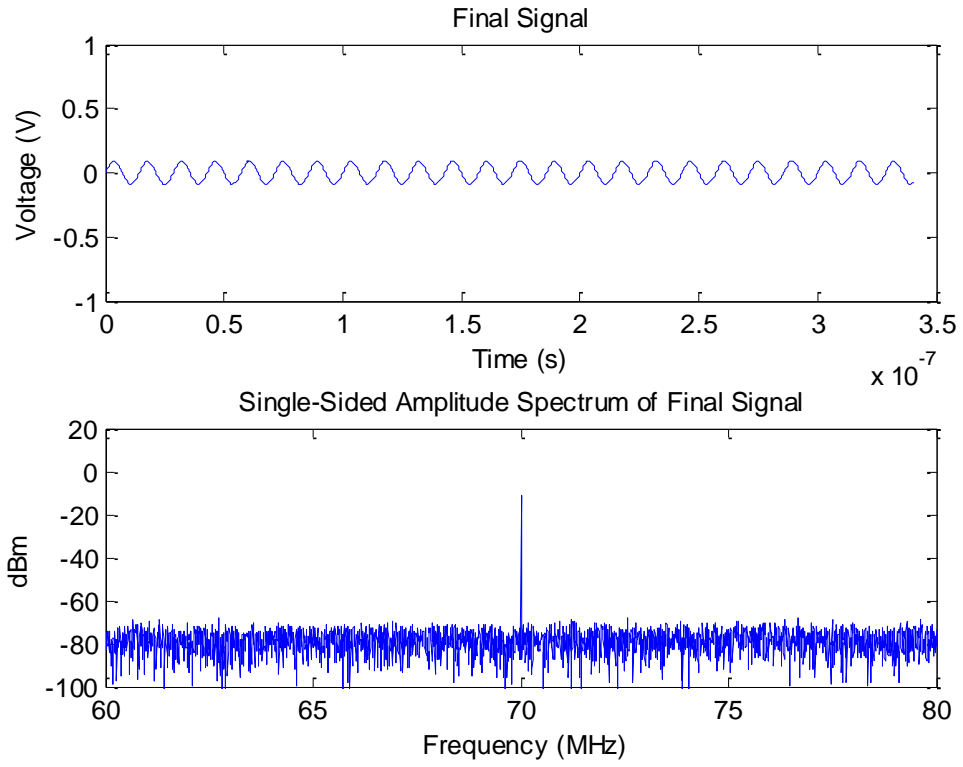**Figure 53: External Modulation Model - Signal and Amplitude Spectrum after Front-End Losses**

```
SNR =

   63.9692


LNA Parameters
  Gain of LNA (dB): 30
  Output P1dB of LNA (dBm): 10
  Noise Figure of LNA (dB): 2
  System Bandwidth (GHz): 1
Plot signal and amplitude spectrum of current signal?(y/n): y
```

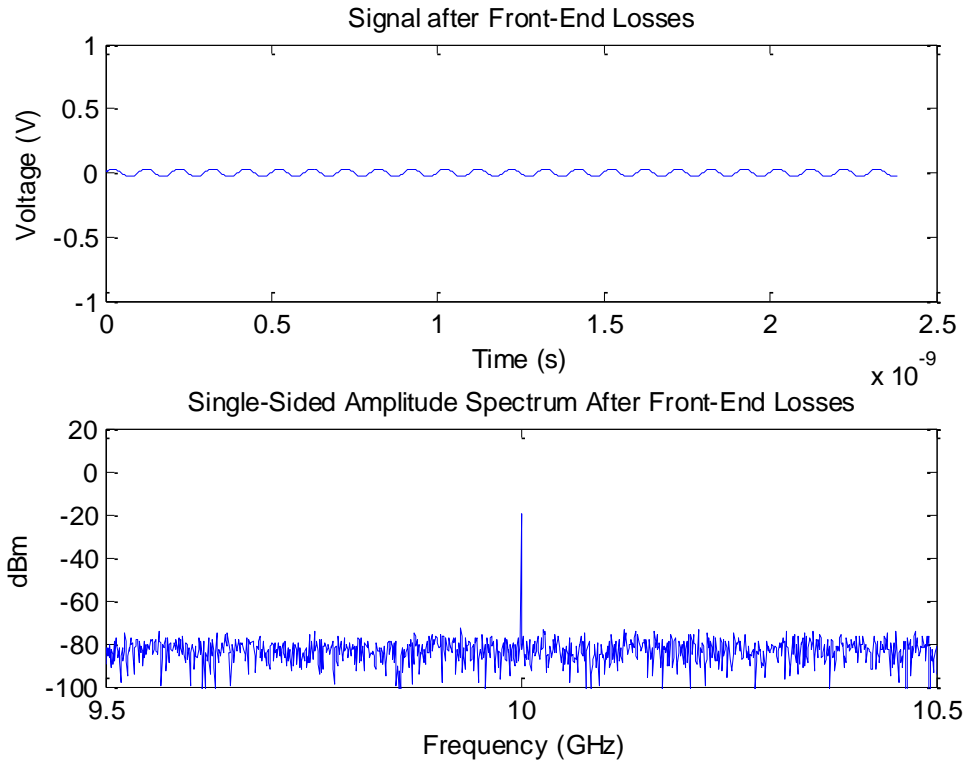**Figure 54: External Modulation Model - Signal and Amplitude Spectrum after LNA**

```
SNR =

   61.9759



Specify Type of Link
  1) Coaxial
  2) Analog Optical (Component Level - External Modulation)
  3) Analog Optical (Component Level - Direct Modulation)
  4) Analog Optical (Link Level)
Enter #: 2

Analog Optical Link Component Parameters (External Modulation)
  Transmitter Parameters
    Total excess modulator loss (dB): 4
    Vpi (V): 5.5
    DC bias voltage of modulator (V): 2.75
    Optical output power from CW laser being input into
modulator (W): .01
  Fiber Parameters
    Fiber Attenuation (dB/km): .5
    Length of Fiber (km): .03
  Receiver Parameters
```

```
   Photodiode responsivity (A/W): .5
  System Bandwidth (GHz): 1
Plot signal and amplitude spectrum of current signal?(y/n): y
```
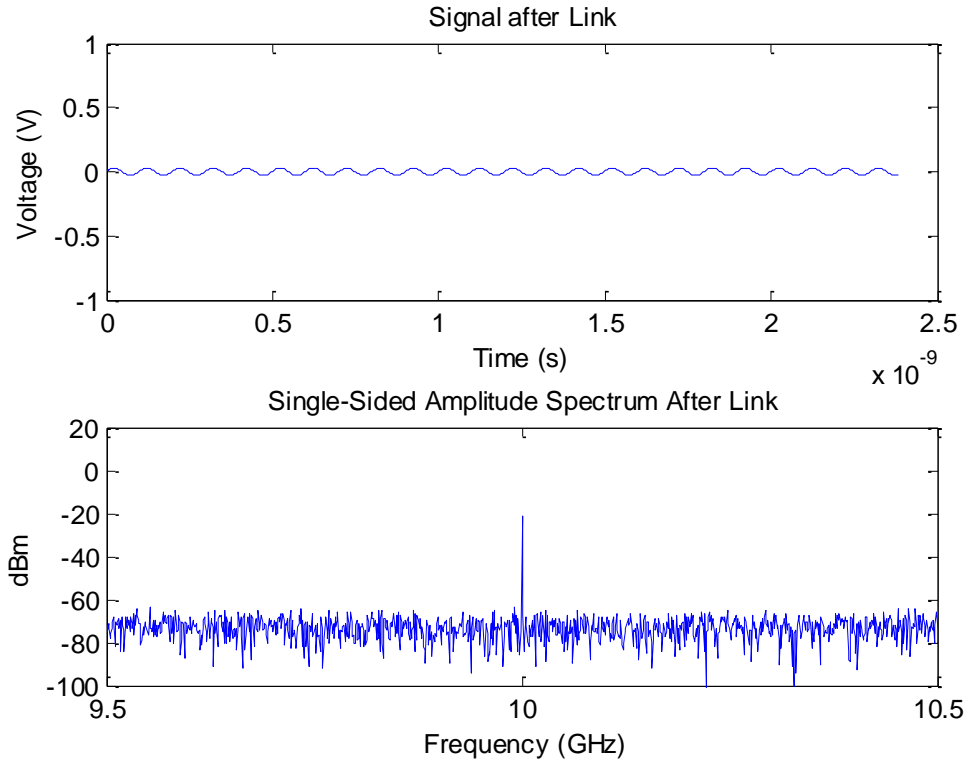

Figure 55: External Modulation Model - Signal and Amplitude Spectrum after Link

```
  SNR =

    53.3200


RCVR Parameters
  Gain of RCVR (dB): 10
  Output P1dB of RCVR (dBm): 10
  Noise Figure of RCVR (dB): 7
  Output Frequency of RCVR (MHz): 70
  System Bandwidth (MHz): 20
Plot signal and amplitude spectrum of final signal?(y/n): y
```

Figure 56: External Modulation Model - Final Signal and Amplitude Spectrum

```
SNR =

    68.7381
```

Appendix F : Sample Model Execution – Analog Optical Link (Link Level)

```
>> RadarReceiver
Signal Setup:
  Frequency of Main Signal (GHz): 10
  Average Power of Main Signal (dBm): -19
  System Bandwidth (GHz): 1
Plot signal and amplitude spectrum of initial signal?(y/n): y
```
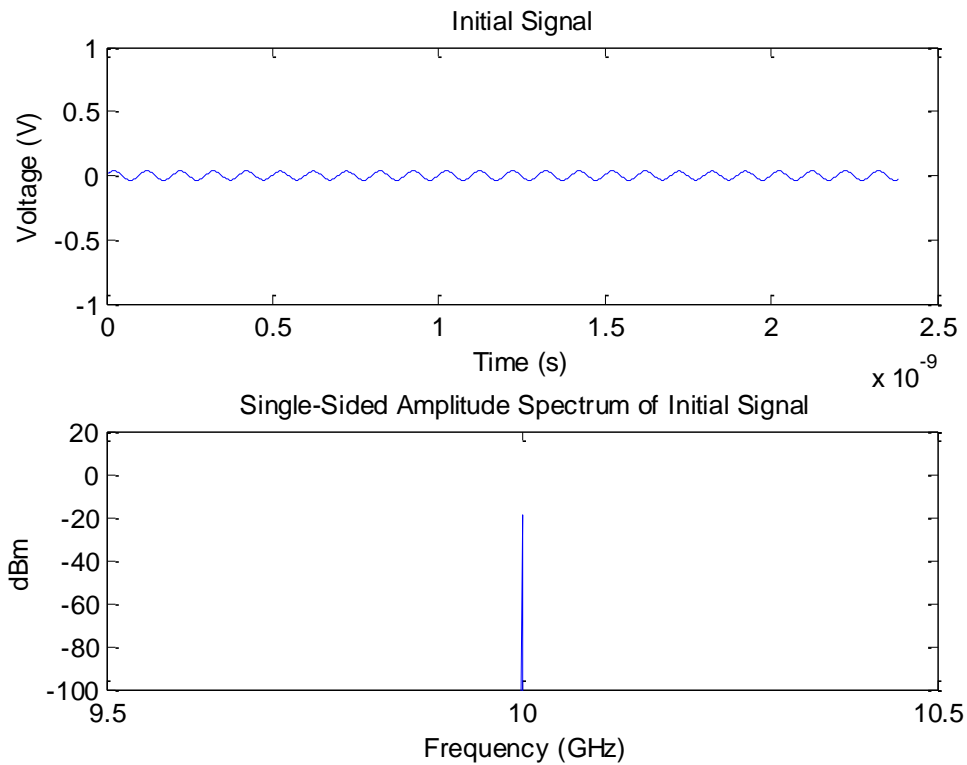

Figure 57: Analog Optical Link Model - Initial Signal and Amplitude Spectrum

```
Front-End Parameters
  Gain of Front-End (dB): -1
  Noise Figure of Front-End (dB): 1
  System Bandwidth (GHz): 1
Plot signal and amplitude spectrum of current signal?(y/n): y
```

Figure 58: Analog Optical Link Model - Signal and Amplitude Spectrum after Front-End Losses

```
SNR =

    63.9800


LNA Parameters
  Gain of LNA (dB): 30
  Output P1dB of LNA (dBm): 10
  Noise Figure of LNA (dB): 2
  System Bandwidth (GHz): 1
Plot signal and amplitude spectrum of current signal?(y/n): y
```
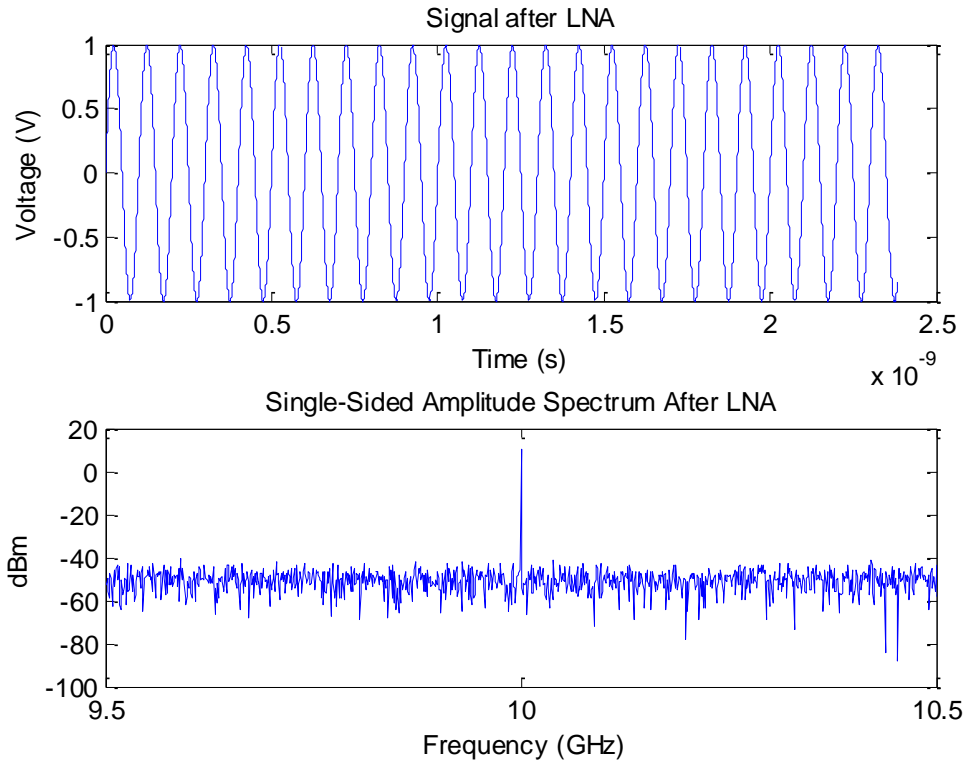
Figure 59: Analog Optical Link Model - Signal and Amplitude Spectrum after LNA

```
SNR =

   61.9713



Specify Type of Link
  1) Coaxial
  2) Analog Optical (Component Level - External Modulation)
  3) Analog Optical (Component Level - Direct Modulation)
  4) Analog Optical (Link Level)
Enter #: 4

Analog Optical Link Parameters
  Attenuation Before Link
    Gain (dB): -24
    Noise Figure (dB): 24
  Link
    Gain (dB): 18
    Output P1dB (dBm): 4
    Noise Figure (dB): 20
  Attenuation After Link
    Gain (dB): -4
    Noise Figure (dB): 4
```

```
System Bandwidth (GHz): 1
Plot signal and amplitude spectrum of current signal?(y/n): y
```
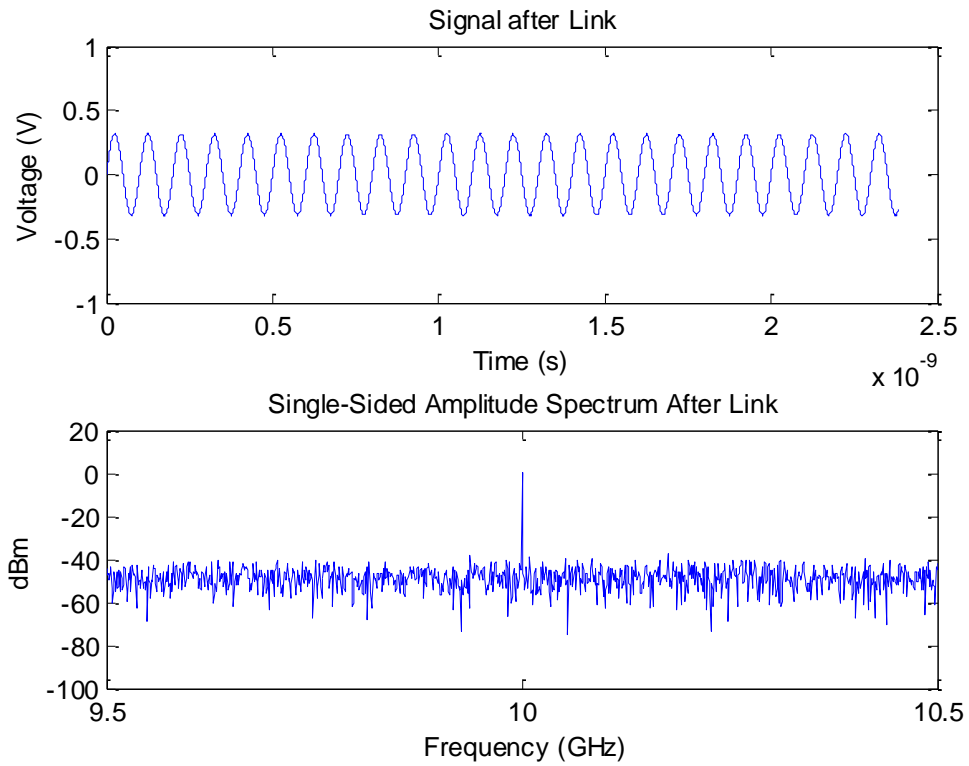

**Figure 60: Analog Optical Link Model - Signal and Amplitude Spectrum after Link**

```
SNR =

   49.7081


RCVR Parameters
  Gain of RCVR (dB): 10
  Output P1dB of RCVR (dBm): 10
  Noise Figure of RCVR (dB): 7
  Output Frequency of RCVR (MHz): 70
  System Bandwidth (MHz): 20
Plot signal and amplitude spectrum of final signal?(y/n): y
```
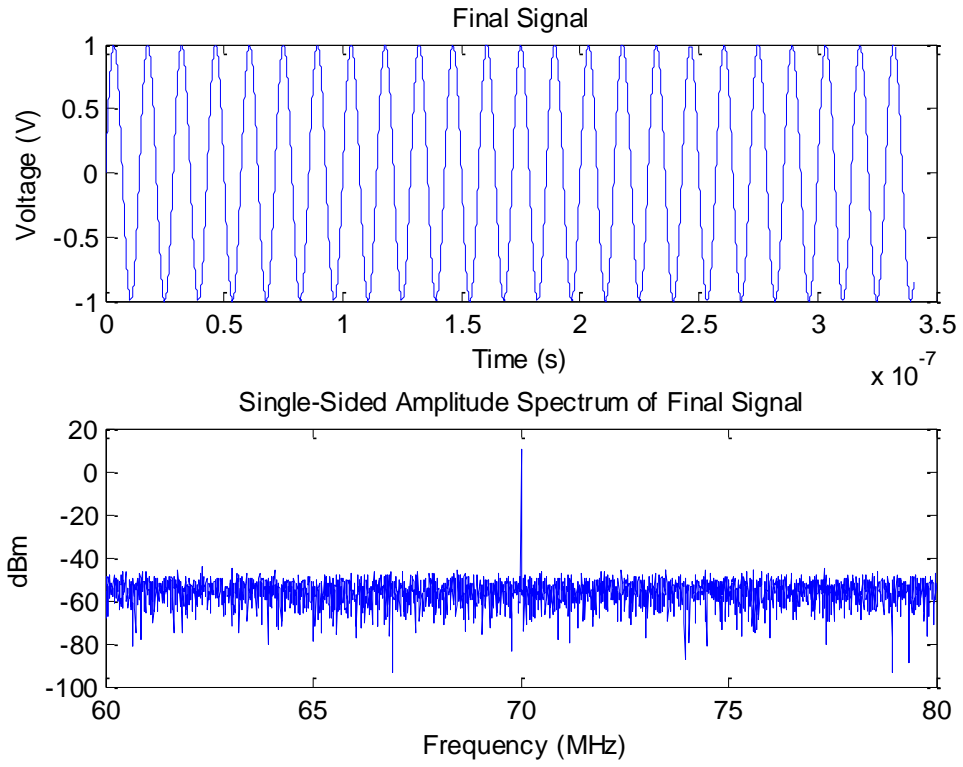
Figure 61: Analog Optical Link Model - Final Signal and Amplitude Spectrum

```
SNR =

    66.6930
```

Appendix G : Sample Model Execution – Saturation

```
>> RadarReceiver
Signal Setup:
  Frequency of Main Signal (GHz): 10
  Average Power of Main Signal (dBm): -10
  System Bandwidth (GHz): 1
Plot signal and amplitude spectrum of initial signal?(y/n): y
```
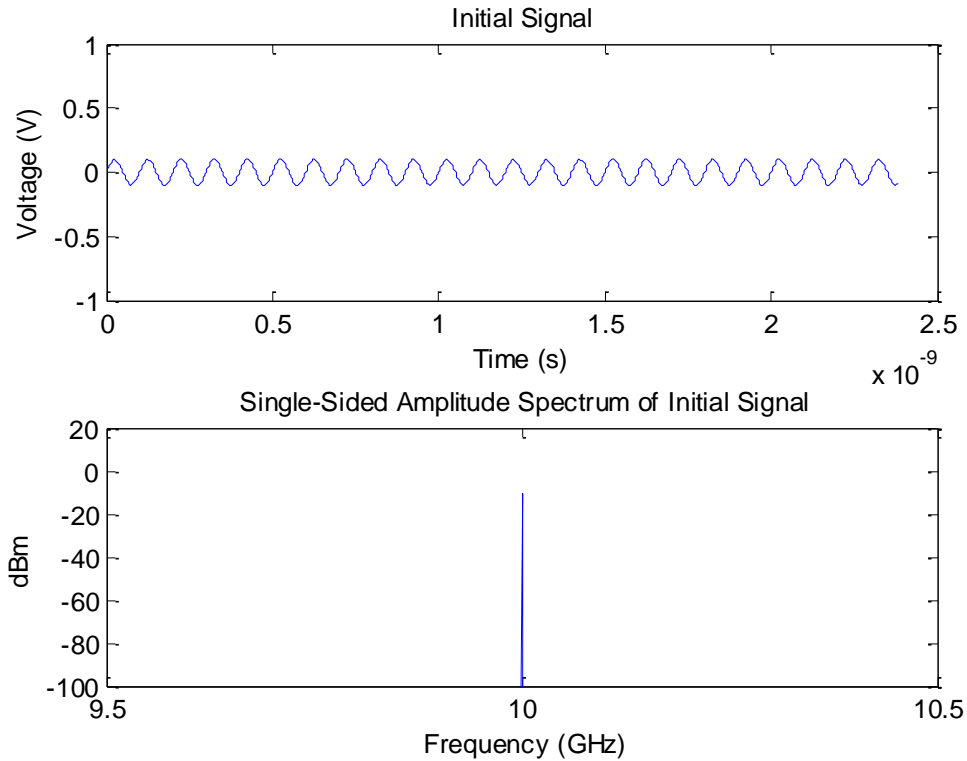

Figure 62: Coaxial Model with Saturation - Initial Signal and Amplitude Spectrum

```
Front-End Parameters
  Gain of Front-End (dB): -1
  Noise Figure of Front-End (dB): 1
  System Bandwidth (GHz): 1
Plot signal and amplitude spectrum of current signal?(y/n): y
```
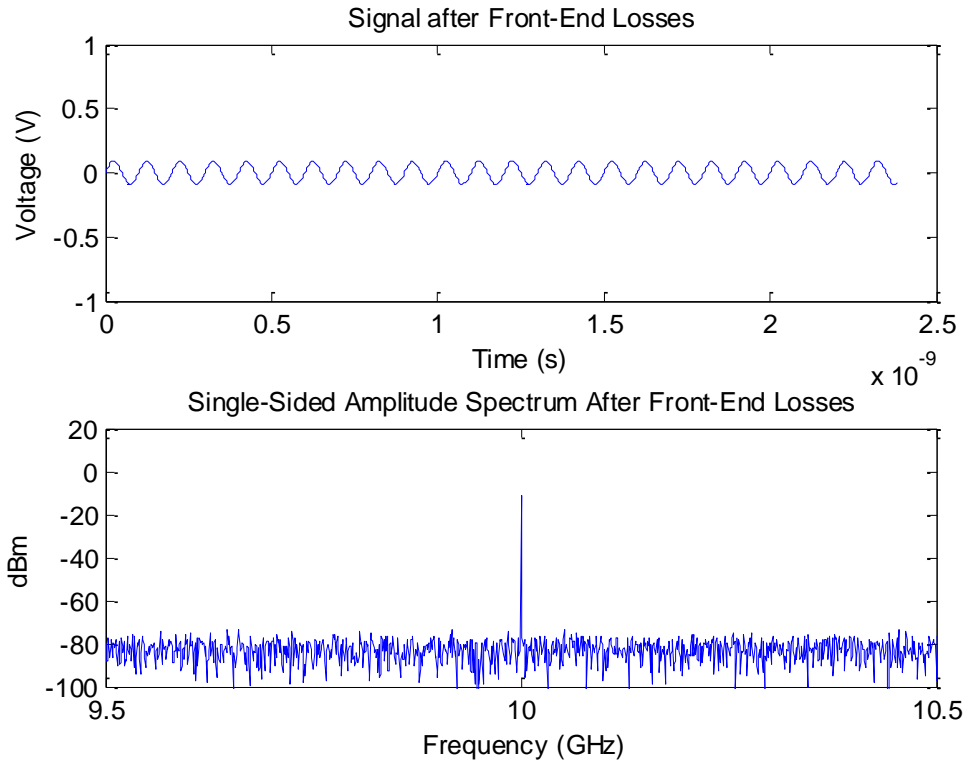
Figure 63: Coaxial Model with Saturation - Signal and Amplitude Spectrum after Front-End Losses

```
SNR =

    72.9768



LNA Parameters
  Gain of LNA (dB): 30
  Output P1dB of LNA (dBm): 10
  Noise Figure of LNA (dB): 2
  System Bandwidth (GHz): 1
Plot signal and amplitude spectrum of current signal?(y/n): y
```
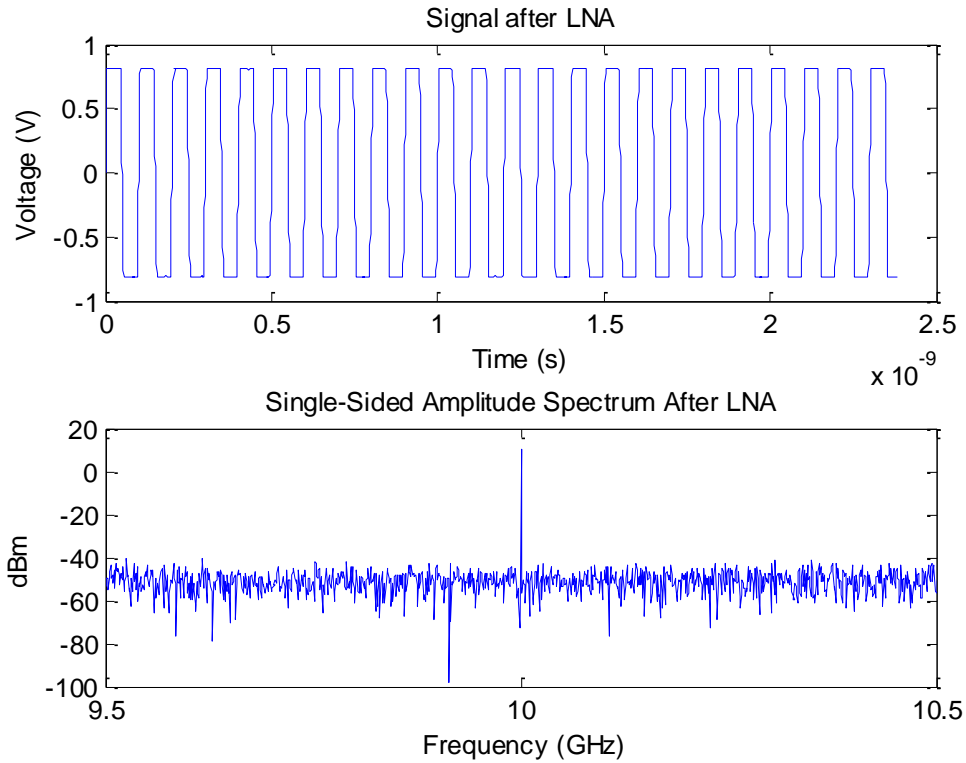
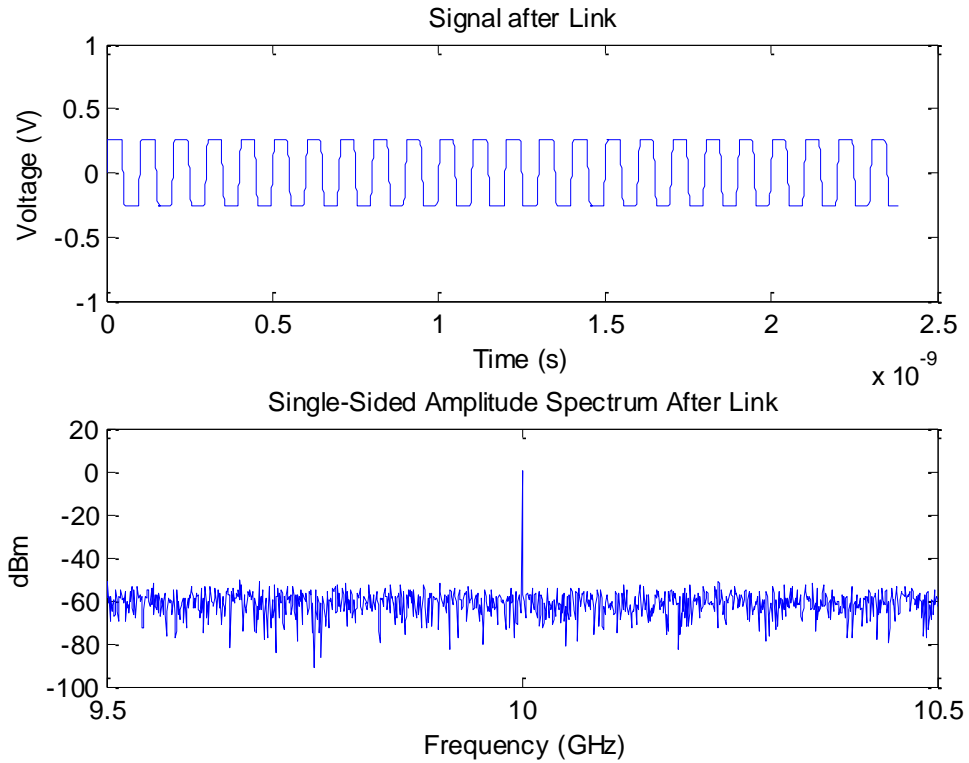**Figure 64: Coaxial Model with Saturation - Signal and Amplitude Spectrum after LNA**

```
SNR =

   62.5617



Specify Type of Link
  1) Coaxial
  2) Analog Optical (Component Level - External Modulation)
  3) Analog Optical (Component Level - Direct Modulation)
  4) Analog Optical (Link Level)
Enter #: 1

Coaxial Link Parameters
  Gain of Link (dB): -10
  Noise Figure of Link (dB): 10
  System Bandwidth (GHz): 1
Plot signal and amplitude spectrum of current signal?(y/n): y
```

Figure 65: Coaxial Model with Saturation - Signal and Amplitude Spectrum after Link

```
SNR =

   62.3784


RCVR Parameters
  Gain of RCVR (dB): 10
  Output P1dB of RCVR (dBm): 10
  Noise Figure of RCVR (dB): 7
  Output Frequency of RCVR (MHz): 70
  System Bandwidth (MHz): 20
Plot signal and amplitude spectrum of final signal?(y/n): y
```
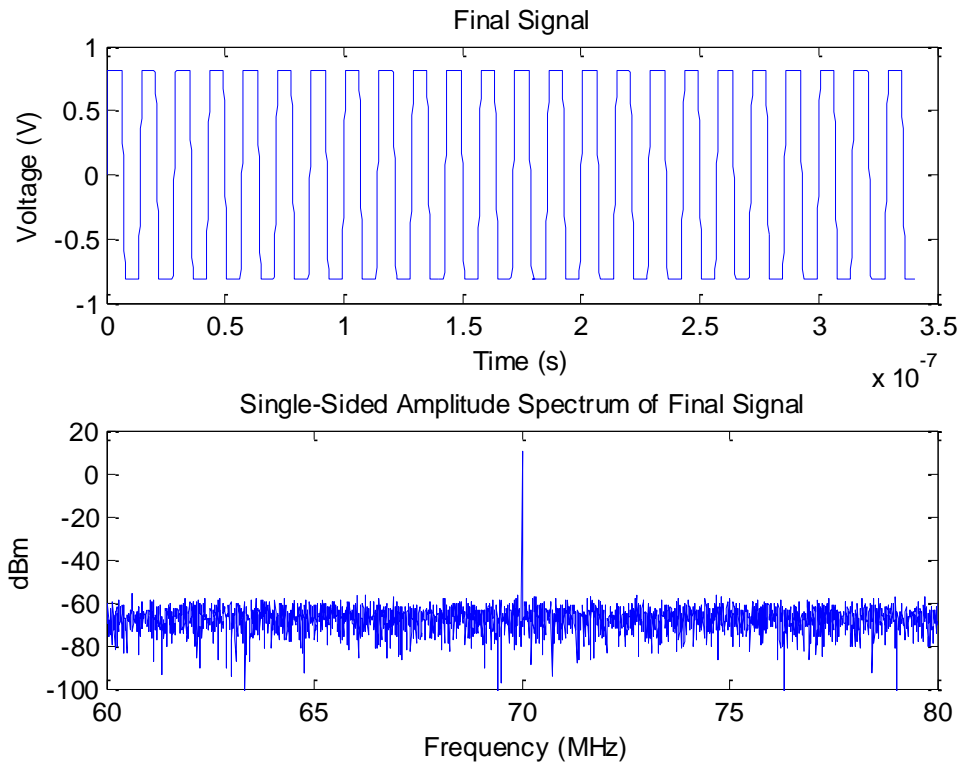
Figure 66: Coaxial Model with Saturation - Final Signal and Amplitude Spectrum

```
SNR =

    78.6034
```

Appendix H : Sample Model Execution – Small Signal

```
>> RadarReceiver
Signal Setup:
  Frequency of Main Signal (GHz): 10
  Average Power of Main Signal (dBm): -60
  System Bandwidth (GHz): 1
Plot signal and amplitude spectrum of initial signal?(y/n): y
```
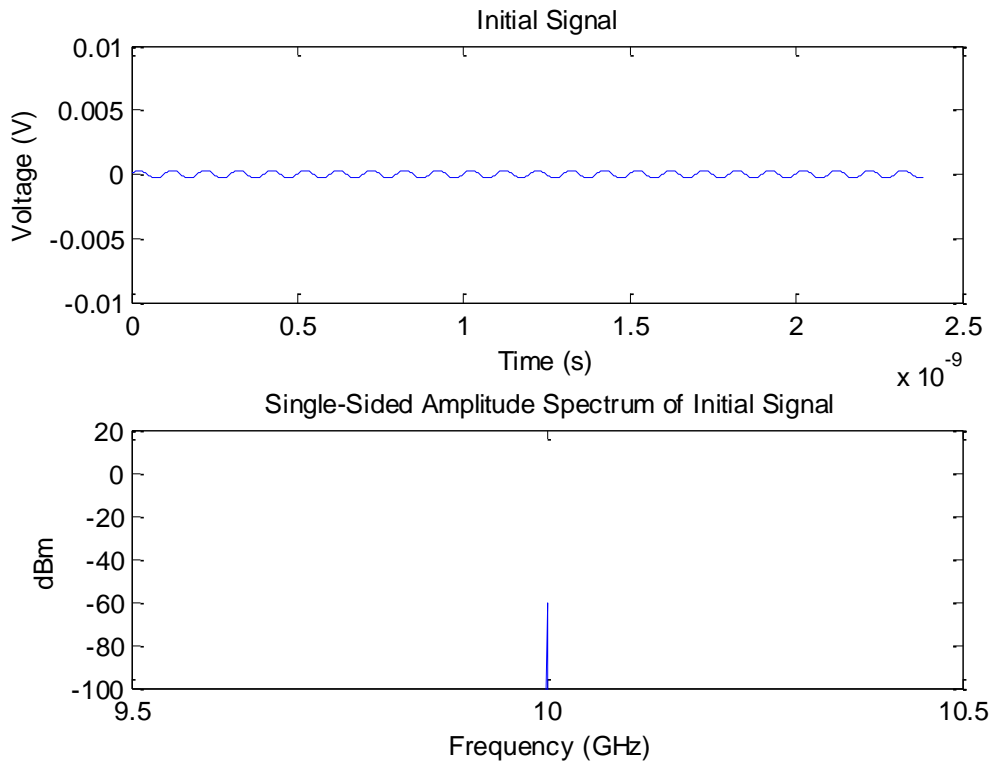

Figure 67: Coaxial Model (Small Signal) - Initial Signal and Amplitude Spectrum

```
Front-End Parameters
  Gain of Front-End (dB): -1
  Noise Figure of Front-End (dB): 1
  System Bandwidth (GHz): 1
Plot signal and amplitude spectrum of current signal?(y/n): y
```
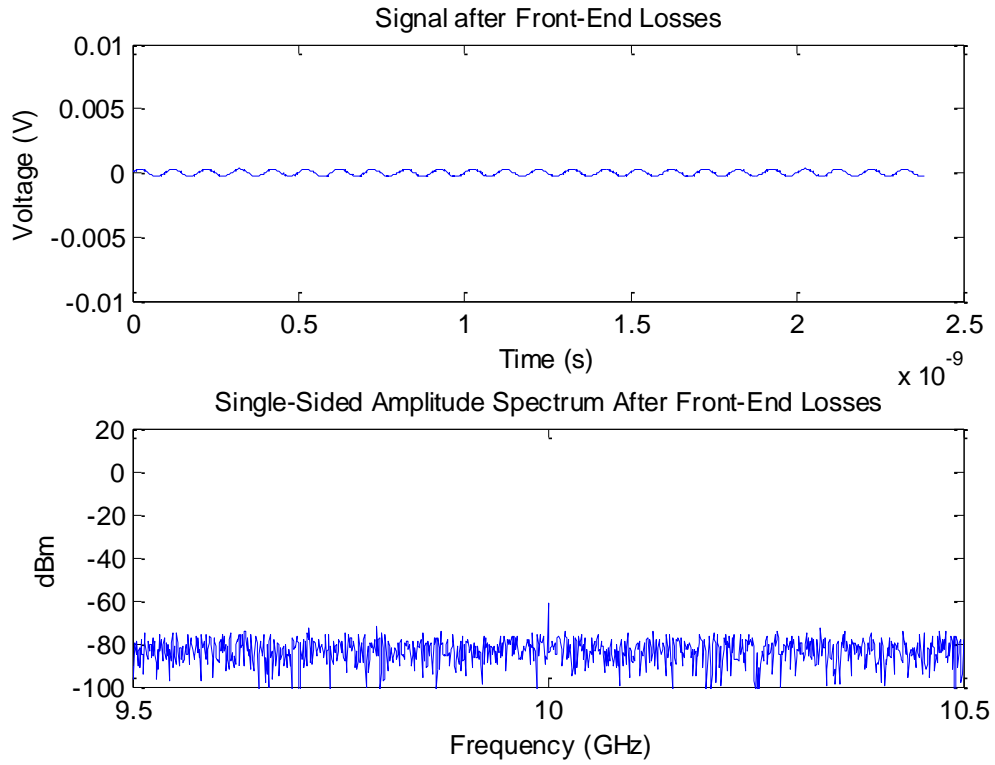
Figure 68: Coaxial Model (Small Signal) - Signal and Amplitude Spectrum after Front-End Losses

```
SNR =

   22.9729



LNA Parameters
  Gain of LNA (dB): 30
  Output P1dB of LNA (dBm): 10
  Noise Figure of LNA (dB): 2
  System Bandwidth (GHz): 1
Plot signal and amplitude spectrum of current signal?(y/n): y
```
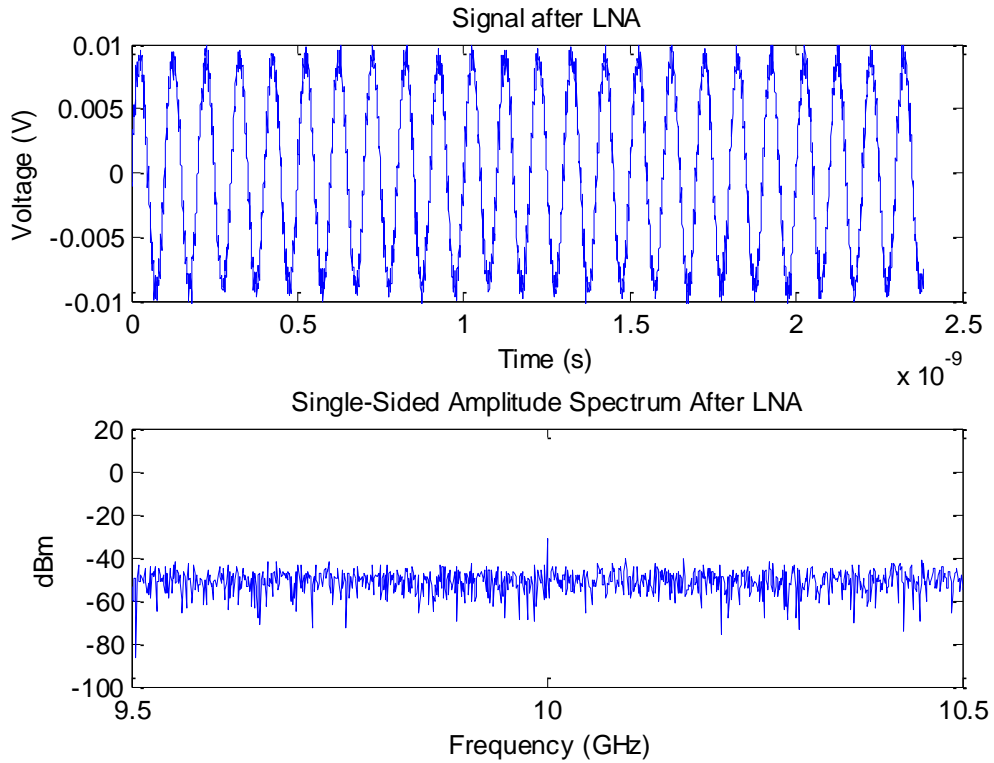
Figure 69: Coaxial Model (Small Signal) - Signal and Amplitude Spectrum after LNA

```
SNR =

   20.9783



Specify Type of Link
  1) Coaxial
  2) Analog Optical (Component Level - External Modulation)
  3) Analog Optical (Component Level - Direct Modulation)
  4) Analog Optical (Link Level)
Enter #: 1

Coaxial Link Parameters
  Gain of Link (dB): -10
  Noise Figure of Link (dB): 10
  System Bandwidth (GHz): 1
Plot signal and amplitude spectrum of current signal?(y/n): y
```
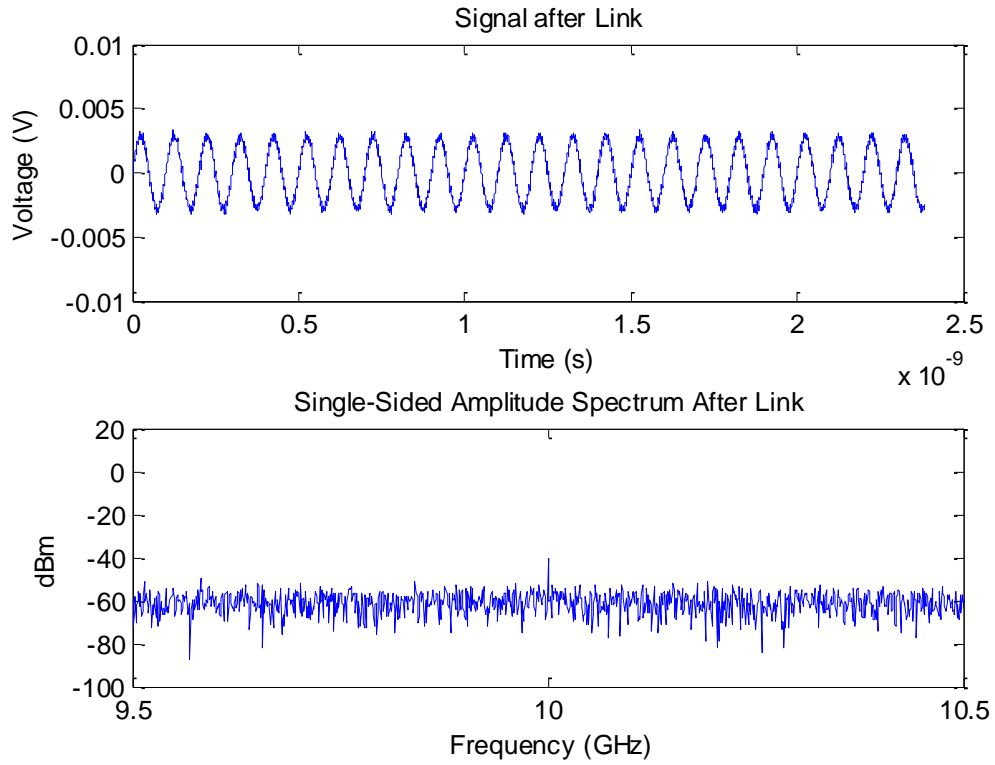
Figure 70: Coaxial Model (Small Signal) - Signal and Amplitude Spectrum after Link

```
SNR =

   20.9551


RCVR Parameters
  Gain of RCVR (dB): 10
  Output P1dB of RCVR (dBm): 10
  Noise Figure of RCVR (dB): 7
  Output Frequency of RCVR (MHz): 70
  System Bandwidth (MHz): 20
Plot signal and amplitude spectrum of final signal?(y/n): y
```
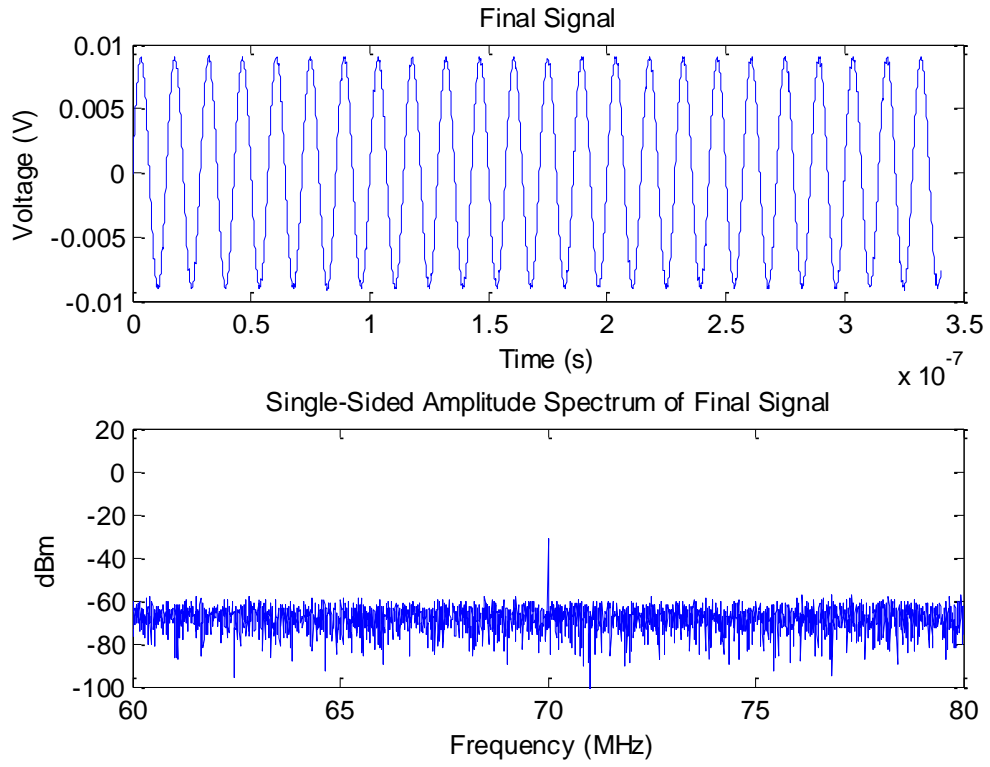
Figure 71: Coaxial Model (Small Signal) - Final Signal and Amplitude Spectrum

```
SNR =

   37.8300
```